1978

A Dynamic Model for the Simulation of Water Re-Use Units.

David Milton Starks
Louisiana State University and Agricultural & Mechanical College

A DYNAMIC MODEL FOR THE SIMULATION OF WATER RE-USE UNITS

A Dissertation

Submitted to the Graduate Faculty of the
Louisiana State University and
Agricultural and Mechanical College
in partial fulfillment of the
requirements for the degree of
Doctor of Philosophy

in

The Department of Chemical Engineering

by
David Milton Starks
B.S., Louisiana State University, 1975
M.S., Louisiana State University, 1977
August 1978

ACKNOWLEDGEMENTS

Dr. Cecil L. Smith is especially appreciated for the assistance, advice, and encouragement given during my undergraduate and graduate studies at LSU. His warm and friendly manner contributed greatly to the enjoyment of this research effort.

Drs. Bryant, Corripio, Groves, and Jones are sincerely thanked for serving on the advisory and examining committees.

The support of the U. S. Army Medical Research and Development Command is also acknowledged. Thanks go to Mr. Mitch Small, Maj. Walter Lambert, and Capt. Barry Peterman for their assistance. Mitch is especially remembered for his numerous courtesies which helped make our stay in Maryland an experience that will always be fondly remembered.

Appreciation is expressed to the secretarial staff at the Department of Chemical Engineering. Hazel LaCoste is thanked for the many favors done and especially for handling the financial aspects of my travels connected with this research. Linda McCain is thanked for her assistance in typing the several reports generated during this project.

Mrs. Charlotte Smith is appreciated for always being a courteous and dependable communication link between myself and her sometimes hard to reach husband, Cecil.

For the superb job of typing this dissertation, I would like to thank Mrs. Mary McDaniel.

The Dr. Charles E. Coates Memorial Fund which provided financial support in the preparation of this manuscript is also appreciated.

Foremost, I would like to gratefully acknowledge the patience, kindness, encouragement, understanding and love shown to me by my wife, Faye; my parents, Nell and Clarence Starks; and my grandmother, Mrs. Effie K. Starks.

TABLE OF CONTENTS

LIST OF TABLES

ABSTRACT

This dissertation presents the development of a flexible dynamic model for use in the design and analysis of waste water for re-use processing systems.

The work was divided into two phases:

1. Development of mechanistic models of several unit processes prominent in the water re-use area. These include models of tubular ultrafiltration, hollow fiber reverse osmosis, ultraviolet radiation enhanced ozonation, and hypochlorination.

   Methodology for evaluating model parameters from experimental data is also given.

2. Development of a dynamic process flow simulator package which consolidates the component models developed under phase 1 into an integrated model.

The results of an example simulation of a water processing unit similar to a design proposed under contract to the U. S. Army Medical Research and Development Command are presented.

CHAPTER I

INTRODUCTION

Over the past several years, the U. S. Army Medical Research and Development Command (USAMRDC) has been involved in the development of water re-use systems for purposes such as the support of field medical units. Given the spectrum of possible applications, the technology in the water re-use area is being developed.

The design objectives for these systems will vary considerably depending on the specific application, but included in the set of important considerations are the following:

1. Output capacity
2. Fractional recovery and product quality
3. Size and weight
4. Power consumption
5. Operational complexity and maintenance requirements
6. Equipment and operating costs

In early investigations, membrane separation emerged as a promising technology. Advantages of membrane systems include:

1. Compact design
2. Low capital cost
3. Low operating cost
4. Simple operation
5. High removal efficiencies for many contaminants
6. Low sensitivity to shock loads

These advantages were recognized in previous studies (13) which concluded that reverse osmosis would be selected as the central element in most re-use applications. These studies indicated the need for effective pretreatment of the wastes to prevent fouling of the reverse osmosis modules. In addition, post-treatment would be required for the removal of residual organic contaminants which pass through the reverse osmosis membranes.

Several additional processes have been evaluated and retained for possible use in water re-use systems. Waste equalization was selected to dampen fluctuations in hydraulic loading and concentrations of "bad actor" contaminants (i.e., contaminants which are difficult to treat or may be detrimental in subsequent processing steps). Ultrafiltration was selected for pretreatment and is the key to successful and efficient operation of subsequent processes. Ultrafiltration can achieve essentially complete rejection of suspended solids at very high water recoveries while exhibiting all the advantages listed above for membrane separation systems. Compared to reverse osmosis, ultrafiltration is particularly well suited to the treatment of "dirty" process streams since the unit productivity of ultrafiltration membranes is much higher allowing effective use of "open" module configurations which, if fouled, can be readily cleaned. In addition, ultrafiltration membranes are generally less susceptible to damage by "bad-actor" constituents and temperature excursions. Removal of suspended solids by ultrafiltration pretreatment permits the utilization of highly compact, narrow-flow-channel reverse osmosis modules. Ozonation was selected for evaluation as a post-treatment process and is capable of effectively removing a variety of organics from wastewater. Chlorination was selected as a

final process step because of the need to prevent the growth of microorganisms during product water storage and the need to disinfect any water discharged to the environment. While ozone is a very effective disinfectant, it is unstable, and after it decomposes, biological contamination can occur.

The Army has supported the development of a pilot plant incorporating each of the unit processes mentioned. The main objective of this program is the acquisition of data characterizing the operation of the various component processes.

In the design and analysis of water re-use systems, mathematical modeling is recognized as a vehicle for investigating the operating characteristics of these systems as well as an aid in control system design. Several factors which are important in the development of such a model are listed below:

1. The model must be inherently flexible with regards to modifications in the unit processes used, piping arrangements, equipment sizing, etc.
2. Due to the projected cyclical and somewhat stochastic nature of most waste streams likely to be encountered, such water processing units never reach steady state. Therefore, the model must necessarily be dynamic in nature.
3. It is expected that the water re-use technology and associated processes being developed, with modifications, would be appealing to groups other than the military. Thus, since future applications are at the present indeterminant, the methodology of adapting the model to any of several - indeed, some even unknown - waste waters should be developed rather

than creating a model specific to one waste water type.

The subject of the present work is the development of a dynamic model of a water treatment element incorporating the unit processes described subject to the constraints enumerated above. This task was divided into two phases:

1. Development of component models for each of the major unit processes involved. Each of these models was created by writing the basic equations describing the particular system and coding a FORTRAN IV program to solve the equations.

   Several of these models require values for parameters such as mass transfer coefficients or reaction rate orders which must be determined from experimental data. It is expected that these parameters are highly dependent upon the operating conditions chosen and waste water being processed.

   In keeping with the goal of developing the capability of extending the model to other applications areas, documentation for the determination of model parameters has received a high priority.

   Chapters II, III, IV, and V describe the model development process for the ultrafiltration (UF), reverse osmosis (RO), ozonation with ultraviolet radiation (UV), and hypochlorination (HC) units, respectively.

2. Development of a dynamic process flow simulation package which combines the component models completed during the first phase into an integrated model. Easily described units such as holding tanks are implemented as part of the flow simulator.

Also, models of additional or modified unit processes are easily incorporated into the flow simulator.

To make this integrated model as flexible as possible, the plant configuration - the process units, as well as the origin and destination of every process stream - is specified by the input data.

Chapter VI documents the process flow simulator package. As an example and test case, a study of the integrated model simulating the operation of a water processing unit similar to the one proposed for the MUST WPE (Medical Unit, Self-Contained, Transportable Water Processing Element) was performed. The MUST WPE development program was also supported by the Army.

The results are presented in a technical report to the USAMRDC (12).

CHAPTER II

THE ULTRAFILTRATION SYSTEM MODEL

INTRODUCTION

In this chapter, the development of the ultrafiltration module model from basic equations is presented, the solution technique is outlined, and an analysis of parameter estimation considerations is given.

Listings of the computer programs comprising the model are included in the report, "A Mathematical Model of a Tubular Ultrafiltration Unit for Water Re-Use Systems". Examples of program runs along with the results of a parameter sensitivity analysis study are presented in the same report. (1)

DEVELOPMENT OF BASIC EQUATIONS AND METHODS USED

The model equations developed characterize the operation of the Abcor HFD ultrafiltration unit shown in Figure 2.1. Contaminated water enters the tube at z=0 and flows in the z direction. The water at z=L is collected as concentrate. While in the tube, some of the water and contaminants pass through the membrane attached to the tube's inner surface and are collected as permeate.

Each ultrafiltration tube is modeled as a long hollow cylinder with a semi-permeable membrane adhering to the inner surface of the tube. The membrane acts as an extra fine mesh, retaining suspended solids and some very large organics, but passing water and much of the dissolved solids. During operation, a thin boundary layer is assumed to form at the membrane through which water must pass before reaching the tube

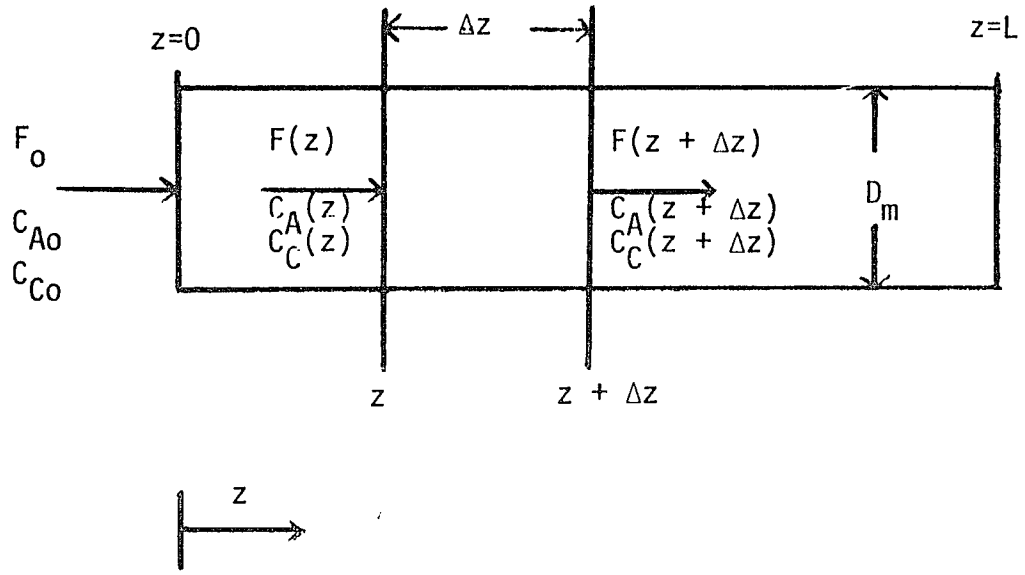

where:

z = Axial coordinate

L = UF tube length

F = Volumetric flow rate

C_A = Concentration of total solids

C_C = Concentration of total organic carbon

D_m = UF tube diameter

o = Indicates inlet conditions

Figure 2.1. Diagram of One Ultrafiltration Module Tube for Material Balance Formulations

wall. Detailed equations derived from writing component and overall material balances for the bulk and boundary layer sections of the tube form the basis of the model.

Formulation of Equations

At the present, the model is concerned with three contaminants in the feed:

1. Suspended solids
2. Dissolved solids
3. TOC (Total Organic Carbon)

As written, the model assumes that the effect of suspended solids and dissolved solids on the flux of contaminants through the membrane is the same, permitting the dissolved and suspended solids to be lumped into a single contaminant, the total solids for the feed and concentrate streams. Since experimental evidence indicates that the membrane achieves essentially complete rejection of suspended solids, the permeate is assumed to be comprised of water, dissolved solids, and TOC.

In most configurations, the residence time of liquid in the UF tubes will be negligible in comparison with the dynamic contribution of associated equipment. Therefore, a steady state formulation has been used.

Total Solids

A steady state material balance on the total solids, being comprised of suspended and dissolved solids and designated 'A', for the slice of tube between z and $z + \Delta z$ shown in Figure 2.1 yields:

Input rate of A = Output rate of A

$$F(z)C_A(z) = F(z + \Delta z)C_A(z + \Delta z) + \pi D_m J_A(z)\Delta z \qquad (1)$$

where: $F(z)$ = fluid volumetric flow rate (m^3/hr)

$C_A(z)$ = concentration of total solids (gm/m^3)

$J_A(z)$ = flux of A through membrane ($gm/hr\text{-}m^2$)

As the permeate contains no suspended solids, J_A must consist entirely of dissolved solids.

TOC (Total Organic Carbon)

A steady state material balance on the TOC, component 'C', for the differential element between z and $z + \Delta z$ shown in Figure 2.1 yields:

Input rate of C = Output rate of C

$$F(z)C_C(z) = F(z + \Delta z)C_C(z + \Delta z) + \pi D_m J_C(z)\Delta z \qquad (2)$$

where: $C_C(z)$ = concentration of TOC (gm/m^3)

$J_C(z)$ = flux of C through membrane ($gm/m^2\text{-}hr$)

Total Material Balance

A steady state total material balance for the differential element in Figure 2.1 yields:

Input rate = Output rate

$$F(z)\rho = F(z + \Delta z)\rho + \pi D_m[J_A(z) + J_B(z) + J_C(z)]\Delta z \qquad (3)$$

where: ρ = total mass density (gm/m^3)

$J_B(z)$ = flux of water, component B, through the membrane ($gm/m^2\text{-}hr$)

Analytical Equations

Equations (1), (2) and (3) are readily converted to differential equations by dividing by Δz and taking the limit as Δz approaches zero. For equation (1), the result is:

$$\frac{d}{dz}[F(z)C_A(z)] = -\pi D_m J_A(z) \qquad (4)$$

Equation (2) becomes:

$$\frac{d}{dz}[F(z)C_C(z)] = -\pi D_m J_C(z) \tag{5}$$

Equation (3) becomes:

$$\frac{d}{dz}F(z) = \frac{-\pi D_m}{\rho}[J_A(z) + J_B(z) + J_C(z)] \tag{6}$$

The boundary conditions are as follows:

$$F(0) = F_o$$

$$C_A(0) = C_{Ao}$$

$$C_C(0) = C_{Co}$$

where: F_o = feed rate to module (m^3/hr)

C_{Ao} = inlet concentration of A (gm/m^3)

C_{Co} = inlet concentration of C (gm/m^3)

Fluxes at the Boundary Layer

To obtain the fluxes J_A, J_B, and J_C, a stagnant boundary layer is imagined to exist near the inner surface of the membrane as shown in Figure 2.2. The following fluxes into and out of the boundary layer are defined:

$$J_A = B(C_{A2} - C_{A3}) \tag{7}$$

$$J_B = \gamma(\Delta P - \Delta\pi) \tag{8}$$

$$J_C = C(C_{C2} - C_{C3}) \tag{9}$$

$$J_{DA} = k_A(C_{A2} - C_{A1}) \tag{10}$$

$$J_{DB} = k_B(C_{B1} - C_{B2}) \tag{11}$$

$$J_{DC} = k_C(C_{C2} - C_{C1}) \tag{12}$$

where: J_{DA} = diffusional flux of solids out of the boundary layer, gm/m^2-hr

J_{DB} = diffusional flux of water into the boundary layer, gm/m^2-hr

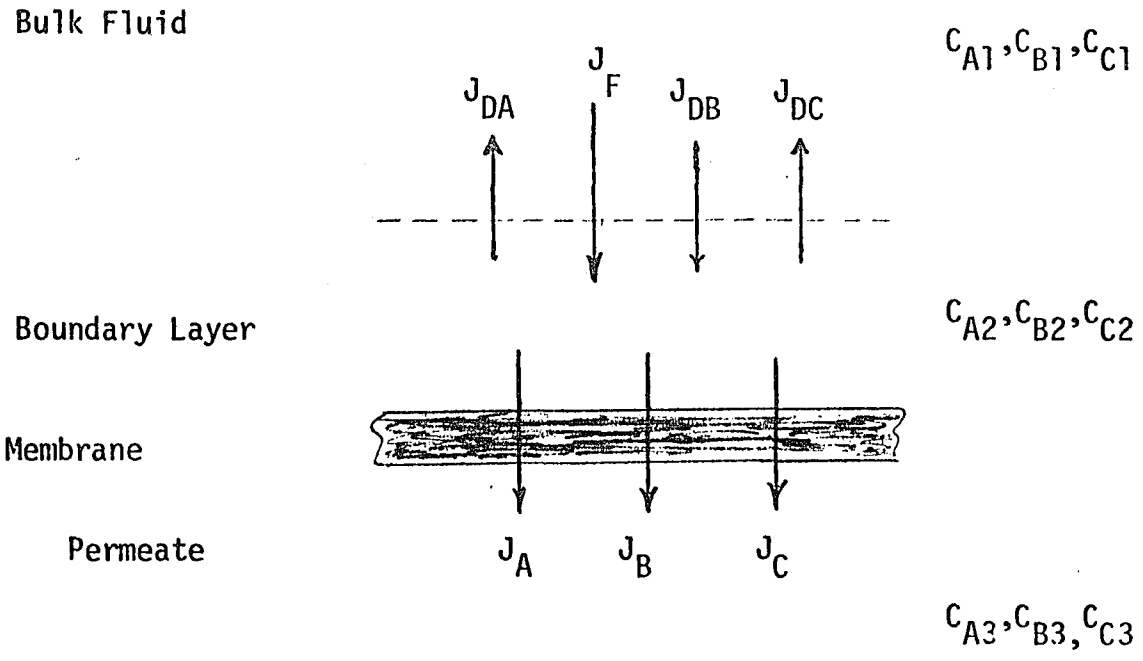

Figure 2.2. Fluxes into and out of boundary layer

J_{DC} = diffusional flux of TOC out of the boundary layer, gm/m^2-hr

C_{A1} = doncentration of A in bulk fluid, gm/m^3

C_{A2} = concentration of A in boundary layer, gm/m^3

C_{A3} = concentration of A in permeate, gm/m^3

C_{B1} = concentration of B in bulk fluid, gm/m^3

C_{B2} = concentration of B in boundary layer, gm/m^3

C_{B3} = concentration of B in permeate, gm/m^3

C_{C1} = concentration of C in bulk fluid, gm/m^3

C_{C2} = concentration of C in boundary layer, gm/m^3

C_{C3} = concentration of C in permeate, gm/m^3

γ = permeability coefficient for pure water, gm/m^2-hr-atm

B = permeability coefficient for dissolved solids, m/hr

C = permeability coefficient for TOC, m/hr

ΔP = pressure drop across membrane, atm

$\Delta\pi$ = osmotic pressure difference across membrane = $\pi_2 - \pi_3$, atm

π_2 = osmotic pressure at boundary layer, atm

π_3 = osmotic pressure of permeate, atm

k_A, k_B, k_C = mass transfer coefficients for solids, water and TOC, respectively, m/hr

The osmotic pressure is related to the concentration of contaminants, C_E, and the absolute temperature, T, by the empirical relationship

$$\pi = f(C_E,T) = \alpha T C_E(1 + \beta C_E)^2 \quad \text{[ref. (3)]} \tag{13}$$

where: α = coefficient, atm-m^3/gm-°K

β = coefficient, m^3/gm

T = absolute temperature, deg Kelvin

C_E = effective contaminant concentration = $C_A + k_E C_C$, gm/m^3

k_E = coefficient expressing the concentration of A equivalent to a unit concentration of C for purposes of osmotic pressure, dimensionless

To obtain $\Delta\pi = \pi_2 - \pi_3$, it is necessary to evaluate π_2 using C_{A2} and C_{C2}; π_3 using C_{A3} and C_{C3}.

The flux J_F due to the bulk flow toward the boundary layer can be obtained by writing a total material balance around the boundary layer:

$$J_F = J_A + J_B + J_C + J_{DA} - J_{DB} + J_{DC} \tag{14}$$

In addition, component balances for component A and for component C can be written:

$$J_F X_{A1} = J_A + J_{DA} \tag{15}$$

$$J_F X_{C1} = J_C + J_{DC} \tag{16}$$

where X_{A1}, X_{C1} = mass fractions of total solids and TOC in bulk stream, respectively.

A component balance can also be written for component B, but it will not be an independent equation.

In addition, the mass fractions X_{A3} and X_{C3} are related to J_A, J_B, and J_C as follows:

$$X_{A3} = \frac{J_A}{J_A + J_B + J_C} \tag{17}$$

$$X_{C3} = \frac{J_C}{J_A + J_B + J_C} \tag{18}$$

where X_{A3}, X_{C3} = mass fractions of total solids and TOC in the permeate, respectively.

The complete set of equations describing the fluxes at the boundary layer is reproduced in Table 2-1.

Table 2-1. Nonlinear Equations for Fluxes at Boundary Layer

Transport Equations

$$J_A = B(C_{A2} - C_{A3})$$

$$J_B = \gamma(\Delta P - \Delta\pi)$$

$$J_C = C(C_{C2} - C_{C3})$$

$$J_{DA} = k_A(C_{A2} - C_{A1})$$

$$J_{DB} = k_B(C_{B1} - C_{B2})$$

$$J_{DC} = k_C(C_{C2} - C_{C1})$$

Osmotic Pressure Relationships

$$\Delta\pi = \pi_2 - \pi_3$$

$$\pi_2 = \alpha T C_{E2}(1 + \beta C_{E2})^2$$

$$\pi_3 = \alpha T C_{E3}(1 + \beta C_{E3})^2$$

$$C_{E2} = C_{A2} + k_E C_{C2}$$

$$C_{E3} = C_{A3} + k_E C_{C3}$$

Material Balances at Boundary Layer

$$J = J_A + J_B + J_C + J_{DA} - J_{DB} + J_{DC}$$

$$J_F X_{A1} = J_A + J_{DA}$$

$$J_F X_{C1} = J_C + J_{DC}$$

$$X_{A3} = \frac{J_A}{J_A + J_B + J_C}$$

$$X_{C3} = \frac{J_C}{J_A + J_B + J_C}$$

Mass Fraction/Density/Concentration Relationships

$$X_{B2} = 1 - X_{A2} - X_{C2} \qquad X_{B3} = 1 - X_{A3} - X_{C3}$$

$$C_{A2} = \rho X_{A2} \qquad C_{A3} = \rho X_{A3}$$

$$C_{B2} = \rho X_{B2} \qquad C_{B3} = \rho X_{B3}$$

$$C_{C2} = \rho X_{C2} \qquad C_{C3} = \rho X_{C3}$$

Mass Transfer Coefficients

Harriott and Hamilton (2) give the following relationship for tubular ultrafiltration modules:

$$N_{Sh} = 0.0096 N_{Re}^{0.913} N_{Sc}^{0.346} \tag{19}$$

where: $N_{Sh} = \frac{kD}{D_x}$ = Sherwood number

$N_{Re} = \frac{DV}{\nu}$ = Reynolds number

$N_{Sc} = \frac{\nu}{D_x}$ = Schmidt number

where: k = mass transfer coefficient, m/hr

ν = kinematic viscosity, m^2/hr

D_x = diffusivity, m^2/hr

D = characteristic length, m

V = linear velocity in axial direction, m/hr

In the case of ultrafiltration modules, D is taken to be the tube diameter.

Since the kinematic viscosity is assumed constant, the only effect of the contaminant concentrations upon the mass transfer coefficients is through the diffusivity, D_x.

For the total solids, component A, the following diffusivity relationship was used:

$$D_{Ax} = [100 a_A X_{A1} + b_A \exp(-100 c_A X_{A1})] \cdot 10^{-10} \tag{20}$$

where: D_{Ax} = diffusivity of A through water and TOC, m^2/hr

a_A, b_A, c_A = coefficients

X_{A1} = bulk mass fraction of A

For the TOC, component C, a constant value of the diffusivity, denoted as D_{Cx}, has been found to be adequate.

The mass transfer coefficient k_A is evaluated by computing D_{Ax} from the bulk flow concentration of total solids and using this value for D_x in equation (19); similarly, k_C is evaluated by replacing D_x with D_{Cx} in equation (19).

Approximations in the Flux Equations

In the ultrafiltration unit, the concentrations of total solids and TOC will be relatively small. Furthermore, the UF membrane will tend to reject these components. For these reasons, the following assumptions will be made:

1. The membrane permeability fluxes J_A and J_C are small compared to J_B.
2. The diffusional fluxes J_{DA}, J_{DB}, and J_{DC} are small compared to J_B.

Table 2-2 presents the equations from Table 2-1 with these approximations included.

Difference Equations

The numerical solution of the differential equations is effected by discretizing in the z-direction using an increment Δz. Therefore, let

$$z_i = i*\Delta z$$

The discrete versions of equations (4), (5), and (6) are the following difference formulations (constant density is assumed).

$$F(z_i)C_A(z_i) = F(z_{i-1})C_A(z_{i-1}) - \pi D_m J_A(z_{i-1})\Delta z \tag{21}$$

$$F(z_i)C_C(z_i) = F(z_{i-1})C_C(z_{i-1}) - \pi D_m J_C(z_{i-1})\Delta z \tag{22}$$

$$F(z_i) = F(z_{i-1}) \frac{-\pi D_m}{\rho} [J_A(z_{i-1}) + J_B(z_{i-1}) + J_C(z_{i-1})]\Delta z \tag{23}$$

Table 2-2. Simplified Equations for Fluxes at the Boundary Layer

Transport Equations

$$J_A = B(C_{A2} - C_{A3})$$

$$J_B = \gamma(\Delta P - \Delta\pi)$$

$$J_C = C(C_{C2} - C_{C3})$$

$$J_{DA} = k_A(C_{A2} - C_{A1})$$

$$J_{DC} \quad k_C(C_{C2} - C_{C1})$$

Osmotic Pressure Relationships

$$\Delta\pi = \pi_2 - \pi_3$$

$$\pi_2 = \alpha T C_{E2}(1 + \beta C_{E2})^2$$

$$\pi_3 = \alpha T C_{E3}(1 + \beta C_{E3})^2$$

$$C_{E2} = C_{A2} + k_E C_{C2}$$

$$C_{E3} = C_{A3} + k_E C_{C3}$$

Material Balance at Boundary Layer

$$J_F = J_B$$

$$J_F X_{A1} = J_A + J_{DA}$$

$$J_F X_{C1} = J_C + J_{DC}$$

$$X_{A3} = \frac{J_A}{J_B}$$

$$X_{C3} = \frac{J_C}{J_B}$$

Mass Fraction/Density/Concentration Relationships

$$X_{B2} = 1 - X_{A2} - X_{C2} \qquad X_{B3} = 1 - X_{A3} - X_{C3}$$

$$C_{A2} = \rho X_{A2} \qquad C_{A3} = \rho X_{A3}$$

$$C_{B2} = \rho X_{B2} \qquad C_{B3} = \rho X_{B_3}$$

$$C_{C2} = \rho X_{C2} \qquad C_{C3} = \rho X_{C3}$$

The boundary conditions become:

$$F(z_o) = F_o$$

$$C_A(z_o) = C_{Ao}$$

$$C_C(z_o) = C_{Co}$$

where $z_o = 0*\Delta z = 0$.

Figure 2.3 illustrates the procedure followed for each value of i from 1 to N, where $N = L/\Delta z$ is the number of increments required.

Algebraic Equations for Fluxes

Block 1 of the procedure in Figure 2.3 requires the computation of J_A, J_B and J_C at z_{i-1} using the values of $F(z_{i-1})$, $C_A(z_{i-1})$, and $C_C(z_{i-1})$ that are presently available. This requires the solution of the set of equations in Table 2-2. As illustrated in Figure 2.4, this entails two nested iteration loops.

For both loops, the interval halving method is used. Various back-substitution methods were tried in the solution of similar equations for the Reverse Osmosis Model but without success. Consequently, the reliability of the interval halving method had to take precedence over computational efficiency.

For the first or outer iteration loop, a value of C_{A2} must be estimated. It is known that $C_{A1} \leq C_{A2} \leq \rho$, which permits interval halving to be utilized.

However, knowing the value of C_{A2} only permits J_{DA} to be calculated. To proceed further, a value is assumed for C_{A3}, which must be in the interval $0 \leq C_{A3} \leq C_{A1}$. This permits J_B to be readily calculated as follows:

$$J_B = k_A \rho \left[\frac{C_{A2}}{C_{A3}} - 1.0\right] , \qquad (24)$$

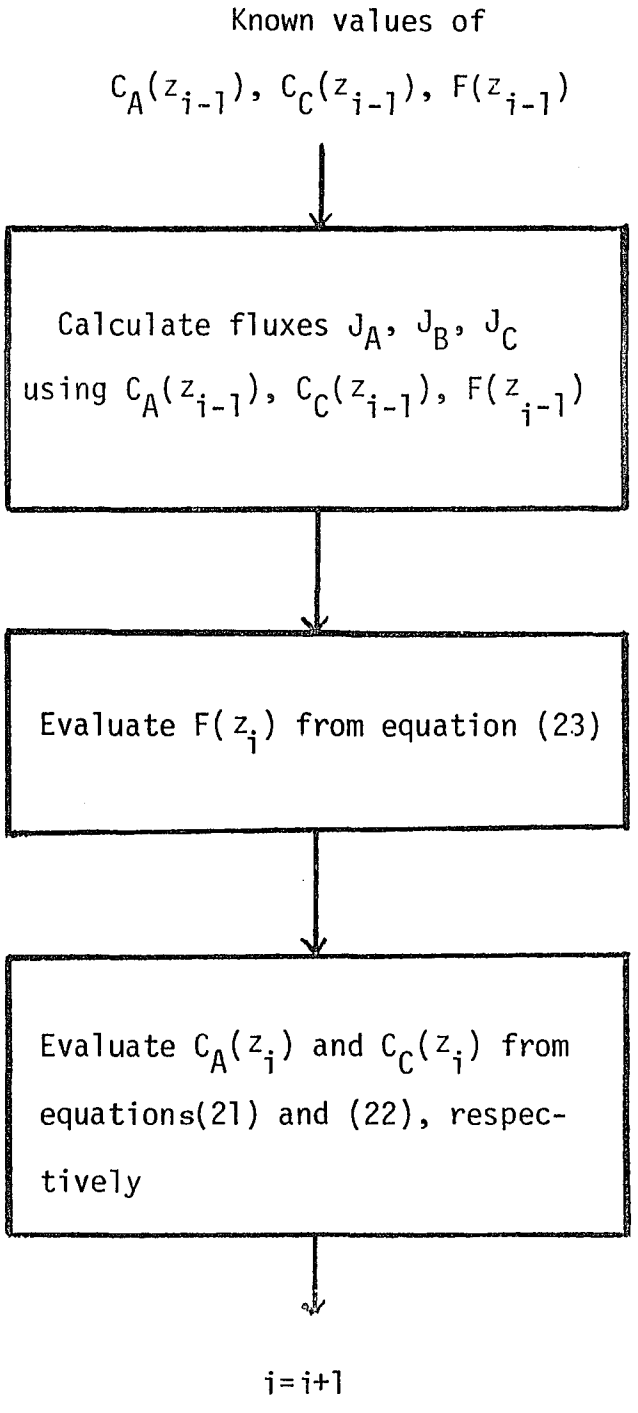

Figure 2.3

Numerical Integration Procedure

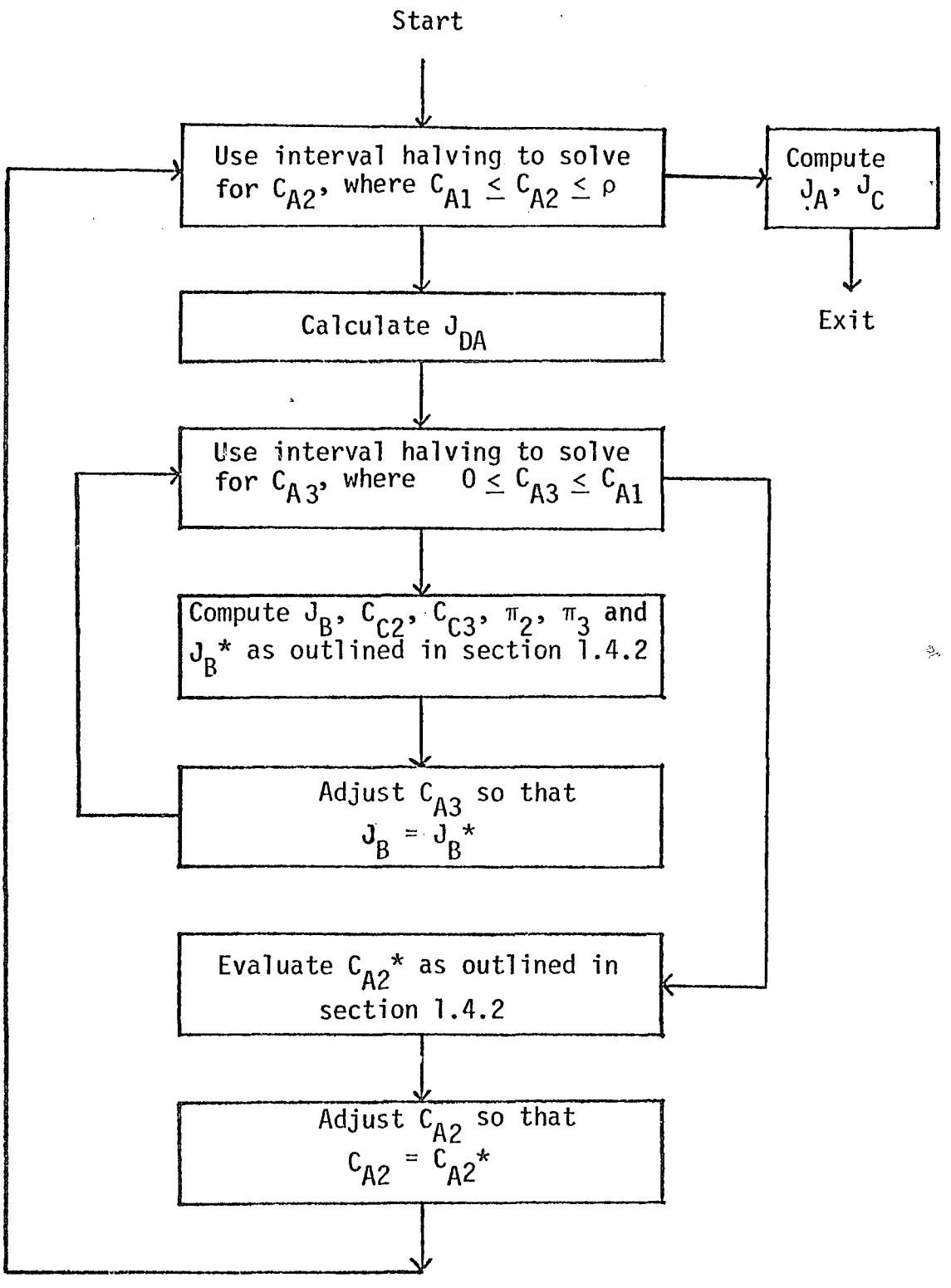

Figure 2.4

Computation of the Fluxes

by combining the following three equations:

$$X_{A3} = J_A/J_B$$

$$C_{A3} = \rho X_{A3}$$

and $J_A = k_A(C_{A2} - C_{A3})$.

The key to the procedure is that C_{C2} and C_{C3} can be calculated from J_B. The equation

$$J_B X_{C1} = J_C + J_{DC}$$

can be written as

$$J_B X_{C1} = C(C_{C2} - C_{C3}) + k_C(C_{C2} - C_{C1}) \tag{25}$$

Furthermore, the equation

$$X_{C3} = \frac{J_C}{J_B}$$

can be written as

$$\frac{C_{C3}}{\rho} = \frac{C(C_{C2} - C_{C3})}{J_B} \tag{26}$$

which can be solved for C_{C3}:

$$C_{C3} = \frac{C \cdot C_{C2}}{J_B/\rho + C} \tag{27}$$

The expression for C_{C3} can be substituted into equation (25) to obtain

$$J_B X_{C1} = C\left(C_{C2} - \frac{C \cdot C_{C2}}{J_B/\rho + C}\right) + k_C(C_{C2} - C_{C1}) \tag{28}$$

or

$$C_{C2} = \frac{J_B X_{C1} + k_C C_{C1}}{k_C + C\left(\frac{J_B/\rho}{J_B/\rho + C}\right)} \tag{29}$$

Now that C_{C2} is known, C_{C3} can be computed using equation (27).

Now that values are available for C_{A2}, C_{C2}, C_{A3}, and C_{C3}, the osmotic pressures π_1 and π_2 can be computed, and then J_B^* can be evaluated using

$$\Delta\pi = \pi_2 - \pi_3$$

and $J_B^* = (\Delta P - \Delta\pi)$.

If the values of J_B and J_B^* do not agree, the value of C_{A3} must be changed. Using the interval halving technique, the interval of uncertainty for C_{A3} is reduced and the computations repeated.

Once a value of C_{A3} is obtained that gives the same value for J_B and J_B^*, the assumption for C_{A2} must be checked. Since values are available for J_B, J_A, and J_{DA}, we can compute C_{A2}^* as follows:

$$J_B X_{A1} = k_A(C_{A2}^* - C_{A1}) + B(C_{A2}^* - C_{A3}) \tag{30}$$

rewritten as

$$C_{A2}^* = \frac{J_B X_{A1} + k_A C_{A1} + B C_{A3}}{k_A + B} \tag{31}$$

If C_{A2}^* is not equal to C_{A2}, a new value for C_{A2} must be assumed. The interval halving logic permits the interval of uncertainty for C_{A2} to be reduced and the calculations repeated.

Using this procedure, the nonlinear flux equations are solved for each integration step.

Since the degree of concentration per pass through the ultrafiltration module is small, a simple Euler integration method was employed. This resulted in a reasonably accurate solution with minimal computational effort.

PARAMETER ESTIMATION CONSIDERATIONS

Values of several key variables, such as mass transfer coefficients and osmotic pressure correlation coefficients, must be determined for use within the model.

To estimate these values, a Pattern Search strategy (8) is used to minimize a cost function which penalizes for model deviations from experimental results.

Cost Function

The cost function used in this study is the sum of weighted relative squared differences between the model and experimental data for the following items characteristic of the behavior of the ultrafiltration unit:

1. Permeate flux
2. Permeate solids concentration
3. Permeate total organic carbon concentration

The algebraic formulation of the cost function is given below:

$$COST = \sum_{i=1}^{n} Z_i \left[W_{Fi} \left(\frac{F_{e,i} - F_{m,i}}{F_{e,i}} \right)^2 + W_{Di} \left(\frac{C_{Ae,i} - C_{Am,i}}{C_{Ae,i}} \right)^2 + W_{Ti} \left(\frac{C_{Ce,i} - C_{Cm,i}}{C_{Ce,i}} \right)^2 \right]$$

where: COST = cost function to be minimized

i = data point identifier

n = number of data points

Z_i = weighting factor of point i relative to other data points

W_{Fi} = weighting factor for flux for data point i ($0 \leq W_{Fi} \leq 1$)

W_{Di} = weighting factor for total solids concentration for data point i ($0 \leq W_{Di} \leq 1$)

W_{Ti} = weighting factor for TOC concentration for data point i ($0 \leq W_{Ti} \leq 1$)

$F_{e,i}$ = experimental value of permeate flux for data point i

$F_{m,i}$ = permeate flux predicted by model for data point i

$C_{Ae,i}$ = experimental permeate total solids concentration for data point i

$C_{Ce,i}$ = experimental permeate TOC concentration for data point i

$C_{Cm,i}$ = permeate TOC concentration predicted by model for data point i

$C_{Am,i}$ = permeate total solids concentration predicted by model for data point i

In addition to the requirement that the weighting factors W_{Fi}, W_{Di}, and W_{Ti} must each be less than 1.0, they should logically sum to 1.0 for each point i:

$$W_{Fi} + W_{Di} + W_{Ti} = 1.0$$

The pattern search technique was chosen to effect the minimization of the cost function for several reasons:

1. The method is straightforward and easy to use.
2. The method is relatively insensitive to numerical error; i.e., no partial derivatives are evaluated.
3. The method generally converges to an optimum in a reasonable amount of time.
4. The domain of the search may be easily constrained.
5. The method is fairly well known.

A listing of the pattern search program is presented in reference (9).

Parameters to be Evaluated

Table 2-3 lists the parameters whose values have been obtained by the parameter estimation procedure. The parameters γ, B, and C may only be obtained from the operation of the Ultrafiltration Module itself.

Of the remaining parameters, four (a_A, b_A, c_A and D_{Cx}) are required for the mass transfer relationships and three (α, β, and k_E) are required for the osmotic pressure correlation. It should be possible to develop experimental procedures to evaluate these independently of the UF module test, but in the absence of such experiments, these seven parameters are also evaluated from the UF test data.

Data Requirements

The following data will be required to properly obtain numerical values for the adjustable parameters within the full range of expected operating conditions - including data for pure water.

A. Specifics of Module Configuration and Geometry
    1. Number of 10 foot sections joined together to form one tube (dimensionless)
    2. Number of tubes used in the module (dimensionless)
    3. Inner diameter of tube (m)

B. Operating Test Data
    1. Feed conditions
        a. Inlet volumetric flow rate (m^3/hr)
        b. Inlet total solids concentration (gm/m^3 = mg/l)
        c. Inlet TOC concentration (gm/m^3 = gm/l)
        d. Inlet pressure (atm)
        e. Temperature (°K)

Table 2-3. Ultrafiltration Model Parameters

γ	Membrane pure water permeability coefficient
B	Membrane total solids permeability coefficient
C	Membrane TOC permeability coefficient
a_A	Coefficient in diffusivity relationship for A
b_A	Coefficient in diffusivity relationship for A
c_A	Coefficient in diffusivity relationship for A
D_{Cx}	Diffusivity of TOC in water and dissolved solids
α	Coefficient in osmotic pressure correlation
β	Coefficient in osmotic pressure correlation
k_E	Mass of dissolved solids equivalent to a unit mass of TOC for use in the osmotic pressure correlation

2. Permeate Conditions

   a. Average permeate flux (gm/m^2-hr)

   b. Permeate total solids concentration (gm/m^3 = mg/l)

   c. Permeate TOC concentration (gm/m^3 = mg/l)

   d. Back-pressure on permeate (atm)

3. Other

   a. Pressure at tube outlet (atm)

The required test data is summarized in Figure 2.5.

In addition to the above, test data on the concentrate would be useful but not necessary. The desirable data would be the following:

a. Flow rate of concentrate (m^3/hr)

b. Concentrate total solids concentration (gm/m^3 = mg/l)

c. Concentrate TOC concentration (gm/m^3 = mg/l)

From the feed and permeate data, the concentrate flow rate and concentrations can be calculated by material balances. But when data is available on the concentrate, a material balance can be used to ascertain the consistency of the data.

Additional Relationships

In addition to the osmotic pressure and mass transfer correlations, two other correlations could be included.

First, the density of the fluid could be a function of the concentration. The simplest density-concentration relationship is a linear equation of the following form:

$$\rho = \sum_i \rho_i x_i$$

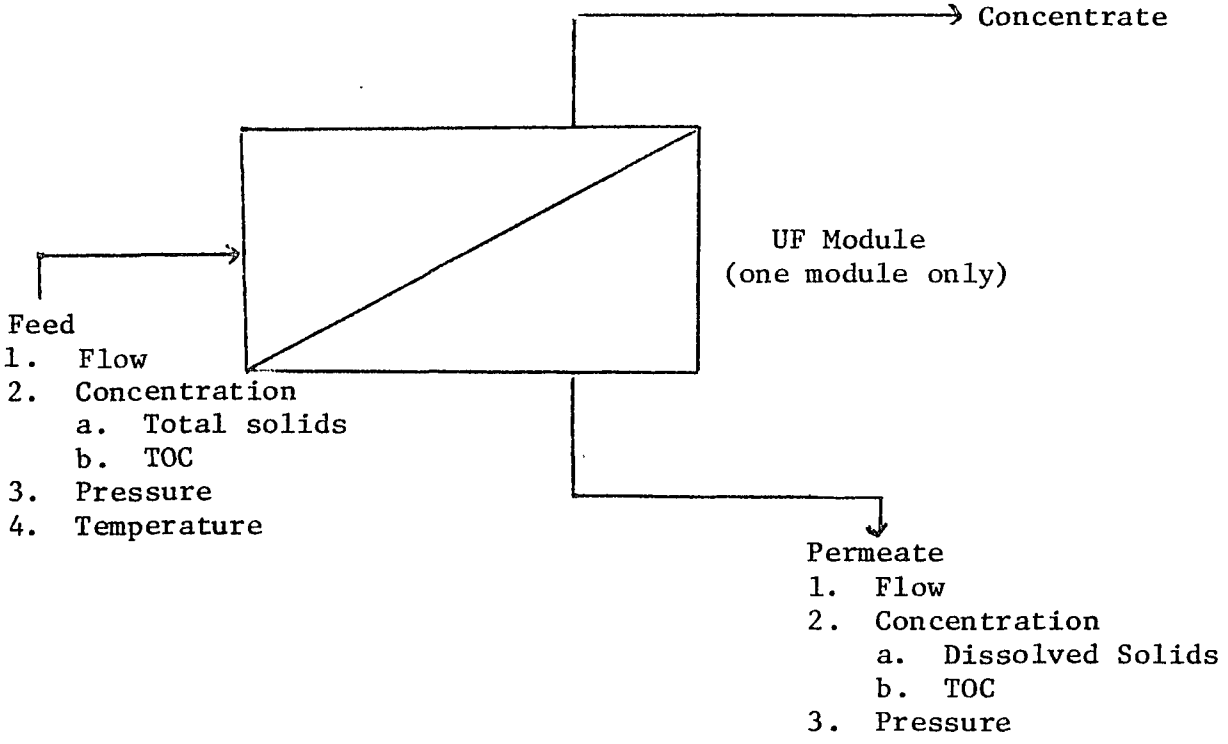

Figure 2.5

Data Requirements for Parameter Fit

where: ρ = fluid density

ρ_i = density of component i

x_i = mass fraction of component i

In this case, mass fractions instead of mole fractions are used because the molecular weight of the contaminant is not known. A temperature dependence could also be included by making the ρ_i's functions of temperature.

Second, the kinematic viscosity could also be a function of concentration and temperature. However, no relationships of this kind have been found necessary.

SUMMARY

This chapter presented the development of the ultrafiltration module model. The model equations for this unit were written and the solution technique employed was described.

The method of evaluating the model parameters from available experimental data was presented.

CHAPTER III

THE REVERSE OSMOSIS SYSTEM MODEL

INTRODUCTION

In this chapter, the development of the reverse osmosis module model from basic material balances is presented, the solution method is outlined, and an analysis of parameter estimation considerations is given.

Listings of the computer programs comprising the model are included in the report, "A Mathematical Model of the Hollow Fiber Reverse Osmosis Unit for Water Re-Use Systems". Examples of program runs along with the results of a parameter sensitivity analysis study are presented in the same report. (6)

DEVELOPMENT OF BASIC EQUATIONS AND METHODS USED

The model equations developed characterize the operation of the Dupont B-10 Reverse Osmosis Separator as illustrated in Figure 3.1. Contaminated water enters via the high pressure feed tube. Flowing in the radial direction, contaminated water becomes progressively more concentrated as water preferentially permeates through the membrane wall into the inner bore of the fibers as illustrated in Figure 3.2. Concentrate is collected at the flow screen and moves axially towards the concentrate outlet. Purified water collected inside the fibers exits the module as permeate.

Using the same justification as in the case of ultrafiltration, the dynamics of the reverse osmosis module are assumed negligible in comparison to associated equipment.

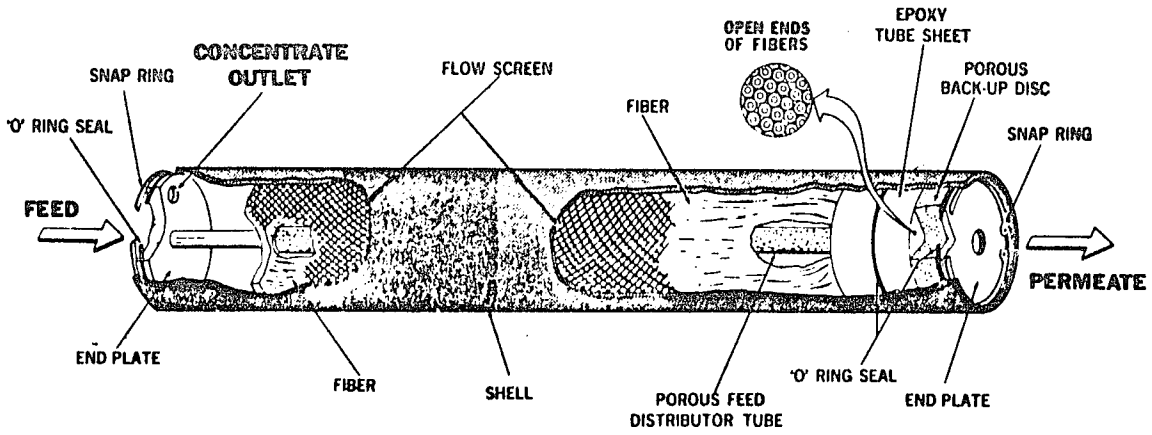

Figure 3-1. Dupont B-10 Reverse Osmosis Separator

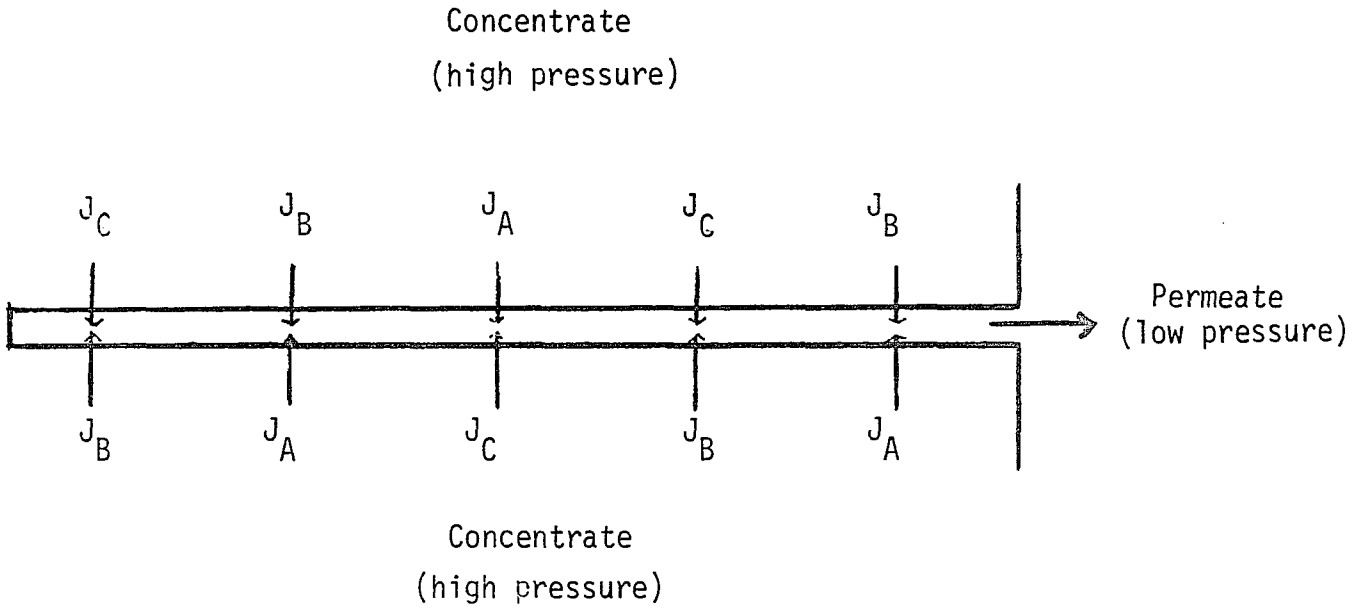

Figure 3.2

Permeation into Inner Bore of Hollow Fibers

Formulation of Equations

To develop the area available for the flux of water and contaminants into the fiber bore, let N_f be the number of perfectly straight, evenly distributed fibers parallel to the axial direction per unit of cross sectional area. Collectively, these idealized fibers would have the same fluxes of water and contaminants as the actual fiber configuration.

Thus the area available for flux is:

Number of fibers per unit area of cross section of the module	x	Outside surface area of one ideal hollow fiber	x	module cross-sectional area under consideration

For the slice of module between r and r + Δr, the area available for flux becomes:

$$(N_f)(\pi D_F L)[\pi(r + \Delta r)^2 - \pi(r)^2]$$

where: D_F is the outside diameter of the fiber (m)

L is the length of the fibers (m)

Dissolved Solids

A steady state material balance on the dissolved solids, component 'A', for the differential element in Figure 3.3 yields:

Input rate of A = Output rate of A

$$(2\pi rL)\ V(r)\ C_A(r) = 2\pi(r + \Delta r)LV(r + \Delta r)\ C_A(r + \Delta r) + J_A(r)(N_f \pi D_F L)[\pi(r + \Delta r)^2 - \pi r^2] \quad (1)$$

where: $V(r)$ = radial velocity of fluid (m/hr)

$C_A(r)$ = concentration of A (gm/m^3)

$J_A(r)$ = flux of A into inner channel of hollow fibers ($gm/hr\text{-}m^2$)

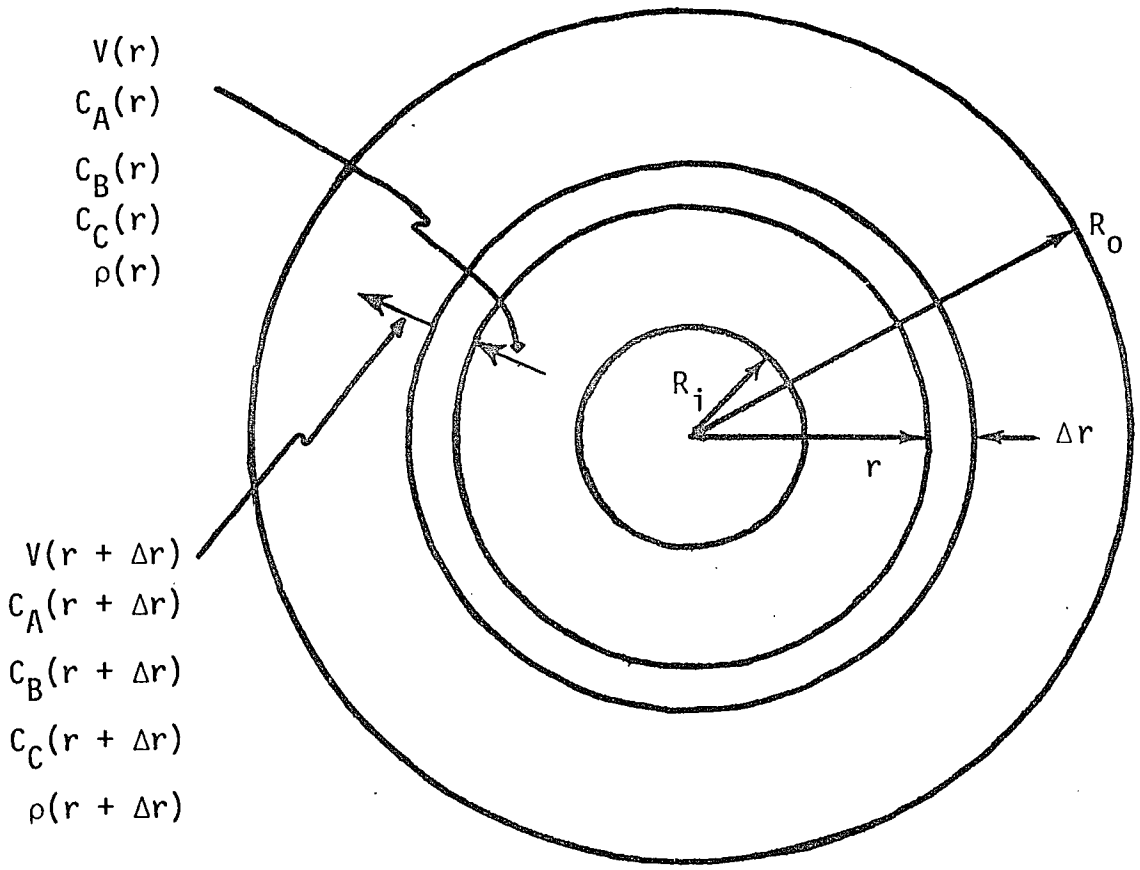

Figure 3.3. Differential element used to derive material balance equations.

TOC (Total Organic Carbon)

A steady state material balance on the TOC, component 'C', for the differential element in Figure 3.3 yields:

Input rate of C = Output rate of C

$$(2\pi rL)V(r)C_C(r) = 2\pi(r + \Delta r)LV(r + \Delta r)C_C(r + \Delta r) + J_C(r)(N_f\pi D_F L)[\pi(r + \Delta r)^2 - \pi r^2] \quad (2)$$

where: $C_C(r)$ = TOC concentration (gm/m^3)

$J_C(r)$ = flux of C into inner channel of hollow fibers ($gm/hr\text{-}m^2$)

Total Material Balance

Similarly, a steady state total material balance on the differential element in Figure 3.3 yields:

Input rate = Output rate

$$(2\pi rL)V(r)\rho(r) = [2\pi(r + \Delta r)L]V(r + \Delta r)\rho(r + \Delta r) + [J_A(r) + J_B(r) + J_C(r)](N_f\pi D_F L)[\pi(r + \Delta r)^2 - \pi r^2] \quad (3)$$

where: $\rho(r)$ = total mass density (gm/m^3)

$J_B(r)$ = flux of water, component B, into the fiber bore ($gm/m^2\text{-}hr$)

In addition, a steady state material balance on component 'B' can be written to obtain an equation analogous to equation (1). However, this equation is not necessary as it becomes a dependent equation when equations (1), (2), and (3) are used in the model.

Analytical Equations

Equations (1), (2), and (3) are readily converted to differential equations by taking the limit as Δr approaches zero. For equation (1), the result is:

$$\frac{d}{dr}[rV(r)C_A(r)] = -N_f\pi D_F rJ_A(r) \quad (4)$$

Equation (3) becomes:

$$\frac{d}{dr}[rV(r)C_C(r)] = -N_f\pi D_F rJ_C(r) \quad (5)$$

Equation (4) becomes:

$$\frac{d}{dr}[rV(r)\rho(r)] = -N_f\pi D_F r[J_A(r) + J_B(r) + J_C(r)] \quad (6)$$

The boundary conditions are as follows:

$$V(R_i) = F_o/(2\pi R_i L)$$

$$C_A(R_i) = C_{Ao}$$

$$C_C(R_i) = C_{Co}$$

where: F_o = Feed rate to module, m^3/hr

C_{Ao} = Inlet concentration of A, gm/m^3

C_{Co} = Inlet TOC concentration, gm/m^3

R_i = Radius of feed distribution tube

Fluxes at the Boundary Layer

To obtain the fluxes J_A, J_B, and J_C, a stagnant boundary layer is imagined to exist near the outer surface of the hollow fibers as shown in Figure 3.4. The following fluxes into and out of the boundary layer are defined:

$$J_A = B(C_{A2} - C_{A3}) \quad (7)$$

$$J_B = \gamma(\Delta P - \Delta\pi) \quad (8)$$

$$J_C = C(C_{C2} - C_{C3}) \quad (9)$$

$$J_{DA} = k_A(C_{A2} - C_{A1}) \quad (10)$$

$$J_{DB} = k_B(C_{B1} - C_{B2}) \quad (11)$$

$$J_{DC} = k_C(C_{C2} - C_{C1}) \quad (12)$$

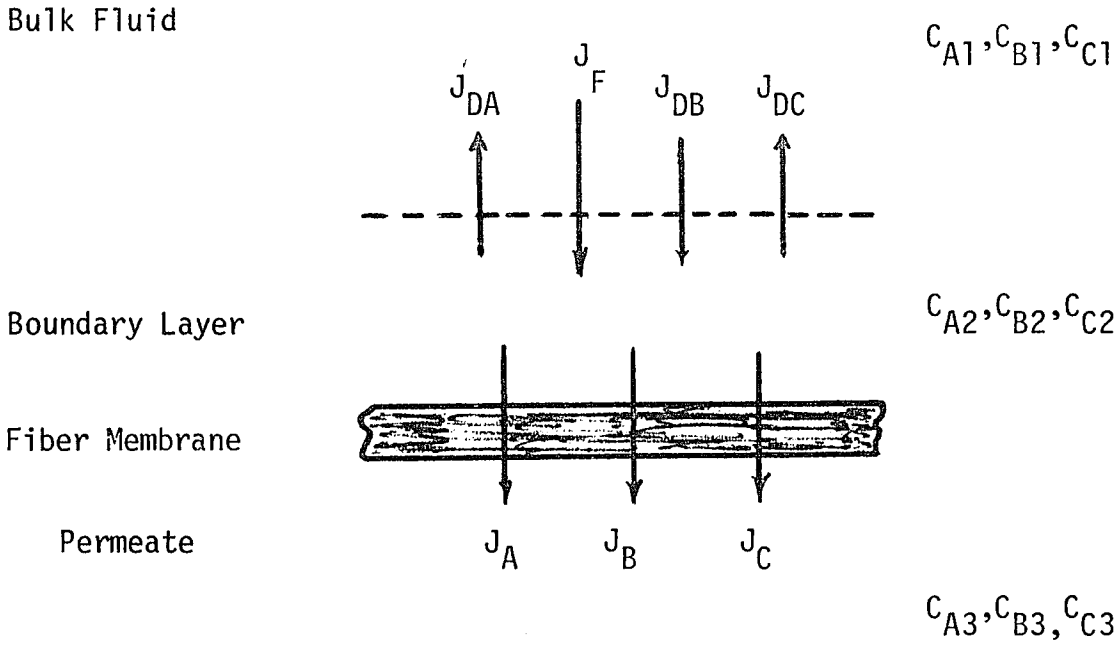

Figure 3.4. Fluxes into and out of boundary layer

where: J_{DA} = diffusional flux of contaminant out of the boundary layer, gm/m^2-hr

J_{DB} = diffusional flux of water into the boundary layer, gm/m^2-hr

J_{DC} = diffusional flux of TOC out of the boundary layer, gm/m^2-hr

C_{A1} = concentration of A in bulk fluid, gm/m^3

C_{A2} = concentration of A in boundary layer, gm/m^3

C_{A3} = concentration of A in permeate, gm/m^3

C_{B1} = concentration of B in bulk fluid, gm/m^3

C_{B2} = concentration of B in boundary layer, gm/m^3

C_{B3} = concentration of B in permeate, gm/m^3

C_{C1} = concentration of C in bulk fluid, gm/m^3

C_{C2} = concentration of C in boundary layer, gm/m^3

C_{C3} = concentration of C in permeate, gm/m^3

γ = permeability coefficient for pure water, gm/m^2-hr-atm

B = permeability coefficient for dissolved solids, m/hr

C = permeability coefficient for TOC, m/hr

ΔP = pressure drop across membrane, atm

$\Delta\pi$ = osmotic pressure difference across membrane = $\pi_2 - \pi_3$, atm

π_2 = osmotic pressure at boundary layer, atm

π_3 = osmotic pressure of permeate, atm

k_A, k_B, k_C = mass transfer coefficients for solids, water, and TOC, respectively, m/hr

The osmotic pressure is related to the concentration of contaminants, C_E, and the absolute temperature, T, by the empirical relationship

$$\pi = f(C_E,T) = \alpha T C_E (1 + \beta C_E)^2 \quad \text{[ref. (3)]} \tag{13}$$

where: α = coefficient, atm-m^3/gm-°K

β = coefficient, m^3/gm

T = absolute temperature, deg Kelvin

C_E = effective contaminant concentration = $C_A + k_E C_C$, gm/m^3

k_E = coefficient expressing the concentration of A equivalent to a unit concentration of C for purposes of osmotic pressure, dimensionless

To obtain $\Delta\pi = \pi_2 - \pi_3$, it is necessary to evaluate π_2 using C_{A2} and C_{C2}; π_3 using C_{A3} and C_{C3}.

The flux J_F due to the bulk flow toward the boundary layer can be obtained by writing a total material balance around the boundary layer:

$$J_F = J_A + J_B + J_C + J_{DA} - J_{DB} + J_{DC} \tag{14}$$

In addition, component balances for component A and for component C can be written:

$$J_F X_{A1} = J_A + J_{DA} \tag{15}$$

$$J_F X_{C1} = J_C + J_{DC} \tag{16}$$

where X_{A1}, X_{C1} = mass fractions of dissolved solids and TOC in the bulk stream, respectively.

A component balance can also be written for component B, but it will not be an independent equation.

In addition, the mass fractions X_{A3} and X_{C3} are related to J_A, J_B, and J_C as follows:

$$X_{A3} = \frac{J_A}{J_A + J_B + J_C} \tag{17}$$

$$X_{C3} = \frac{J_C}{J_A + J_B + J_C} \tag{18}$$

The complete set of equations describing the fluxes at the boundary layer is reproduced in Table 3-1.

Effect of Flow Velocity on Mass Transfer Coefficients

Harriott and Hamilton (2) give the following relationship for tubular ultrafiltration modules:

$$N_{Sh} = 0.0096 N_{Re}^{0.913} N_{Sc}^{0.346} \quad (19)$$

where: $N_{Sh} = \frac{kD}{D_x}$ = Sherwood number

$N_{Re} = \frac{DV}{\nu}$ = Reynolds number

$N_{Sc} = \frac{\nu}{D_x}$ = Schmidt number

where: k = mass transfer coefficient, m/hr

ν = kinematic viscosity, m^2/hr

D_x = diffusivity, m^2/hr

D = characteristic length, m

V = velocity, m/hr

A similar modified relationship is postulated to exist for RO modules.

First, the Reynolds number must be computed for flow across a tube bank instead of for flow inside a tube. For heat exchanger bundles, the Reynolds number is normally computed as follows (7):

$$N_{Re} = \frac{D_o W}{\mu S_m} \quad (20)$$

where: W = mass flow rate, gm/hr

D_o = outside diameter of tubes, m

μ = viscosity, gm/m-hr

S_m = area available for flow, m^2

Table 3-1. Nonlinear Equations for Fluxes at Boundary Layer

Transport Equations

$$J_A = B(C_{A2} - C_{A3})$$

$$J_B = \gamma(\Delta P - \Delta\pi)$$

$$J_C = C(C_{C2} - C_{C3})$$

$$J_{DA} = k_A(C_{A2} - C_{A1})$$

$$J_{DB} = k_B(C_{B1} - C_{B2})$$

$$J_{DC} = k_C(C_{C2} - C_{C1})$$

Osmotic Pressure Relationships

$$\Delta\pi = \pi_2 - \pi_3$$

$$\pi_2 = \alpha T C_{E2}(1 + \beta C_{E2})^2$$

$$\pi_3 = \alpha T C_{E3}(1 + \beta C_{E3})^2$$

$$C_{E2} = C_{A2} + k_E C_{C2}$$

$$C_{E3} = C_{A3} + k_E C_{C3}$$

Material Balances at Boundary Layer

$$J = J_A + J_B + J_C + J_{DA} - J_{DB} + J_{DC}$$

$$J_F X_{A1} = J_A + J_{DA}$$

$$J_F X_{C1} = J_C + J_{DC}$$

$$X_{A3} = \frac{J_A}{J_A + J_B + J_C}$$

$$X_{C3} = \frac{J_C}{J_A + J_B + J_C}$$

Mass Fraction/Density/Concentration Relationships

$$X_{B2} = 1 - X_{A2} - X_{C2} \qquad X_{B3} = 1 - X_{A3} - X_{C3}$$

$$\rho_2 = \rho_A X_{A2} + \rho_B X_{B2} + \rho_C X_{C2} \qquad \rho_3 = \rho_A X_{A3} + \rho_B X_{B3} + \rho_C X_{C3}$$

$$C_{A2} = \rho_2 X_{A2} \qquad C_{A3} = \rho_3 X_{A3}$$

$$C_{B2} = \rho_2 X_{B2} \qquad C_{B3} = \rho_3 X_{B3}$$

$$C_{C2} = \rho_2 X_{C2} \qquad C_{C3} = \rho_3 X_{C3}$$

In determining S_m, the space occupied by the tubes must be accounted for.

For the RO module, the total area of radius r would be $2\pi rL$, from which the area taken up by the fibers must be subtracted. Assuming a uniform fiber density, the fibers would occupy some fraction, say f_F, of the total area. Thus, the net area for flow would be $2\pi rL(1-f_F)$. The Reynolds number becomes

$$N_{Re} = \frac{D_o W}{\mu(2\pi rL(1-f_F))} = \frac{D_o V}{\nu(1-f_F)} \tag{21}$$

Of course, with these considerations, one would not expect the exponent of 0.913 for the Reynolds number nor the coefficient 0.0096 to be valid for RO. Thus, the following relationship will be used:

$$\frac{kD_o}{D_x} = c_1 \left(\frac{D_o V}{\nu(1-f_F)}\right)^{e_1} \left(\frac{\nu}{D_x}\right)^{e_2} \tag{22}$$

where c_1, e_1 and e_2 must be evaluated from experimental data.

To use Equation (22) directly, five parameters would have to be evaluated from test data:

$$c_1,\ e_1,\ e_2,\ D_x \text{ and } f_F$$

As presently being collected, the RO test data does not permit D_x, f_F, c_1 and e_2 to be evaluated independently, since the equation can be written as follows:

$$k = \left(\frac{c_1 D_x^{1-e_2} \nu^{e_2}}{D_o(1-f_F)^{e_2}}\right) (N'_{Re})^{e_1} = C_1 (N'_{Re})^{e_1} \tag{23}$$

where $N'_{Re} = \frac{D_o V}{\nu}$

The same values for the exponent e_1 will be used for both components, but different values will be used for C_1.

Approximations in the Flux Equations

In the reverse osmosis unit, the concentrations of dissolved solids and TOC will be relatively small. Furthermore, the RO membrane will tend to reject these components. For these reasons, the following assumptions will be made:

1. The membrane permeability fluxes J_A and J_C are small compared to J_B.
2. The diffusional fluxes J_{DA}, J_{DB}, and J_{DC} are small compared to J_B.
3. The density is that of water, namely ρ_B.

Table 3-2 presents the equations from 3-1 with these approximations included.

Solution Method

The solution method basically consists of numerically integrating the differential equations (4), (5), and (6) resulting from the total and component material balances. However, this is somewhat complicated by the fact that the fluxes must be determined at each increment by solving the set of nonlinear equations summarized in Table 3-2.

Difference Equations

The numerical solution of the differential equations is effected by discretizing in the r-direction using an increment Δr. Therefore, let

$$r_i = R_i + i\Delta r$$

The discrete versions of equations (4), (5), and (6) are the following difference formulations (constant density is assumed).

Table 3-2. Simplified Equations for Fluxes at the Boundary Layer

Transport Equations

$$J_A = B(C_{A2} - C_{A3})$$

$$J_B = \gamma(\Delta P - \Delta\pi)$$

$$J_C = C(C_{C2} - C_{C3})$$

$$J_{DA} = k_A(C_{A2} - C_{A1})$$

$$J_{DB} = k_B(C_{B1} - C_{B2})$$

$$J_{DC} \quad k_C(C_{C2} - C_{C1})$$

Osmotic Pressure Relationships

$$\Delta\pi = \pi_2 - \pi_3$$

$$\pi_2 = \alpha T C_{E2}(1 + \beta C_{E2})^2$$

$$\pi_3 = \alpha T C_{E3}(1 + \beta C_{E3})^2$$

$$C_{E2} = C_{A2} + k_E C_{C2}$$

$$C_{E3} = C_{A3} + k_E C_{C3}$$

Material Balance at Boundary Layer

$$J_F = J_B$$

$$J_F X_{A1} = J_A + J_{DA}$$

$$J_F X_{C1} = J_C + J_{DC}$$

$$X_{A3} = \frac{J_A}{J_B}$$

$$X_{C3} = \frac{J_C}{J_B}$$

Mass Fraction/Density/Concentration Relationships

$$X_{B2} = 1 - X_{A2} - X_{C2} \qquad X_{B3} = 1 - X_{A3} - X_{C3}$$

$$C_{A2} = \rho X_{A2} \qquad C_{A3} = \rho X_{A3}$$

$$C_{B2} = \rho X_{B2} \qquad C_{B3} = \rho X_{B_3}$$

$$C_{C2} = \rho X_{C2} \qquad C_{C3} = \rho X_{C3}$$

$$\rho = \rho_B$$

$$r_i V(r_i) C_A(r_i) = r_{i-1} V(r_{i-1}) C_A(r_{i-1}) - N_f \pi D_F r_i J_A(r_{i-1}) \Delta r \quad (24)$$

$$r_i V(r_i) C_C(r_i) = r_{i-1} V(r_{i-1}) C_C(r_{i-1}) - N_f \pi D_F r_i J_C(r_{i-1}) \Delta r \quad (25)$$

$$\rho r_i V(r_i) = \rho r_{i-1} V(r_{i-1}) - N_f \pi D_F r_i [J_A(r_{i-1}) + J_B(r_{i-1}) + J_C(r_{i-1})] \Delta r \quad (26)$$

A similar set of equations is obtained by simply re-writing equations (1), (2), and (3) derived from the differential elements (let $r_i = r + \Delta r$ and $r_{i-1} = r$):

$$2\pi r_i L V(r_i) C_A(r_i) = 2\pi r_{i-1} L V(r_{i-1}) C_A(r_{i-1}) - J_A(r_{i-1}) N_f \pi D_F L [\pi r_i^2 - \pi r_{i-1}^2] \quad (27)$$

$$2\pi r_i L V(r_i) C_C(r_i) = 2\pi r_{i-1} L V(r_{i-1}) C_A(r_{i-1}) - J_C(r_{i-1}) N_f \pi D_F L] \pi r_i^2 - \pi r_{i-1}^2] \quad (28)$$

$$2\pi r_i L \rho V(r_i) = 2\pi r_{i-1} L \rho V(r_{i-1}) - [J_A(r_{i-1}) + J_B(r_{i-1}) + J_C(r_{i-1})] N_f \pi D_F L [\pi r_{i-1}^2 - \pi r_{i-1}^2] \quad (29)$$

Using the approximation $\pi r_i^2 - \pi r_{i-1}^2 \approx 2\pi r_i \Delta r$, equations (27), (28), and (29) would reduce to equations (24), (25), and (26). However, equations (27), (28), and (29) will be used to generate the numerical solution.

The boundary conditions are:

$$V(R_i) = F_o/(2\pi R_i L)$$

$$C_A(R_i) = C_{Ao}$$

$$C_C(R_i) = C_{Co}$$

Figure 3.5 illustrates the procedure followed for each value of i from 1 to N, where $N = (R_o - R_i)/\Delta r$ is the number of increments required. (R_o is the outer radius of the fiber bundle.)

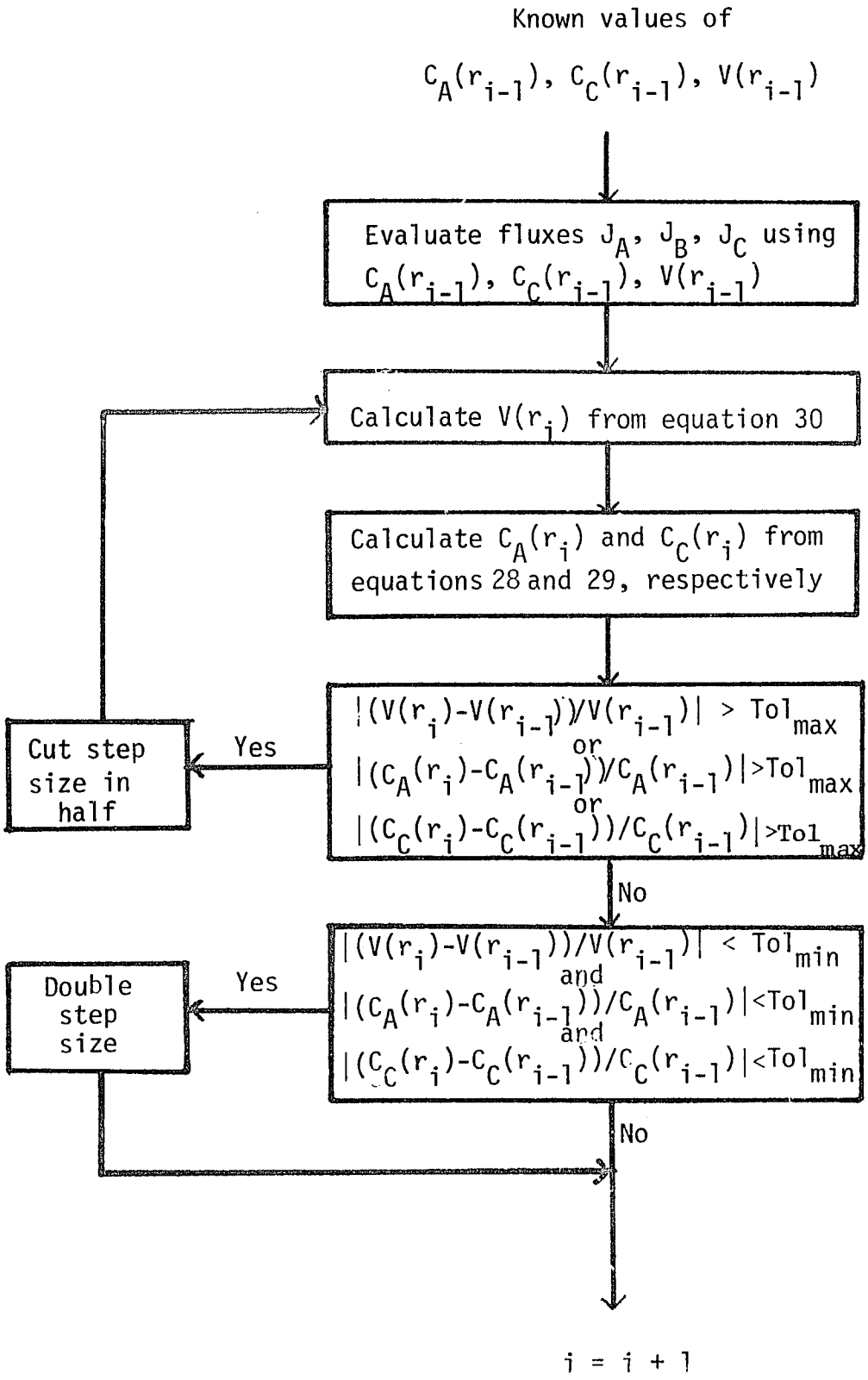

Figure 3.5

Numerical Integration Procedure

Algebraic Equations for Fluxes

Block 1 of the procedure in Figure 3.5 requires the computation of J_A, J_B, and J_C at r_i using the values of $V(r_{i-1})$, $C_A(r_{i-1})$, and $C_C(r_{i-1})$ that are presently available. This requires the solution of the set of equations in Table 3-2. As illustrated in Figure 3.6, this entails two nested iteration loops.

For both loops, the interval halving method is used. Various back-substitution methods were tried, but without success. (See Appendix A of reference (6)). The equations proved to be highly nonlinear, and with varying degrees of sensitivity. Consequently, the reliability of the interval halving method had to take precedence over computational efficiency.

For the first or outer iteration loop, a value of C_{A2} must be estimated. It is known that $C_{A1} \leq C_{A2} \leq \rho$, which permits interval halving to be utilized.

However, knowing the value of C_{A2} only permits J_{DA} to be calculated. To proceed further, a value is assumed for C_{A3}, which must be in the interval $0 \leq C_{A3} \leq C_{A1}$. This permits J_B to be readily calculated as follows:

$$J_B = k_A \rho \left(\frac{C_{A2}}{C_{A3}} - 1.0\right), \tag{30}$$

by combining the following three equations:

$$X_{A3} = J_A/J_B$$

$$C_{A3} = \rho X_{A3}$$

and $$J_A = k_A(C_{A2} - C_{A3}).$$

The key to the procedure is that C_{C2} and C_{C3} can be calculated from J_B. The equation

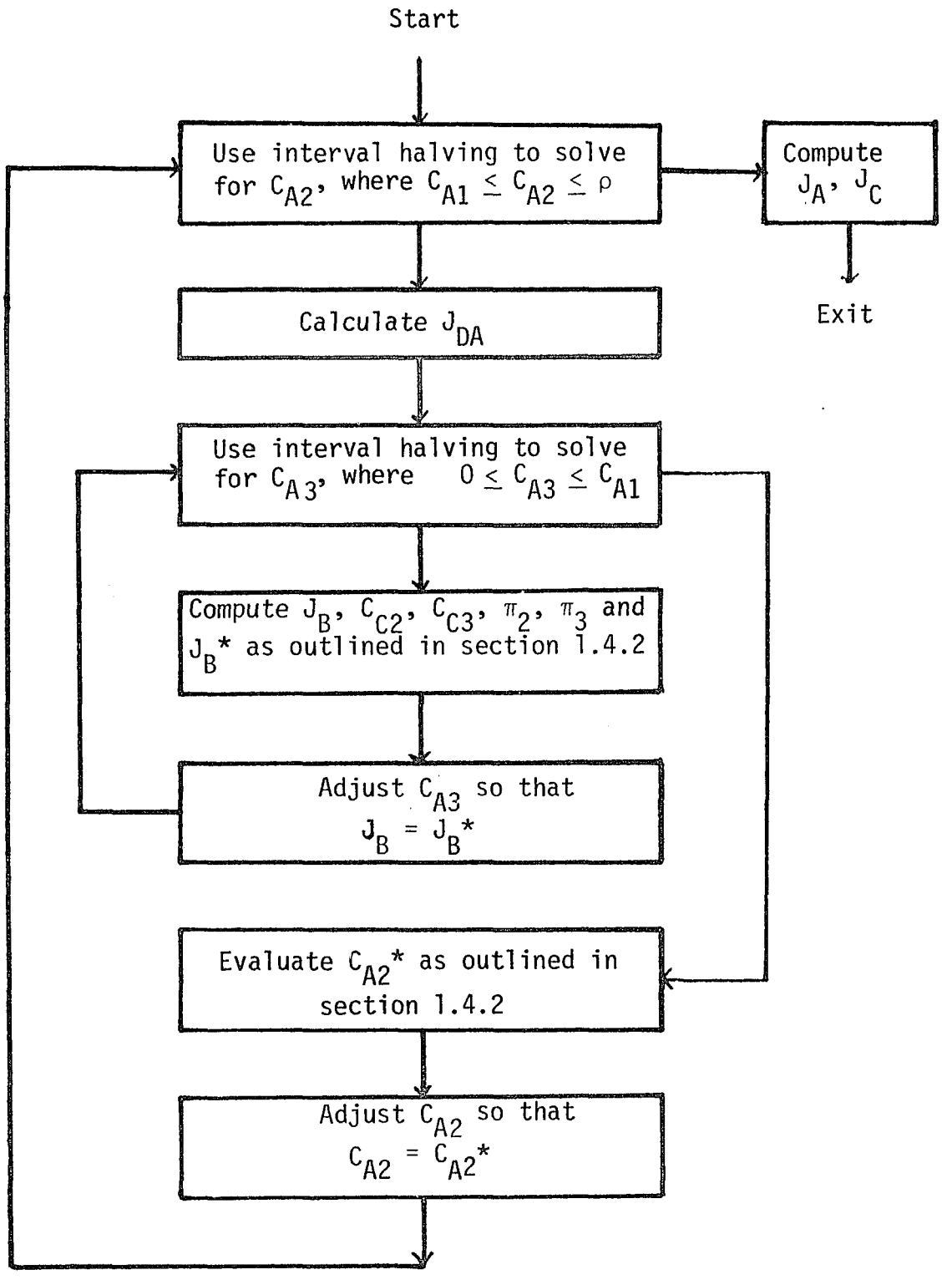

Figure 3.7

Computation of the Fluxes

$$J_B X_{C1} = J_C + J_{DC}$$

can be written as

$$J_B X_{C1} = C(C_{C2} - C_{C3}) + k_C(C_{C2} - C_{C1}) \tag{31}$$

Furthermore, the equation

$$X_{C3} = \frac{J_C}{J_B}$$

can be written as

$$\frac{C_{C3}}{\rho} = \frac{C(C_{C2} - C_{C3})}{J_B} \tag{32}$$

which can be solved for C_{C3}:

$$C_{C3} = \frac{C \cdot C_{C2}}{J_B/\rho + C} \tag{33}$$

The expression for C_{C3} can be substituted into equation (31) to obtain

$$J_B X_{C1} = C(C_{C2} - \frac{C \cdot C_{C2}}{J_B/\rho + C}) + k_C(C_{C2} - C_{C1}) \tag{34}$$

or

$$C_{C2} = \frac{J_B X_{C1} + k_C C_{C1}}{k_C + C\,(\frac{J_B/\rho}{J_B/\rho + C})} \tag{35}$$

Now that C_{C2} is known, C_{C3} can be computed using equation (33).

Now that values are available for C_{A2}, C_{C2}, C_{A3}, and C_{C3}, the osmotic pressures π_1 and π_2 can be computed, and then J_B^* can be evaluated using

$$\Delta\pi = \pi_2 - \pi_3$$

and $J_B^* = (\Delta P - \Delta\pi)$.

If the values of J_B and J_B^* do not agree, the value of C_{A3} must be changed. Using the interval halving technique, the interval of uncertainty for C_{A3} is reduced and the computations repeated.

Once a value of C_{A3} is obtained that gives the same value for J_B and J_B^*, the assumption for C_{A2} must be checked. Since values are available for J_B, J_A, and J_{DA}, we can compute C_{A2}^* as follows:

$$J_B X_{A1} = k_A(C_{A2}^* - C_{A1}) + B(C_{A2}^* - C_{A3})$$

rewritten as

$$C_{A2}^* = \frac{J_B X_{A1} + k_A C_{A1} + B C_{A3}}{k_A + B}$$

If C_{A2}^* is not equal to C_{A2}, a new value for C_{A2} must be assumed. The interval halving logic permits the interval of uncertainty for C_{A2} to be reduced and the calculations repeated.

Using this procedure, the nonlinear flux equations are solved for each integration step.

The solution method flow charted in Figure 3.5 was chosen to insure numerical accuracy and to reduce the computational effort required whenever possible. For values of r near R_i, the radial velocity gradient is steep, and a small step size is required. At values of r near R_o, the magnitude of the radial velocity gradient is much smaller, and a larger step size may be used. (See Figure 3.7).

An added advantage of this solution method is that even if the step size must be reduced, the solution to the flux equations - which requires the major portion of total computation time - is not recomputed.

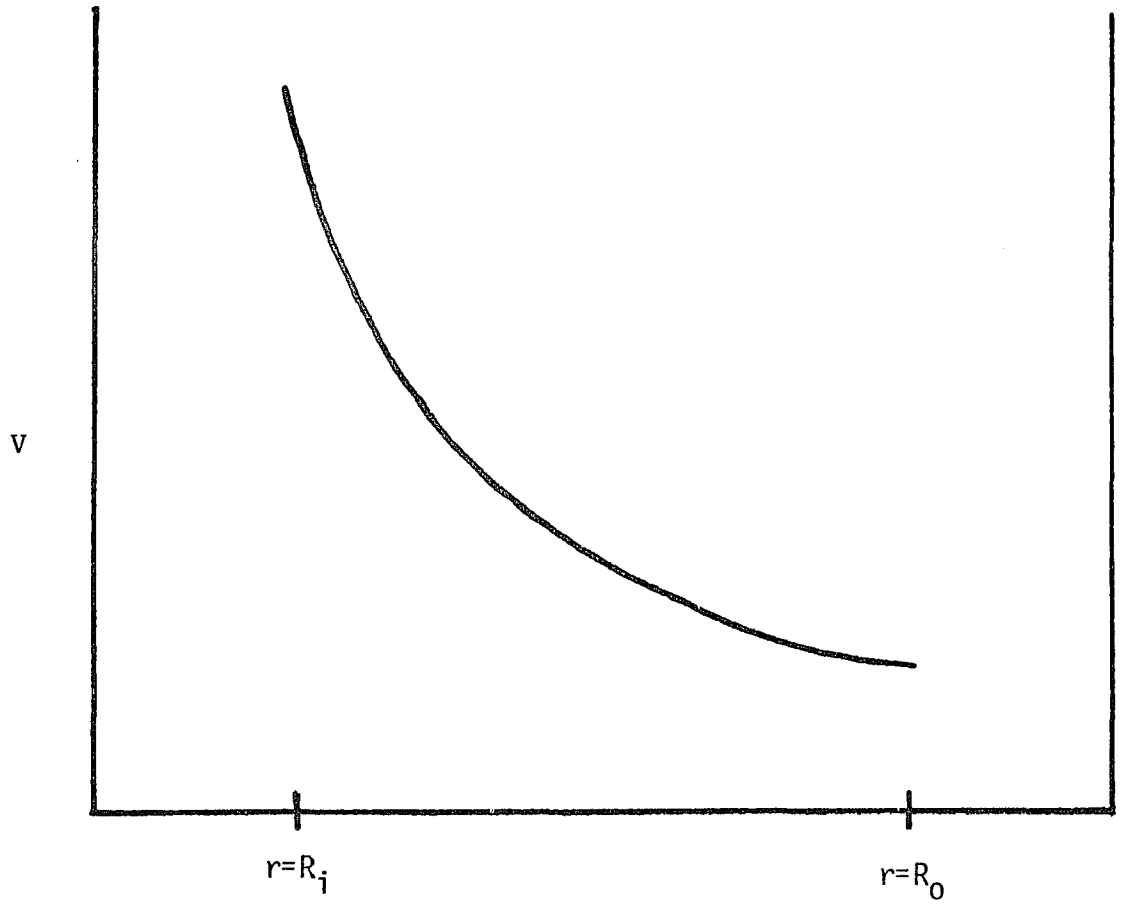

Figure 3.7

Expected Radial Velocity Profile

PARAMETER ESTIMATION CONSIDERATIONS

Values of several key variables, such as mass transfer coefficients and osmotic pressure correlation coefficients, must be determined for use within the model.

To estimate these values, the Pattern Search strategy discussed in reference (8), is again used to minimize a cost function which penalizes for model deviations from experimental results.

Cost Function

The cost function used in this study is the sum of weighted relative squared differences between the model and experimental data. The following items are compared in the evaluation:

1. Permeate flow rate
2. Permeate solids concentration
3. Concentration of total organic carbon in the permeate

The algebraic formulation of the cost function is given below:

$$COST = \sum_{i=1}^{n} z_i \left[W_{Fi} \left(\frac{F_{e,i} - F_{m,i}}{F_{e,i}} \right)^2 + W_{Di} \left(\frac{C_{Ae,i} - C_{Am,i}}{C_{Ae,i}} \right)^2 + W_{Ti} \left(\frac{C_{Ce,i} - C_{Cm,i}}{C_{Ce,i}} \right)^2 \right]$$

where: COST = cost function to be minimized

i = data point identifier

n = number of data points

z_i = weighting factor of point i relative to other data points

W_{Fi} = weighting factor for permeate flow for data point i ($0 \leq W_{Fi} \leq 1$)

W_{Di} = weighting factor for dissolved solids concentration for data point i ($0 \leq W_{Di} \leq 1$)

W_{Ti} = weighting factor for TOC concentration for data point i ($0 \leq W_{Ti} \leq 1$)

$F_{e,i}$ = experimental value of permeate flux for data point i

$F_{m,i}$ = permeate flow predicted by model for data point i

$C_{Ae,i}$ = experimental permeate dissolved solids concentration for data point i

$C_{Ce,i}$ = experimental permeate TOC concentration for data point i

$C_{Cm,i}$ = permeate TOC concentration predicted by model for data point i

$C_{Am,i}$ = permeate dissolved solids concentration predicted by model for data point i

In addition to the requirement that the weighting factors W_{Fi}, W_{Di}, and W_{Ti} must each be less than 1.0, they should logically sum to 1.0 for each point i:

$$W_{Fi} + W_{Di} + W_{Ti} = 1.0$$

Parameters to be Evaluated

Table 3.3 lists the parameters whose values have been obtained by the parameter estimation procedure. The parameters N_f, γ, B, and C may only be obtained from the operation of the RO module itself.

Of the remaining parameters, three of these (C_{1A}, C_{1C}, and e_1) are required for the mass transfer relationships and three (α, β, and k_E) are required for the osmotic pressure relationship. It should be possible to develop experimental procedures to evaluate these independently of the RO module test, but in the absence of these independent experiments, these six parameters are also evaluated from the RO test data.

Table 3-3. Reverse Osmosis Model Parameters

N_f	Number of ideal fibers per unit cross-sectional area of the fiber bundle
γ	Permeability coefficient for pure water
B	Permeability coefficient for dissolved solids
C	Permeability coefficient for TOC
e_1	Exponent of Reynolds number in mass transfer correlation
α	Coefficient in osmotic pressure correlation
β	Coefficient in osmotic pressure correlation
k_E	Mass of dissolved solids equivalent to a unit mass of TOC for use in the osmotic pressure correlation
C_{1A}	Coefficient in mass transfer correlation for A
C_{1C}	Coefficient in mass transfer correlation for C

Data Requirements

The following data will be required to properly obtain numerical values for the adjustable parameters within the full range of expected operating conditions - including data for pure water.

A. Specifics of Module Configuration and Geometry

1. Length of fiber containing section of module (m)
2. Inner diameter of module (m)
3. Outer diameter of feed distribution pipe (m)
4. Outer diameter of hollow fibers (m)

B. Operating Test Data

1. Feed conditions
   a. Inlet volumetric flow rate (m^3/hr)
   b. Inlet dissolved solids concentration (gm/m^3 = mg/l)
   c. Inlet TOC concentration (gm/m^3 = mg/l)
   d. Inlet pressure (atm)
   e. Temperature (°K)
2. Permeate Conditions
   a. Flow rate of permeate (m^3/hr)
   b. Permeate solids concentration (gm/m^3 = mg/l)
   c. Permeate TOC concentration (gm/m^3 = mg/l)
   d. Back-pressure on permeate (atm)

The required test data is summarized in Figure 3.8.

In addition to the above, test data on the concentrate would be useful but not necessary. The desirable data would be the following:

a. Flow rate of concentrate (m^3/hr)
b. Concentrate dissolved solids concentration (gm/m^3 = mg/l)

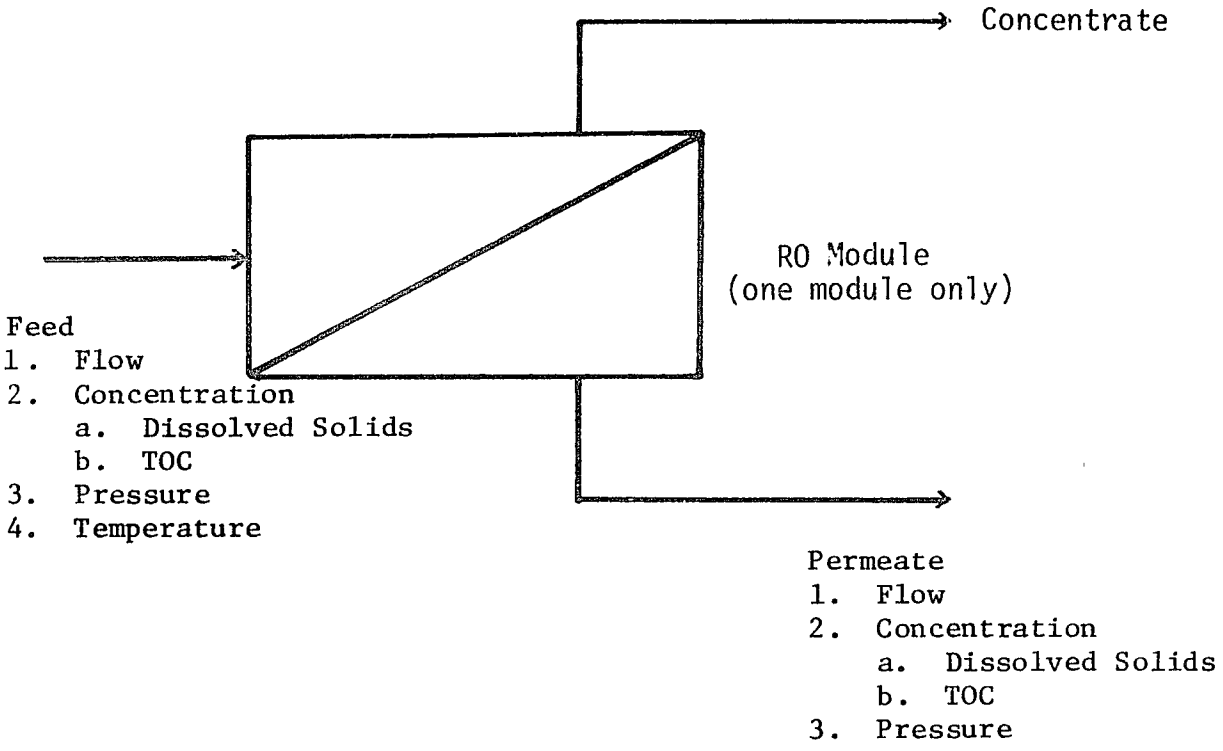

Figure 3.8

Data Requirements for Parameter Fit

c. Concentrate TOC concentration (gm/m^3 = mg/l)

d. Back-pressure on concentrate (atm)

From the feed and permeate data, the concentrate flow rate and concentration can be calculated by material balances. But when data is available on the concentrate, a material balance can be used to ascertain the consistency of the data.

In the absence of back-pressure data on the concentrate, it must be assumed that the pressure drop from feed to concentrate is small, which seems reasonable at low flow rates. On the other hand, the interpretation of pressure drop data raises the question as to which of the following is the major contributor to the pressure drop:

1. Feed distribution
2. Flow across the fibers
3. Concentrate outlet flow screen

For best performance of the unit, any major pressure drop is hopefully not caused by the first two.

Additional Relationships

In addition to the osmotic pressure and mass transfer correlations, two other correlations could be included.

First, the density of the fluid could be a function of the concentration. The simplest density-concentration relationship is a linear equation of the following form:

$$\rho = \Sigma \rho_i x_i$$

where: ρ = fluid density

ρ_i = density of component i

x_i = mass fraction of component i

In this case, mass fractions instead of mole fractions are used because the molecular weight of the contaminant is not known. A temperature dependence could also be included by making the ρ_i's functions of temperature.

Second, the kinematic viscosity could also be a function of concentration and temperature. However, no relationships of this kind have been found necessary.

SUMMARY

This chapter presented the development of the reverse osmosis module model. The model equations for this unit were written and discussed. The solution technique employed to solve these equations was described. The method of evaluating the model parameters from available experimental data was presented.

CHAPTER IV

THE OZONATION CONTACTING SYSTEM MODEL

INTRODUCTION

In this chapter, the development of the ozonation contacting system model from basic equations is presented, the solution method is outlined and an analysis of parameter estimation considerations is given.

Listings of the computer programs comprising the model are included in the report, "A Mathematical Model of an Ozonation Contacting Unit for Water Re-Use Systems". Examples of program runs along with the results of a parameter sensitivity analysis study are presented in the same report. (8)

DEVELOPMENT OF BASIC EQUATIONS AND METHODS USED

The ozone contactor chosen for post Reverse Osmosis treatment varies slightly from the design by Alfred Torricelli (10) shown in Figure 4.1. The purpose of the contactor is to oxidize organic compounds to carbon dioxide using gaseous ozone.

During normal operation, contaminated water enters the pre-contactor, flows sequentially through each of six stages, and exits as purified water. Ozone dispersed in a carrier gas (usually air) is sparged through each of the stages, collected at the head space above each stage, and sparged through the pre-contactor.

This flow path for the gas results in a high utilization of ozone. This is particularly important since the power requirements for ozone generation are usually high.

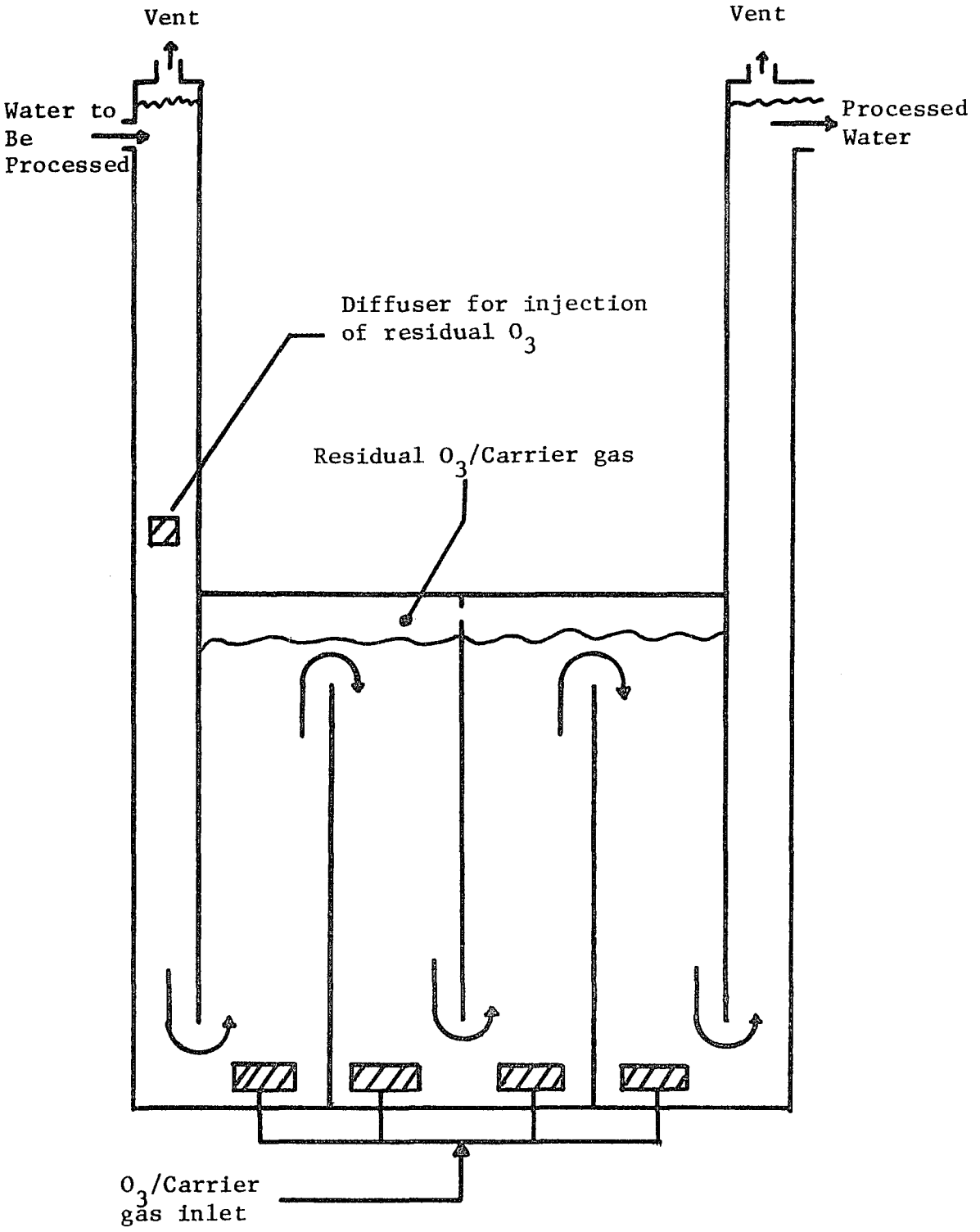

Figure 4.1. Torricelli Ozone Contactor Schematic

Turbulence produced by the bubbles of gas swirling upward through the column of liquid and the significant liquid residence time cause the aqueous phase of each stage to approach the perfectly mixed state. The bubbles are assumed to be of uniform size and shape, and each is considered to maintain a uniform velocity through the contactor. These assumptions have been used by others (9).

Mass Transfer of Ozone from Gas to Liquid Phase

A steady state material balance on ozone between x and x + Δx for the gas phase of the contactor stage shown in Figure 4.2 gives:

Input = Output

$$G(t)Z(x,t) = G(t)Z(x + \Delta x,t) + (k_L a)(A\Delta x)(C_Z^*(x,t) - C_Z(t)) \quad (1)$$

where: A = cross sectional area of cylinder, m^2

k_L = liquid phase mass transfer coefficient, m/hr

a = interfacial area of bubbles per unit of liquid volume, m^2/m^3

G(t) = flow rate of ozone-free gas, Kgm-moles/hr

$C_Z(t)$ = liquid phase concentration of ozone, Kgm-moles/m^3

$C_Z^*(x,t)$ = liquid phase concentration of ozone in equilibrium with Z(x,t), Kgm-moles/m^3

Z(x,t) = moles ozone/mole ozone-free gas

x = axial coordinate, m

t = time, hr

A form of Henry's Law, equation (2), is used to relate the equilibrium liquid and gas phase concentrations of ozone.

$$y_{O_3}^* = K_H x_{O_3}^* \quad (2)$$

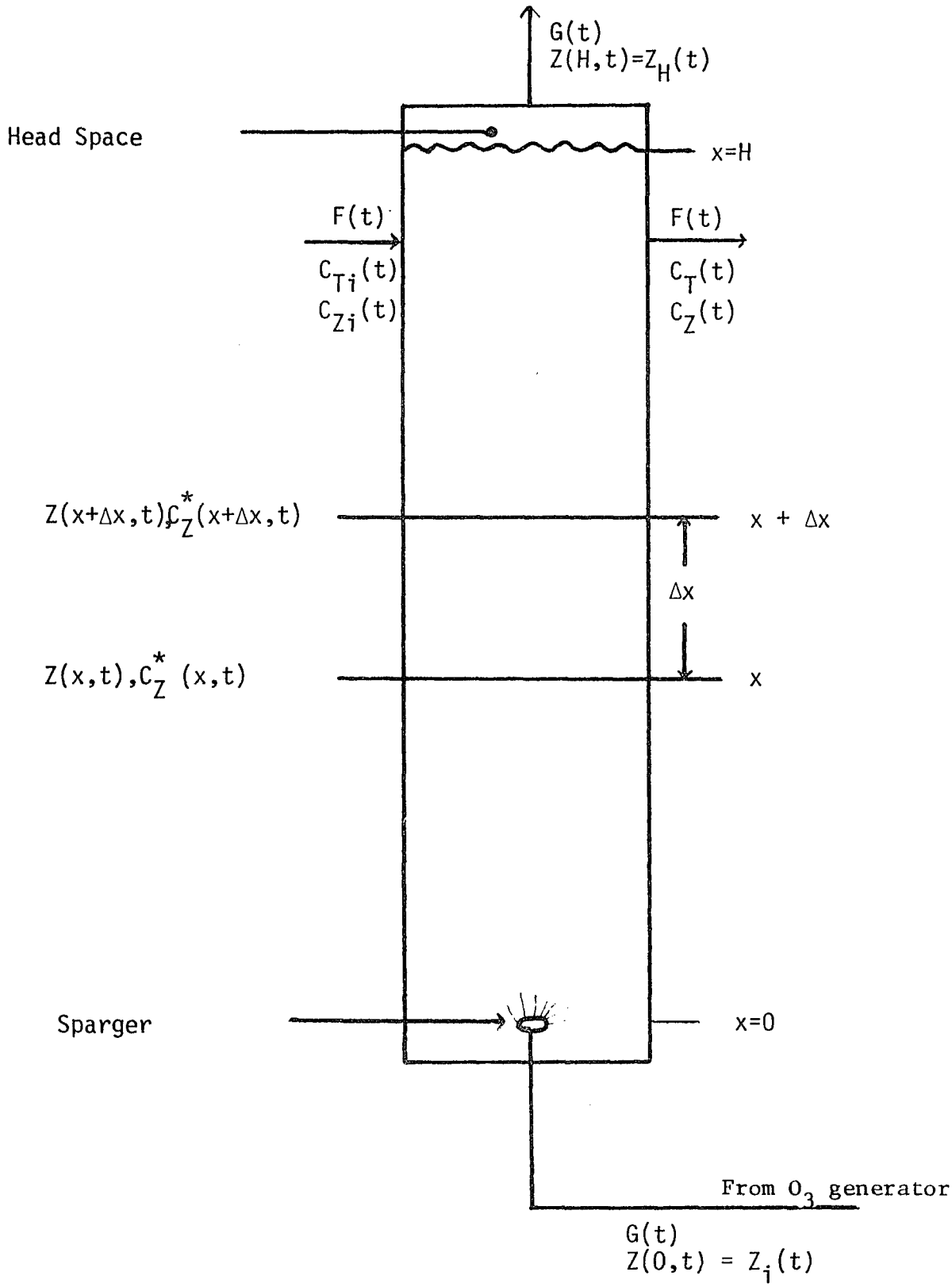

Figure 4.2

Contactor Stage
(UV Lamps Not Shown)

where: $y^*_{O_3}$ = equilibrium gas phase mole fraction of ozone

$x^*_{O_3}$ = equilibrium liquid phase mole fraction of ozone

K_H = Henry's Law constant

It is easily shown that:

$$y_{O_3} = Z/(1 + Z)$$

where: y_{O_3} = any gas phase mole fraction of ozone.

Z = any gas phase mole fraction of ozone expressed as moles of ozone per mole of ozone free gas.

Also:

$$C_Z^* = \rho_L x^*_{O_3} \tag{4}$$

where: ρ_L = molar liquid density, Kgm-moles/m^3

Combining equations (2), (3), and (4) gives:

$$C_Z^*(x,t) = \left(\frac{Z(x,t)}{1 + Z(x,t)}\right)\left(\frac{\rho_L}{K_H}\right) \tag{5}$$

Substituting this result into the material balance equation (1) gives:

$$G(t)Z(x,t) - G(t)Z(x + \Delta x,t) = (k_L a)(A\Delta x)\left[\frac{Z(x,t)}{1+Z(x,t)}\left(\frac{\rho_L}{K_H}\right) - C_Z(t)\right] \tag{6}$$

Dividing by Δx and taking the limit as Δx goes to zero produces:

$$G(t)\frac{\partial Z(x,t)}{\partial x} = -(k_L a)A\left[\left(\frac{Z(x,t)}{1 + Z(x,t)}\right)\left(\frac{\rho_L}{K_H}\right) - C_Z(t)\right] \tag{7}$$

The boundary conditions are as follows:

$Z(0,t) = Z_i(t)$

$G(t) = G_i(t)$ (assumption resulting from very short gas holding time)

$Z(x,0)$ is known (usually zero)

where: $Z_i(t)$ = inlet concentration of ozone in gas phase

$G_i(t)$ = inlet gas flow rate

Note that if $Z_i(t)$ is small,

$$\frac{Z(x,t)}{1 + Z(x,t)} \approx Z(x,t).$$

The relationship between $k_L a$ and x is the subject of some dispute among various researchers. Yoshida and Akita (9) report that the mass transfer coefficient is independent of position in the contacting columns. However, Eckenfelder (9) and Aiba (9) conclude that $k_L a$ may be correlated as:

$$k_L a = \frac{QG_o^M (H-x)^P}{V}$$

where: Q = constant

G_o = volumetric gas flow rate

M = exponent of G_o

P = exponent of the submergence depth, (H-x), H = height

V is not defined.

Note that this correlation also provides a basis for determining the effect of changes in gas flow rate upon the mass transfer of ozone.

From the small amounts of ozone transferred and from the very short residence time of the gas as compared to that of the water it is assumed that the effect of any change in Z(x=0) has an immediate impact upon Z(x=H). Thus:

$$G(t) \frac{dZ(x)}{dx} = -(k_L a)(A)\left[\frac{Z(x)\rho_L}{K_H} - C_Z(t)\right] \qquad (9)$$

with the boundary condition, $Z(0) = Z_i(t)$.

The solution to equation (9) is:

$$Z(x) = Z_i(t)*M_1(x) + (1. - M_1(x)) \frac{C_Z(t)K_H}{\rho_L} \tag{10}$$

where: $$M_1(x) = \exp\left(\frac{-\rho_L Q G_o^{M-1} A}{K_H V \rho_g (p+1)} [(H-x)^{p+1} + H^{p+1}]\right) \tag{11}$$

$$Z_H = Z(x=H) = Z_i(t)*M_1(H)+(1- M_1(H)) \frac{C_Z(t)K_H}{\rho_L} \tag{12}$$

If the height of liquid in the column is constant, as is normally the case, $M_1(H)$ becomes:

$$M_1(H) = \exp\left(\frac{-\rho_L Q' G_o^{M-1} A}{K_H V \rho_g}\right)$$

where $Q' = \frac{QH^{p+1}}{p+1}$ = constant

Reaction of Ozone with Organic Contaminants

An unsteady state material balance on TOC in the liquid phase is developed:

Input - Output = Accumulation

Input = $F(t)C_{Ti}(t)$

Output = $F(t)C_T(t) + V*R_T(C_T(t),C_Z(t))$

$$\text{Accumulation} = \frac{V*dC_T(t)}{dt}$$

$$\frac{dC_T(t)}{dt} = (C_{Ti}(t) - C_T(t))/\tau - R_T(C_T(t),C_Z(t)) \tag{13}$$

B.C. $C_T(0)$ is known;

$C_Z(0)$ is known.

where: V = liquid volume, m^3

$\tau = V/F$ = liquid mean residence time, hr

$R_T(C_T(t),C_Z(t))$ = reaction rate of TOC and liquid phase ozone, $\frac{\text{gm TOC}}{m^3 hr}$

C_T = concentration of TOC in the stage, gm/m^3

C_{Ti} = concentration of TOC entering the stage, gm/m^3

F = volumetric flow rate, m^3/hr

Liquid Phase Concentration of Ozone

$$\text{Input} = F(t)C_{Zi}(t) + G(t)\rho_g(Z_i(t) - Z_H(t))$$

$$\text{Output} = F(t)C_Z(t) + V^*[\alpha R_T(C_T(t),C_Z(t)) + R_d(C_Z(t))]$$

$$\text{Accumulation} = V\frac{d}{dt}C_Z(t)$$

Combining terms in the usual form gives:

$$\frac{d}{dt}C_Z(t) = (C_{Zi}(t) - C_Z(t))/\tau + (G(t)\rho_g/V)(Z_i(t) - Z_H(t)) - \alpha R_T(C_T(t),C_Z(t)) - R_d(C_Z(t)) \quad (14)$$

B.C. $C_Z(0)$ is known.

$C_T(0)$ is known.

where: ρ_g = molar density of gas, Kgm-moles/m^3

R_d = auto decomposition reaction of ozone, Kgm-mole-O_3/m^3-hr

α = moles ozone required to convert one gm of TOC to carbon dioxide, Kgm-mole-O_3/gm TOC

Rate Equations

The following forms for rate equations have been chosen:

$$R_T = kC_T^{e_T}C_Z^{e_Z} \quad (15)$$

$$R_d = k_d C_Z^{e_d} \tag{16}$$

where: k = reaction rate constant of O_3-TOC reaction

e_T = reaction order of TOC for O_3-TOC reaction

e_Z = reaction order of C_Z for O_3-TOC reaction

k_d = reaction rate constant for decomposition reaction

e_d = order of decomposition reaction

Ultraviolet (UV) radiation is assumed to affect the rate constants k and k_d in the following manner:

$$k = k_o(1 + \mu)^2, \ \mu \geq 0 \tag{17}$$

$$k_d = k_{do}(1 + \mu)^2, \ \mu \geq 0 \tag{18}$$

where: k_o = k in the absence of UV radiation

k_{do} = k_d in the absence of UV radiation

μ = parameter indicative of the effects of ultraviolet radiation upon k and k_d. μ=0 in the absence of UV radiation.

Steady State Model

To reduce the computational effort required to evaluate parameters such as the liquid phase mass transfer coefficient and the reaction rate constants, a steady state model of the contacting stage was developed:

Steady state mass transfer of ozone from gas to liquid phase:

$$G \frac{dZ(z)}{dx} = -(k_L a)(A)\left[\left(Z(x) \frac{\rho_L}{K_H} - C_Z\right)\right] \tag{19}$$

B.C. $Z(0) = Z_i$

Steady state balance on total organic carbon:

$$(C_{Ti} - C_T)/\tau = R_T \tag{20}$$

Steady state balance on dissolved ozone in the liquid phase:

$$(C_{Zi} - C_Z)/\tau + (G\rho_g/V)(Z_i - Z_H) = \alpha R_T + R_d \qquad (21)$$

Steady State Solution Method

Since the reaction rate equations are nonlinear, solving the steady state equations involves a trial and error process. The solution method employed is described below and flowcharted in Figure 4.3.

The first step is to assume a value for C_T. Next, C_Z can be calculated from a combination of equations (15) and (20) expressed as:

$$C_Z = [(\frac{(C_{Ti} - C_T)}{\tau})/(kC_T^{e_T})]^{1/e_Z} \qquad (22)$$

Once C_Z is known, either equation (7) or (19) is integrated from x=0 to x=H to obtain Z(x) at x=H. If Z_i is small,

$$\frac{Z_i}{1+Z_i} \approx Z_i,$$

and equation (19) should be chosen since it is analytically integrable in x, thereby avoiding the computational overhead associated with integrating equation (7) numerically.

By re-arranging and combining equations (15),(16) and (21), a check on the previous estimate of C_T may be computed:

$$C_T^* = \{[\frac{(C_{Zi}-C_Z)}{\tau} + (\frac{G\rho_g}{V})(Z_i - Z(x=H)) - k_d C_Z^{e_d}]/(\alpha k C_Z^{e_z})\}^{1/e_T} \qquad (22)$$

If C_T^* is significantly different from C_T, a new estimate for C_T is determined and the process repeated. An interval halving technique has been used in this study to perform the iterative solution.

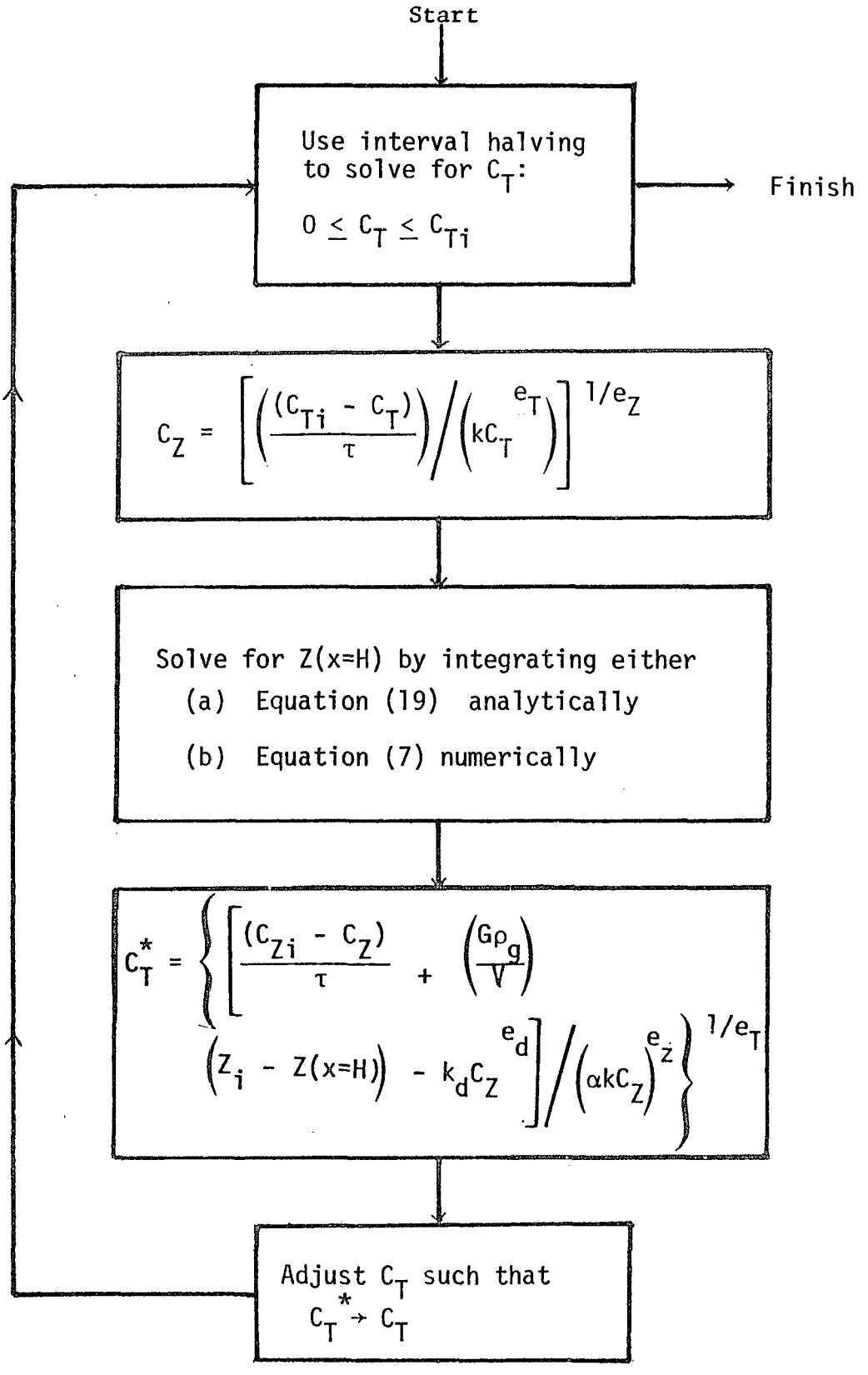

Figure 4.3. Steady State Solution Method

Unsteady State Solution Method

The unsteady state solution of the contactor stage requires that the set of nonlinear ordinary differential equations repeated below be integrated in time from a given initial condition.

Total organic carbon:

$$\frac{dC_T(t)}{dt} = \frac{(C_{Ti}(t) - C_T(t))}{\tau} - kC_T(t)^{e_T}C_Z(t)^{e_Z} \qquad (13)$$

Liquid phase ozone:

$$\frac{dC_Z(t)}{dt} = \frac{(C_{Zi}(t) - C_Z(t))}{\tau} + \frac{G(t)\rho_g}{V}[Z_i(t) - Z_H(t)] - \alpha R_T - R_d \qquad (14)$$

Boundary Conditions:

$C_T(0)$, $C_Z(0)$, $Z_i(t)$ are known

A simple forward difference integration technique was tried but without success. Due to the fast transfer of ozone from the gas to liquid phase from an initial condition of $C_Z = 0$, an unacceptably small time increment was required for stable integration.

The backward difference technique does not suffer from this instability problem. The derivative is evaluated not at the beginning of the time step where it is at a maximum, but rather at the end of the integration period where it is at a minimum.

The backward difference integration formulation of equation (14) appears as follows. The subscript n denotes evaluation at time t; the subscript n+1 denotes evaluation at time t+1.

$$C_{Zn+1} = C_{Zn} + \Delta t \left\{\frac{(C_{Zi,n+1} - C_{Zn+1})}{\tau} + \left(\frac{G_{n+1}\rho_g}{V}\right)(1-M_1(H))\right.$$

$$\left.(Z_{i,n+1} - \frac{C_{Zn+1}K_H}{\rho_L}) - \alpha k C_{Tn+1}^{e_T} C_{Zn+1}^{e_Z} - k_d C_{Zn+1}^{e_d}\right\} \qquad (23)$$

The problem now becomes one of solving (23), a nonlinear algebraic equation, for C_{Zn+1}.

We have chosen to linearize the equation in C_{Zn+1} by approximating expressions of the form C_{Zn+1}^{γ} by the following Tayor series expansion (truncated after the linear term):

$$C_{Zn+1}^{\gamma} \approx (1-\gamma)C_{Zn}^{\gamma} + \gamma C_{Zn}^{\gamma-1}C_{Zn+1}$$

where: γ = any arbitrary exponent.

With this approximation, equation (23) becomes, after some gathering of terms,

$$C_{Zn+1} = \frac{C_{Zn} + Q_1\Delta t}{1 + Q_2\Delta t} \tag{24}$$

where: $$Q_1 = \frac{C_{Zi,n+1}}{\tau} + \left(\frac{G_{n+1}\rho_g}{V}\right)(1-M_1(H))(Z_{i,n+1}) - \alpha k C_{Tn+1}^{e_T}(1-e_Z)C_{Zn}^{e_Z} - k_d(1-e_d)C_{Zn}^{e_d} \tag{25}$$

and $$Q_2 = \frac{1}{\tau} + \left(\frac{G_{n+1}\rho_g}{V}\right)(1-M_1(H))\left(\frac{K_H}{\rho_L}\right) + \alpha k C_{Tn+1}^{e_T} e_Z C_{Zn}^{e_Z-1} + k_d e_d C_{Zn}^{e_d-1} \tag{26}$$

A forward difference integration of equation (13) was found adequate. Thus, in the actual numerical solution, equations (25) and (26) were evaluated using C_{Tn} instead of C_{Tn+1}.

The numerical procedure for solving the material balance equations for the total organic carbon and liquid phase ozone concentrations is flow charted in Figure 4.4.

Overall Contactor System Solution Method (Steady State and Dynamic)

The model of the overall ozone contactor - including a precontactor and six stages - consists of the repeated application of the individual

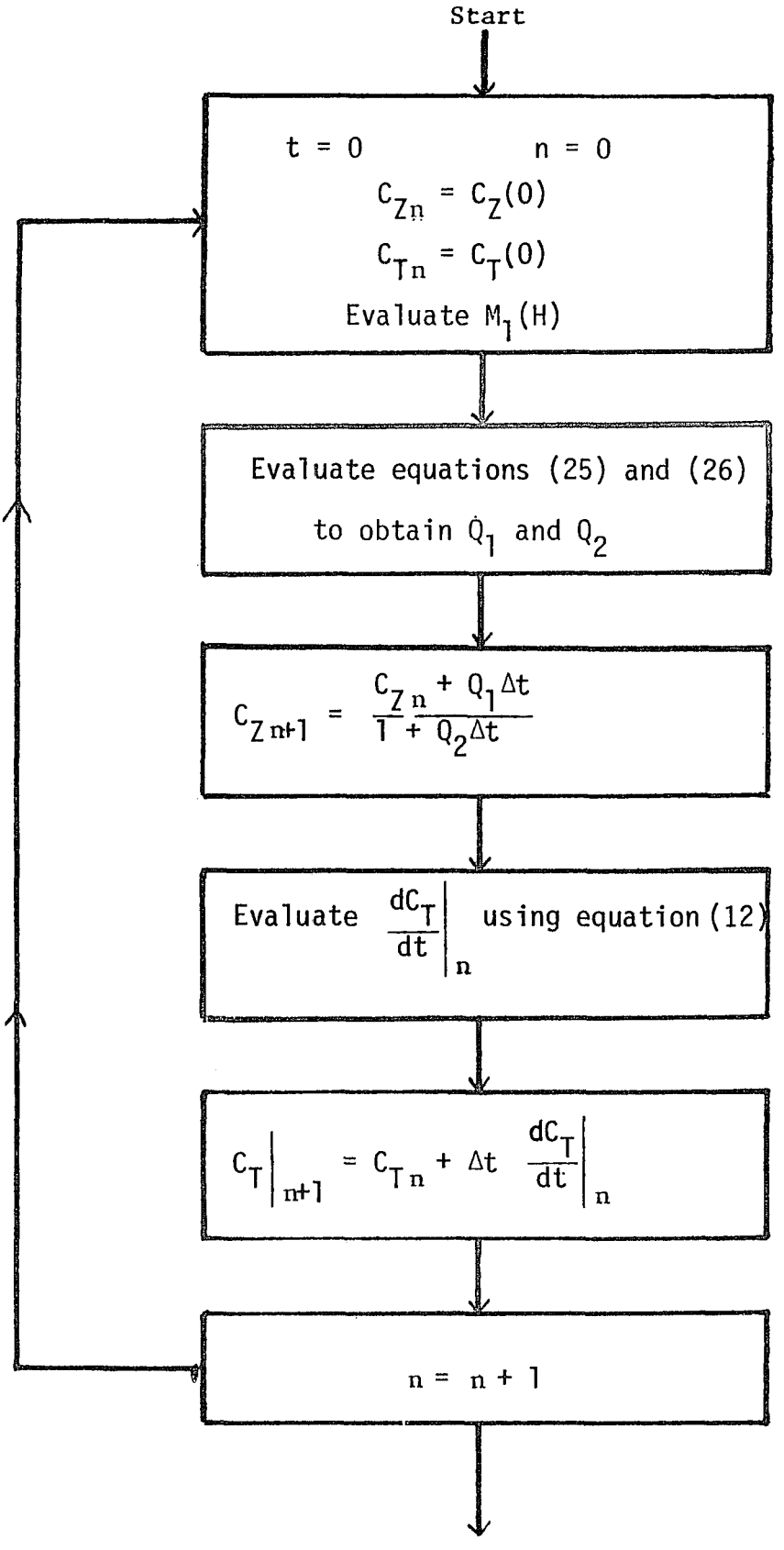

Figure 4.4. Unsteady State Solution Method

contacting stage models. In essence, the overall ozone contactor model connects the individual stages in the proper sequence as illustrated in Table 4-1.

Overall Contactor System Steady State Solution

As the pre-contactor is dependent upon the models of stages one through six, and vice-versa, the solution technique is necessarily iterative. The method used is essentially a back-substitution strategy and is flowcharted in Figure 4.5.

Overall Contactor System Dynamic Solution

Since, for each increment of time, the pre-contactor and stages may be considered independent of each other, the unsteady state solution of the overall contactor is very straightforward. A flow chart is given in Figure 4.6.

PARAMETER ESTIMATION CONSIDERATION

Values of key variables,such as reaction rate coefficients and the mass transfer coefficient, must be determined for use within the model.

To estimate these values, the Pattern Search (4) discussed in Chapter II is again used to minimize a cost function which penalizes for model deviations from experimental results.

Cost Function

The cost function used in this study is the sum of weighted relative squared differences between the model and experimental data. The following items are compared in the evaluation:

1. Off gas ozone concentration
2. Concentration of total organic carbon

Stage	Input From:		Output To:	
	Liquid	Gas	Liquid	Gas
Precontactor	RO Permeate	Stages 1-6	Stage 1	Vented
1	precontactor	O_3 generator	stage 2	precontactor
2	stage 1	O_3 generator	stage 3	precontactor
3	stage 2	O_3 generator	stage 4	precontactor
4	stage 3	O_3 generator	stage 5	precontactor
5	stage 4	O_3 generator	stage 6	precontactor
6	stage 5	O_3 generator	hypochlor-ination unit	precontactor

Table 4-1

Ozone Contactor Configuration

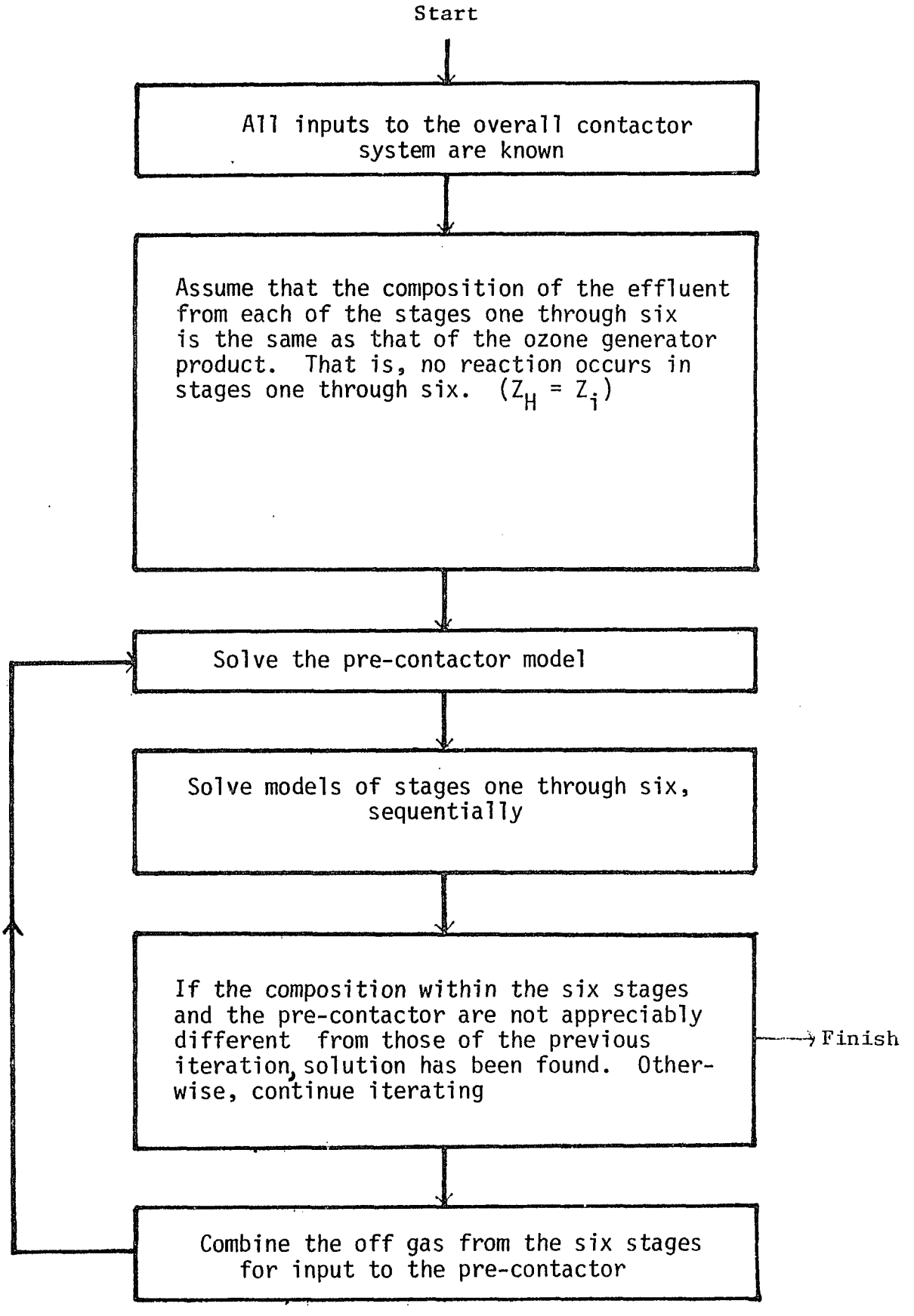

Figure 4.5. Steady State Solution Method for Overall Contacting System

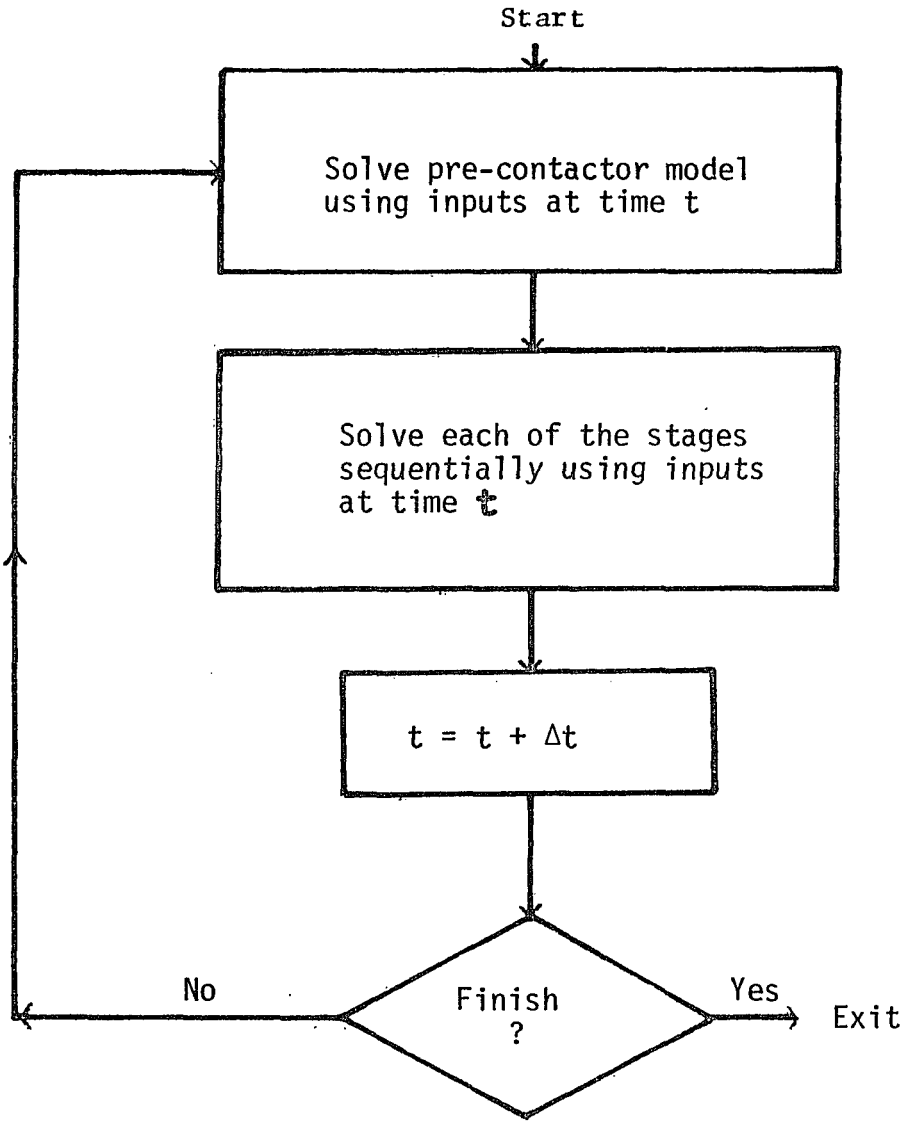

Figure 4.6

Dynamic Solution of Overall Contacting System

3. Concentration of dissolved ozone.

The algebraic formulation of the cost function is given below:

$$COST = \sum_{i=1}^{n} W_{Pi} \{ \sum_{j = \text{precontactor stages}} [W_{ZH_{ij}} (\frac{ZH_{e,ij} - ZH_{m,ij}}{ZH_{e,ij}})^2 + W_{CT_{ij}} (\frac{CT_{e,ij} - CT_{m,ij}}{CT_{e,ij}})^2 + W_{CZ_{ij}} (\frac{CZ_{e,ij} - CZ_{m,ij}}{CZ_{e,ij}})^2] \}$$

where: n = number of data points, dimensionless

W_{Pi} = weighting factor for the point as a whole, dimensionless

$W_{ZH_{ij}}$ = weighting factor for off gas ozone concentration deviations. (Data point i, Stage j), dimensionless

$W_{CT_{ij}}$ = weighting factor for product water TOC concentration deviations. (Data point i, Stage j), dimensionless

$W_{CZ_{ij}}$ = weighting factor for product water dissolved ozone concentration deviations. (Data point i, Stage j), dimensionless

$ZH_{e,ij}$ = experimental reading of off gas ozone concentration. (Data point i, Stage j), moles ozone/mole ozone free gas

$ZH_{m,ij}$ = model prediction of off gas ozone concentration. (Data point i, Stage j), moles ozone/mole ozone free gas

$CT_{e,ij}$ = experimental value of product water TOC concentration. (Data point i, Stage j), gm/m^3

$CT_{m,ij}$ = model prediction of product water TOC concentration. (Data point i, Stage j), gm/m^3

$CZ_{e,ij}$ = experimental value of product water dissolved ozone concentration. (Data point i, Stage j), Kgm $moles/m^3$

$CZ_{m,ij}$ = model prediction of product water dissolved ozone concentration. (Data point i, Stage j), Kgm $moles/m^3$

For the purposes of the cost function, the pre-contactor is considered as though it were a stage.

Parameters to be Evaluated

Table 4-2. lists the model parameters whose values must be determined from experimental data.

Several parameters may be evaluated by appropriate laboratory kinetic analyses, namely α, k_{do}, k_o, e_T, e_Z, and e_d. Since the mass transfer of ozone and the effect of ultraviolet (UV) radiation are directly influenced by the contactor stage configuration, it is felt that Q', M, and μ should be evaluated from actual operating data.

Data Requirements

The following data will be required to properly obtain numerical values for the adjustable parameters within the ozone contacting system model.

1. System Geometry
    a. Precontactor
        1. Height (m)
        2. Width (m)
        3. Length (m)
    b. Stages
        1. Number of stages used
        2. Height (m)
        3. Width (m)
        4. Length (m)

Table 4-2. Ozonation Model Parameters

k_o	TOC - ozone reaction rate constant in the absence of UV radation
e_T	TOC - ozone reaction rate order for TOC
μ_o	Value of μ in the presence of UV radiation
k_{do}	Ozone decomposition reaction rate constant in the absence of UV radiation
e_Z	TOC - ozone reaction rate order for ozone
e_d	Ozone decomposition reaction rate order
α	Moles of ozone required to oxidize one gram of organic carbon
Q'	Constant in correlation for $k_L a$
M	Exponent of G_o in correlation for $k_L a$

c. Specific configuration of interstage piping; i.e., origin and destination of both influents and effluents for each stage - including the pre-contactor (if present)

2. System Input Data
   a. Waste water type
   b. Inlet volumetric flow rate of contaminated water (m^3/hr)
   c. Inlet volumetric flow rate of ozone/carrier gas (m^3/hr)
   d. TOC of RO effluent (gm/m^3)
   e. Ozone concentration of ozone/carrier gas from ozone generator (moles ozone/mole carrier gas)
   f. Operating temperature (°K)
   g. Operating pressure (atm)
3. System Output Data*
   a. TOC levels in pre-contactor and all stages (gm/m^3)
   b. Liquid phase concentration of ozone in pre-contactor and all stages ($Kgm\text{-}moles/m^3$)
   c. Ozone concentration of gaseous effluent from pre-contactor and all stages (gm-moles ozone/gm-mole ozone free gas)

SUMMARY

This chapter presented the development of the ozonation module model. Equations describing the behavior of this unit and the method of evaluating parameters from available experimental data are discussed.

*Note: Not all of the requested system output data may be available; however, the fit program can make use of all data taken. Also, all system output data must be gathered when the entire ozone contacting system is at steady state.

CHAPTER V

THE HYPOCHLORINATION SYSTEM MODEL

INTRODUCTION

In this chapter, the development of the model of the hypochlorination unit from basic material balance equations and the solution method employed are presented.

Although a section on parameter estimation considerations is included to maintain consistency, it is concluded that no adjustable parameters exist.

Listings of the computer programs and the results of example runs are contained in the report, "A Mathematical Model of a Hypochlorination Unit for a Water Re-Use System". (11)

DEVELOPMENT OF BASIC EQUATIONS AND METHODS USED

Ozone is a powerful disinfectant but is highly unstable in aqueous solutions. However, a small residual of free available chlorine, present as either HOCl or OCl^-, is an effective retardant against bacterial growth for sustained periods.

The purpose of the hypochlorination module is to introduce the proper amount of calcium hypochlorite solution to achieve the required disinfectant residual without an excessively high free chlorine concentration.

A diagram of the unit is presented in Figure 5.1 together with the notation pertinent to this chapter.

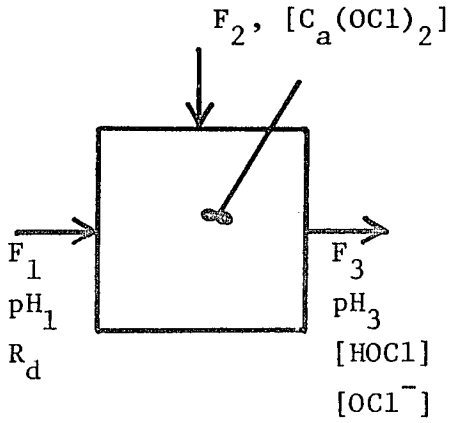

where: [A] represents the concentration of component A.

1,2, and 3 are subscripts designating flow streams.

pH is $-\log_{10}$ of the hydrogen ion concentration.

$Ca(OCl)_2$ is calcium hypochlorite.

HOCl is hypochlorous acid.

OCl^- is the hypochlorite radical.

F is the liquid volumetric flow rate

R_d is the total chlorine demand of the inlet water.

Figure 5.1. Diagram of Hypochlorination Unit

Basic Chemical Reactions

The following reactions occur when $Ca(OCl)_2$ is added to water:

$$Ca(OCl)_2 \rightarrow Ca^{++} + 2HOCl + 2OH^-$$

$$HOCl \rightleftarrows H^+ + OCl^-$$

$$H^+ + OH^- \rightleftarrows H_2O$$

Material Balance

A total material balance on the hypochlorite ion using the hypochlorination unit as a control volume yields:

$$\text{INPUT} - \text{OUTPUT} = \text{ACCUMULATION} \qquad (1)$$

$$\text{INPUT: } 2F_2[Ca(OCl)_2]$$

$$\text{OUTPUT: } F_3[HOCl)] + F_3[OCl^-] + F_1R_d$$

$$\text{ACCUMULATION: } V\frac{d}{dt}([HOCl] + [OCl^-])$$

where: V = volume of mixed tank

t = time

B.C. $[HOCl]_3$ at t=0 is known

$[OCl^-]_3$ at t=0 is known

pH_3 at t=0 is known

It is tacitly assumed in the above and subsequent material balances that the hypochlorination unit approaches the perfectly mixed state. In actuality, the unit is equipped with a mechanical agitator.

Constraints on the Material Balance

The solution to the total material balance must satisfy the following constraints at all times:

$$\frac{[H^+][OCl^-]}{[HOCl]} = K_{eq} \quad \text{(Dissociation relationship for hypochlorous acid)} \qquad (2)$$

and $[H^+][OH^-] = 1.0 \times 10^{-14}$ (Dissociation relationship for water) (3)

or $pH + pOH = 14$

where K_{eq} is the dissociation constant for HOCl.

Solution Method

The unsteady state material balance for the hypochlorite ion may be solved as follows:

1. Given $[HOCl]_3$, $[OCl^-]_3$, pH_3, at time t.
2. Calculate $\frac{d}{dt}([HOCl] + [OCl^-])$ at time t.
3. Calculate $([HOCl] + [OCl^-])$ at time $t + \Delta t$ as

$$([HOCl] + [OCl^-])_{t+\Delta t} = ([HOCl] + [OCl^-])_t + \frac{d}{dt}([HOCl] + [OCl^-])\Big|_t \Delta t \quad (4)$$

To determine [HOCl] at time $t + \Delta t$, the following iterative technique is proposed:

1. Estimate $[HOCl]_{t+\Delta t}$
2. Application of an unsteady state material balance on $[H^+]$ yields:

$$[H^+]_{t+\Delta t} = [H^+]_t + [F_1 10^{-pH_1} + (2F_2[C_a(OCl)_2] - F_3[HOCl]_{t+\Delta t}) - \alpha F_1 R_d - F_3[H^+]_{t+\Delta t} - F_3 X] * \frac{\Delta t}{V} \quad (5)$$

where X = amount of H^+ reacted with OH^- to form H_2O

α = fraction of total chlorine demand satisfied by reactions with HOCl

3. A similar material balance for OH^- yields:

$$[OH^-]_{t+\Delta t} = [OH^-]_t + (F_1 10^{-pOH_1} + 2F_2[Ca(OCl)_2] - F_3[OH^-]_{t+\Delta t} - F_3 X) \frac{\Delta t}{V} \quad (6)$$

4. Since $[OH^-]_{t+\Delta t}[H^+]_{t+\Delta t} = 10^{-14}$, a quadratic equation is formed in X. Once X is computed, $[H^+]_{t+\Delta t}$ and $[OH^-]_{t+\Delta t}$ are easily evaluated.

5. $[OCl^-]_{t+\Delta t}$ is computed as

$$[OCl^-]_{t+\Delta t} = \frac{K_{eq}[HOCl]_{t+\Delta t}}{[H^+]_{t+\Delta t}}$$

6. A check on the value of $[HOCl]_{t+\Delta t}$ first assumed is calculated as:

$$[HOCl)'_{t+\Delta t} = ([HOCl] + [OCl^-])_{t+\Delta t} - [OCl^-]_{t+\Delta t}$$

7. If $[HOCl]_{t+\Delta t} > [HOCl]'_{t+\Delta t}$ the next estimate of [HOCl) should be lowered; otherwise the next estimate of [HOCl] should be raised.

8. Go to step 2 if the successive estimates of [HOCl] are significantly different; otherwise, the solution at this point has been found.

For interval halving, the initial bounds on $[HOCl]_{t+\Delta t}$ are determined from the following relationship:

$$0 \leq [HOCl]_{t+\Delta t} \leq ([HOCl] + [OCl^-])_{t+\Delta t} \qquad (7)$$

In some cases, the hypochlorination mixing tank may be replaced by an inline mixer of very small volume. Since the residence times of inline mixers tend to be very short, a steady state model for this type of hypochlorination unit becomes attractive for two reasons:

1. The model equations and computer programs are simplified.
2. There are none of the problems associated with the numerical integration of stiff equations such as those that would result from a very small liquid holding time.

The steady state model is easily derived from the dynamic model by forcing all time derivatives to zero:

Steady state balance on chlorine:

$$\frac{d}{dt}\left([HOCl] + [OCl^-]\right) = 2F_2[C_a(OCl)_2] - F_3[HOCl] - F_3[OCl^-] - F_1R_d = 0 \quad (8)$$

Steady state balance on H^+:

$$\frac{d}{dt}[H^+] = F_1 10^{-pH_1} + (2F_2[C_a(OCl)_2] - F_3[HOCl]) - F_3[H^+] - F_3X = 0 \quad (9)$$

Steady state balance on OH^-:

$$\frac{d}{dt}[OH^-] = F_1 10^{-pOH_1} + 2F_2[C_a(OCl)_2] - F_3[OH^-] - F_3X = 0 \quad (10)$$

The steady state solution technique is very similar to that for the unsteady state case and is presented here:

1. Estimate [HOCl].
2. The material balance equations for $[H^+]$ and $[OH^-]$ can be combined with the equilibrium relationship for water resulting in a quadratic equation for X as a function of [HOCl]:

$$\{F_1 * 10^{-pH_1} + (2F_2[C_a(OCl)_2] - F_3[HOCl] - F_3X - \alpha F_1R_d\} *$$
$$\{F_1 * 10^{-pOH_1} + 2F_2[C_a(OCl)_2] - F_3X\}/F_3^2 = 10^{-14} \quad (11)$$

   Since [HOCl] has been estimated, X can be computed. $[H^+]$ may then be evaluated.
3. With values available for [HOCl] and $[H^+]$, $[OCl^-]$ is obtained from the dissociation relationship for hypochlorous acid:

   $[OCl^-] = Keq[HOCl]/[H^+]$
4. A check on the estimate of [HOCl] is determined from the total chlorine balance:

$$[HOCl]' = \{2F_2[C_a(OCl)_2] - F_3[OCl^-] - F_1R_d\}/F_3 \quad (12)$$

5. If [HOCl] > [HOCl'], the next estimate of [HOCl] should be lowered; otherwise, it should be increased.

6. If the successive estimates of [HOCl] are significantly different, go to step 1; otherwise, the solution has been found.

An upper bound on [HOCl] may be computed by assuming that none of the [HOCl] formed by the addition of $C_a(OCl)_2$ is reacted or dissociated. That is,

$$0 \leq [HOCl] \leq \frac{2[C_a(OCl)_2]F_2}{F_3} \tag{13}$$

PARAMETER ESTIMATION CONSIDERATIONS

The fraction of the chlorine demand of the inlet water, α, satisfied by reaction with HOCl is the only candidate for a model parameter. However, since α is generally known from laboratory analysis - as is the total chlorine demand, R_d - no parameter estimation procedures are necessary.

Data Requirements

The following data will be required to properly execute the model of the hypochlorination system. Since no fit parameters need be evaluated, no experimental data is necessary.

A. Specifics of Module Configuration and Geometry

1. Volume of mixing system (m^3)

B. Operating Test Data

1. Initial Conditions

a. pH of initial system contents (pH)

b. Concentration of free available chlorine (ppm)

2. Feed Conditions
   a. Inlet volumetric flow rate (m^3/hr)
   b. pH of inlet water (pH)
   c. Total chlorine demand of influent (ppm)
   d. Fraction of total demand in inlet water satisfied by HOCl (dimensionless)
3. Hypochlorite Addition Conditions
   a. Concentration of $C_a(OCl)_2$ ($Kgmole/m^3$)
   b. Flow rate of $C_a(OCl)_2$ solution (m^3/hr)

SUMMARY

The model equations describing the hypochlorination unit process were developed and a solution technique presented in this chapter. No parameter estimation procedure was required.

CHAPTER VI

THE PROCESS FLOW SIMULATOR PACKAGE

INTRODUCTION

This chapter serves to present the overall dynamic simulator. Models of less complicated pieces of equipment, such as mixed tanks, are developed.

Program listings and the results of example runs demonstrating the capabilities of the simulator are contained in a technical report to the U. S. Army (12).

OVERVIEW

The dynamic process simulator is a general purpose computer program capable of simulating the dynamic behavior of a process. The configuration of the process is specified by the input data, along with the parameters that specify the characteristics of the individual items of equipment in the process. This permits a variety of process configurations to be investigated without requiring any changes in the program source code.

While the structure of the simulator is very general, the program as developed has been tailored to meet the needs of water reuse systems. Every reasonable effort has been made to facilitate the superposition of a control system upon the process model.

A considerable commitment has been made to maintaining the integrity of the integrated model. All stream designations in the input data are checked for validity. The simulator also investigates each

stream to make sure that an origin and destination have been specified.

In addition, total and component material blances are performed around the entire process configuration to ascertain the consistency of the model results.

Streams

For the purposes of the simulator, the process is represented by individual pieces of equipment interconnected by process streams.

The status of each stream is specified by a stream vector. The components of this vector define the properties of the stream (flow rate, composition, temperatures, etc.). As currently implemented, the vector consists of the following:

Element	Definition
1	Flow, m^3/hr
2	Concentration of suspended solids, gm/m^3
3	Concentration of dissolved solids, gm/m^3
4	Concentration of total organic carbon, gm/m^3

Each stream is designated within the simulator program by a positive integer.

Equipment

Each piece of equipment in the process is simulated by a routine which is specific to that equipment type.

Most of the equipment types have associated parameters which identify the characteristics that distinguish a particular item of equipment from others of the same type.

For example, many configurations include several holding tanks, i.e., the equalization/pre-screening tank, the ultrafiltration feed tank, and the reverse osmosis feed tank. One distinguishing characteristic here is the initial volume of each tank.

Simulation Method

To simulate operation of a particular configuration, the following steps are executed:

1. Determine the proper equipment type of the next unit as specified in the process configuration.
2. Set up the input and output streams to and from this unit as specified by the process configuration.
3. Set up the parameters which are unique to this particular piece of equipment.
4. Call the equipment routine for this equipment type.
5. If this is the last piece of equipment in the configuration, go to step 6; otherwise, go to step 1.
6. Increment the index of time for the simulation and go to step 1, starting with the first item of equipment.

Equipment Types

The simulator presently recognizes the following types of equipment:

Type	Code
Mixed tank	MT
Overflow tank	ØT

Type	Code
Pump	P
Stream splitter	SP
Stream source	SØ
Stream mixer	SM
Ultrafiltration unit	UF
Reverse Osmosis unit	RØ
UV/ozonation unit	UV
Hypochlorination unit	HC
Sink	SK

Other pieces of equipment can be easily added to the simulator.

ADDITIONAL EQUIPMENT MODELS

The remainder of this chapter is devoted to presenting the remainder of the equipment models. In addition, the parameters specific to each equipment type are described.

Mixed Tank

The mixed tank is described by a total material balance and several component material balances. The total material balance is:

$$\frac{dV}{dt} = \sum_{\text{input}} F_i - \sum_{\text{output}} F_j$$

where: V = volume of liquid in the tank

F_i = flow rate of input stream i

F_j = flow rate of output stream j

Each component material balance is:

$$\frac{d}{dt}(VC) = \sum_{\text{input}} F_i C_i - \sum_{\text{output}} F_j C_j$$

where: C = concentration in the tank

C_i = concentration of input stream

C_j = concentration of output stream

Any combination of input and output streams are permitted. The concentrations of all exit streams are the same as the concentrations in the tank.

For the mixed tank, the following parameters are required:

1. Initial volume of liquid in the tank
2. Initial concentration of suspended solids in the tank
3. Initial concentration of dissolved solids in the tank
4. Initial concentration of total organic carbon in the tank

In the initialization calculations for the mixed tank, the concentrations of all output streams are specified as the initial concentrations in the tank.

Overflow tank

An overflow tank is a mixed tank with an upper limit on the volume. Should this maximum volume be exceeded, the excess influent is discharged via the overflow stream.

The basic equations for the overflow tank are the same as for the mixed tank. The additional equations which provide the overflow capability are as follows:

$$F_l = F_T \text{ for } 0 < V < V_{max}$$

$$F_l = \sum_{input} F_i - \sum_{output} F_j \text{ for } V \geq V_{max}$$

where: F_l = overflow rate

F_T = design overflow rate

V = volume of liquid in tank

V_{max} = maximum volume of liquid in tank

F_i = flow rate of input stream

F_j = flow rate of output stream

Both F_T and V_{max} are data parameters.

The following parameters are required for the overflow tank:

1. Initial volume
2. Initial concentration of suspended solids
3. Initial concentration of dissolved solids
4. Initial concentration of total organic carbon
5. Design overflow rate
6. Maximum volume

In the initialization calculations, the concentrations of all output streams are set equal to the initial concentrations in the tank.

Volumetric Pump

This item of equipment represents either a constant volume pump or a variable volume pump followed by a flow controller.

The basic equation for this pump is as follows:

$$F_1 = F_2 = F_p$$

where: F_p = flow rate through pump

F_1 = flow rate of input stream

F_2 = flow rate of output stream

The concentration of the output stream is set equal to the concentration of the input stream.

The only parameter associated with the pump is F_p.

Stream Splitter

The purpose of this piece of equipment is to split an input stream into two output streams, the flow rate of one output stream being specified.

The flow equation describing this piece of equipment is as follows:

$$F_2 = \begin{cases} F_s \text{ if } F_1 \geq F_s \\ F_1 \text{ if } F_1 < F_s \end{cases}$$

$$F_3 = F_1 - F_2$$

where: F_1 = flow rate of input stream

F_2 = flow rate of first output stream

F_3 = flow rate of second output stream

The concentrations in both output streams are set equal to the input concentration.

The only parameter required is F_s, the design split.

Stream Source

The stream source is designed to simulate the pulse-type input streams that are encountered in water re-use units. The stream is assumed to behave as follows:

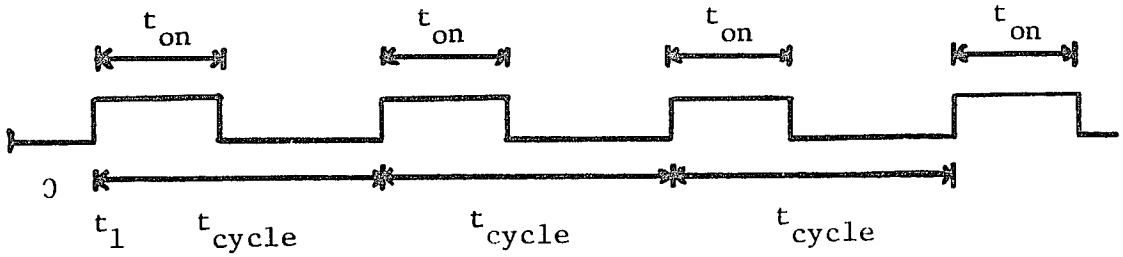

where: t_1 = time of start of first pulse

t_{on} = time duration of pulse

t_{cycle} = time of cycle

During the flow period, the flow rate and concentration must be specified.

For this unit, the following parameters are required:

1. time of first pulse (t_1)
2. time duration of pulse (t_{on})
3. time of cycle (t_{cycle})
4. flow rate during pulse
5. concentration of suspended solids
6. concentration of dissolved solids
7. concentration of total organic carbon

Stream Mixer

The stream mixer is designed to combine several input streams to produce a single output stream.

The flow equations describing this unit are as follows:

$$F_j = \sum_{input} F_i$$

where: F_i = flow rate of input stream

F_j = flow rate of output stream

The equation for concentration is as follows:

$$C_j = \frac{\sum_{input} F_i C_i}{F_j}$$

where: C_i = concentration of input stream

C_j = concentration of output stream

No parameters are required for this unit.

Ultrafiltration Unit

The ultrafiltration unit model is described in Chapter II.

The required parameters are:

1. Length of tubes
2. Diameter of tubes
3. Number of tubes in module
4. Number of integration steps
5. Density of water

Reverse Osmosis Unit

The reverse osmosis unit model is described in Chapter III.

The required parameters are:

1. Length of hollow fibers
2. Outer radius of feed distribution tube
3. Inner radius of module
4. Diameter of hollow fibers
5. Average pressure in concentrate side of module
6. Density of water
7. Operating temperature
8. Average kinematic viscosity of the RO feed solution

Ozonation Unit

The ozonation unit model is described in Chapter IV.

The required parameters are:

1. Inlet ozone/carrier gas concentration
2. Inlet gas flow rate
3. Initial concentration of suspended solids
4. Initial concentration of dissolved solids
5. Initial concentration of total organic carbon

Hypochlorination Unit

The hypochlorination unit model is described in Chapter V.

The required parameters are:

1. Initial pH
2. Initial concentration of free available chlorine (parts per million)
3. Initial concentration of suspended solids
4. Initial concentration of dissolved solids
5. Initial concentration of total organic carbon
6. Feed rate of $C_a(OCl)_2$ solution

Sink

As indicated earlier, all input streams to the process must originate with the source block. Similarly, all streams leaving the process must be inputs to a block called the "Sink". One reason for this is so that each stream must originate with one and only one block and each the destination for each stream must be one and only one block.

Actually, the sink block plays no role in the simulation. The only calculation procedure involved is that the collective stream flows (total and component) are integrated for the material balance calculations.

Each sink block may have up to five input streams. The process configuration may contain multiple sink blocks.

No parameters are required.

SUMMARY

The simulator interconnects each of the unit processes selected in a particular configuration into an integrated dynamic model.

To permit the greatest degree of flexibility, the equipment sizings, initial conditions, and plant configurations are specified by the input data.

CHAPTER VII

CONCLUSIONS

The purpose of this dissertation has been to develop a dynamic model of a water treatment element incorporating the unit processes described in Chapters II-V.

The typical application of this model would be in the simulation of a full scale water treatment unit. Experimental data collected from pilot unit processes over the expected range of operating conditions would be used to determine model parameters.

The component models developed were presented in Chapters II-V. The objective in each case was to compose a model adequately rigorous in a mechanistic sense that would not require an undue expenditure of computational effort. This was readily accomplished in the models of the hypochlorination and ozonation systems.

For the models of the ultrafiltration and reverse osmosis systems, this was not the case. The primary difficulty encountered was the formulation of a suitable solution method for determining the fluxes of material into and out of the boundary layer region.

Methods which generally converged to the solution quickly also tended to have instability set in near operating conditions of high concentrations and low flow rates. Methods which were always stable tended to converge to the solution rather slowly. In view of the general purpose nature of the simulator, a solution method of the latter

variety was chosen for use in the ultrafiltration and reverse osmosis systems models.

The process flow simulator on the whole performs admirably. One feature of the simultor worthy of special note is the total and species material balance calculations performed around the overall process configuration. This simple check quickly provides a good estimate of the integrity of the solution that would require considerable effort to obtain otherwise.

To demonstrate the capabilities of the component models and the simulator, an example simulation was performed. The process configuration chosen for study is similar to the conceptual design of a water treatment unit by the Walden Division of Abcor Inc. (13). Tables 7-1 through 7-3 and Figures 7.1 through 7.5 describe the unit specifications and other background information used.

Model parameters for the unit processes were determined in the manner outlined in Chapters II through V. Tables 7-4 through 7-6 present the results of the parameter estimation experience for the ultrafiltration, reverse osmosis, and ozonation systems models.

Due to the scarcity of useable data, these parameters were determined only to the degree necessary to give reasonable agreement between model predictions and experimental results.

A simple sensitivity analysis was performed for each unit process model by recording the response to purturbations in operating variables and adjustable parameters. While no quantitative judgements were possible, the model responses to these tests were at least qualitatively correct.

Table 7-1. Formulation of Hospital Composite Waste Water

Hospital Composite Waste Water is composed of the following individual waste streams: (An average analysis of each stream is also given).

Waste Streams	Suspended Solids Concentration (gm/m^3)	Dissolved Solids Concentration (gm/m^3)	TOC Concentration (gm/m^3)
Shower	93.	374.	44.
Kitchen	910.	3290.	1120.
Operating Room	2.	1788.	252.
Laboratory	58.	215.	476.
X-Ray	43.	1247.	126.

Data taken from the Walden Report (13).

Table 7-2. Typical Hospital Waste Water Flow Patterns (for 24 hour day)

Waste Type	Time of Pulse (hr)	Pulse Cycle Time (hr)	Pulse Flow Rate (m^3/hr)	Pulse Duration (hr)
Shower	6.0	24.0	1.51	1.5
Shower	16.0	24.0	1.51	3.0
Shower	23.25	24.0	1.51	0.75
Kitchen	8.0	24.0	0.26	2.0
Kitchen	12.0	24.0	0.26	2.0
Kitchen	17.0	24.0	0.26	2.0
Kitchen	23.0	24.0	0.26	1.0
Operating Room	0.0	1.0	0.53	0.25
Laboratory	9.0	24.0	0.19	7.0
X-Ray	9.0	24.0	0.066	8.0

Data taken from the Walden Report (13).

Table 7-3. Unit Descriptions and Specifications

Unit	Description
U1	Equalization Prescreening Tank.
	Initial Volume = 15 m^3
	Initial Concentration of Suspended Solids = 159 $\frac{gm}{m^3}$
	Initial Concentration of Dissolved Solids =1107 $\frac{gm}{m^3}$
	Initial Concentration of TOC = 263 $\frac{gm}{m^3}$
U2	Overflow Tank.
	Initial Volume = 0.35 m^3
	Initial Concentration of Suspended Solids = 159 $\frac{gm}{m^3}$
	Initial Concentration of Dissolved Solids =1107 $\frac{gm}{m^3}$
	Initial Concentration of TOC = 263 $\frac{gm}{m^3}$
	Design Overflow Rate = 0.08 m^3/hr
	Maximum Volume = 0.76 m^3
U3	UF Circulation Pump.
	Pump Flow Rate = 61.32 m^3/hr
U4	UF Module.
	Configuration = 9 tubes
	Temperature = 311°K
	Inlet ΔP = 3.40 atm
	ΔP down UF tubes = 2.04 atm
U5	RO Feed Tank.
	Initial Volume = 0.57 m^3
	Initial Concentration of Suspended Solids = 0.0 $\frac{gm}{m^3}$
	Initial Concentration of Dissolved Solids = 600 $\frac{gm}{m^3}$
	Initial Concentration of TOC = 25 $\frac{gm}{m^3}$

Table 7-3. (cont.)

Unit	Description
U6	RO Battery High Pressure Pump. Pump Flow Rate = 0.95 m^3/hr
U7,U8,U9,U10	RO Modules. Configuration = B-10 Permasep Hollow Fiber Separator Pressure = 54 atm Temperature = 303 °K
U11	Ozone Contacting System. Configuration = 6 stages, precontactor Precontactor Volume = 0.690 m^3 Stage Volume = 0.736 m^3 Gas Flow Rate = 1.698 m^3/hr Inlet O_3 Concentration = .0122 moles O_3/mole carrier gas Inlet Concentration of Suspended Solids = 0.0 $\frac{gm}{m^3}$ Inlet Concentration of Dissolved Solids = 50.0 $\frac{gm}{m^3}$ Inlet Concentration of TOC = 5.0 $\frac{gm}{m^3}$
U12	Hypochlorination Unit. Volume = .252 m^3 Feed Rate of $C_a(OCl)_2$ Solution = $6.42X10^{-5}$ m^3/hr Concentration of $C_a(OCl)_2$ Solution = 0.643 $\frac{Kgmole}{m^3}$ Initial Concentration of Suspended Solids = 0.0 $\frac{gm}{m^3}$ Initial Concentration of Dissolved Solids =50.0 $\frac{gm}{m^3}$ Initial Concentration of TOC = 5.0 $\frac{gm}{m^3}$

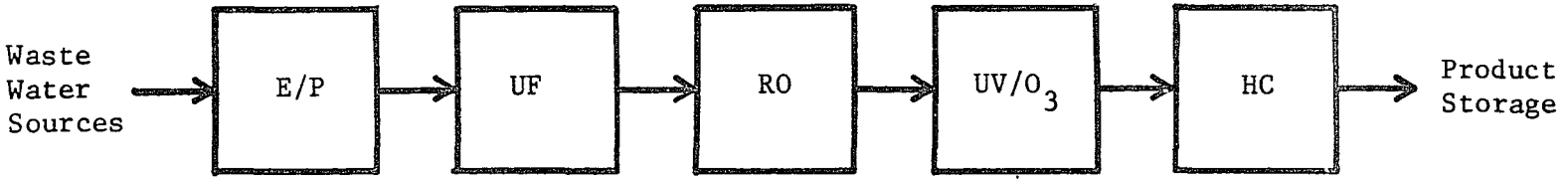

E/P - Equalization/Pre-screening system

UF - Ultrafiltration system

RO - Reverse Osmosis system

UV/O_3 - Ozone Contacting system

HC - Hypochlorination system

Figure 7.1. Example Process Configuration

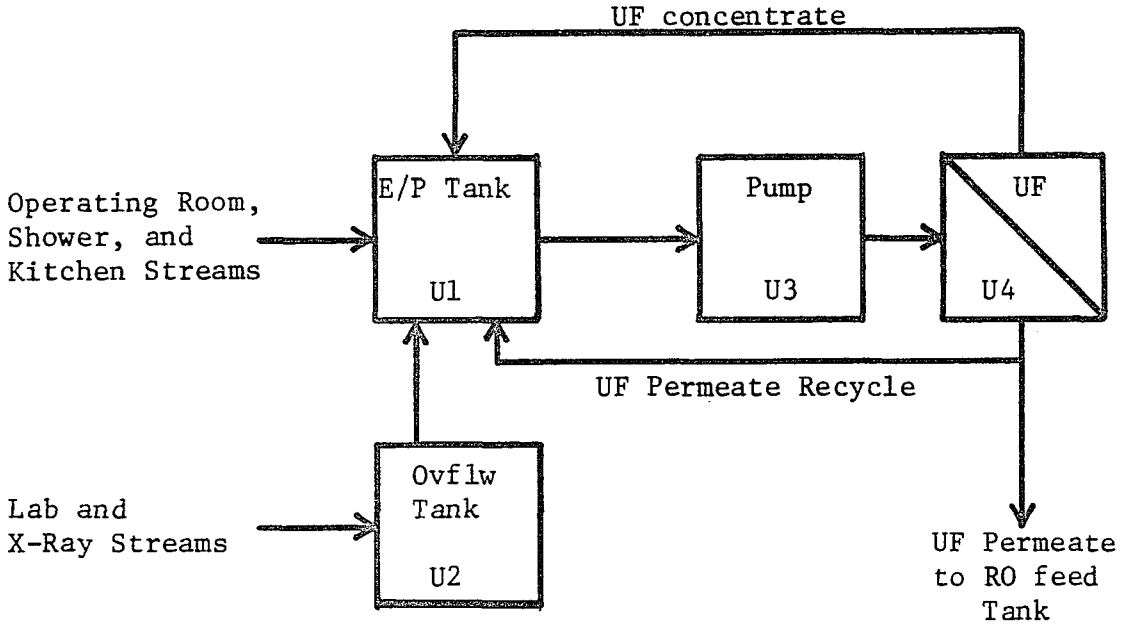

Figure 7.2. Expanded Equalization/Pre-screening and Ultrafiltration Systems

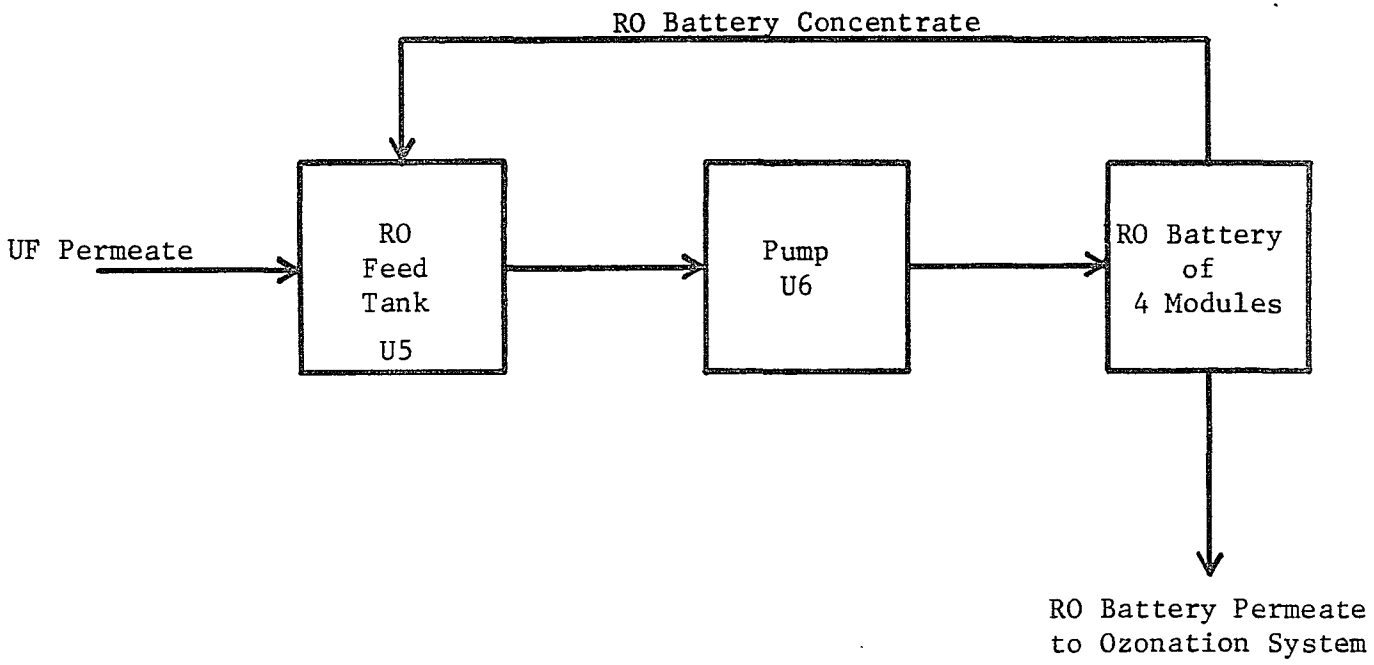

Figure 7.3. Expanded Reverse Osmosis System

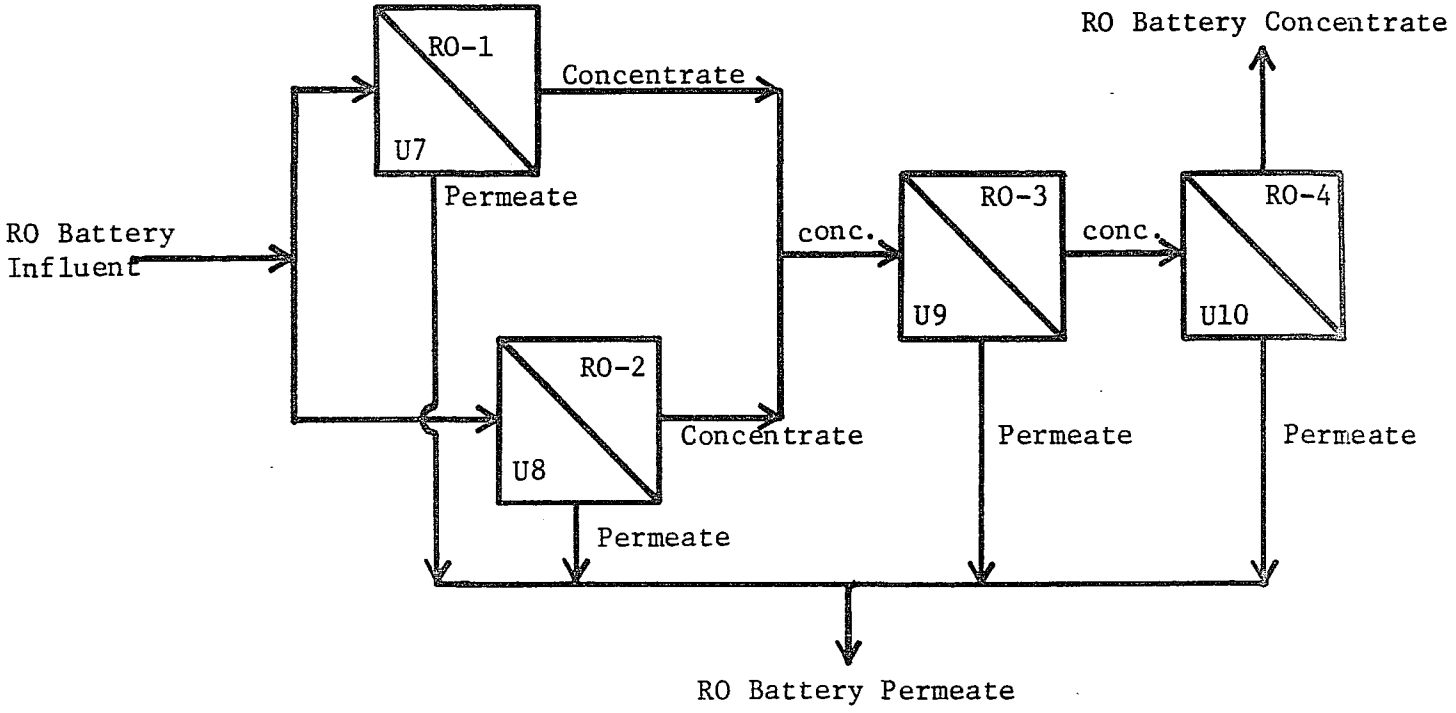

Figure 7.4. Expanded RO Module Battery Diagram

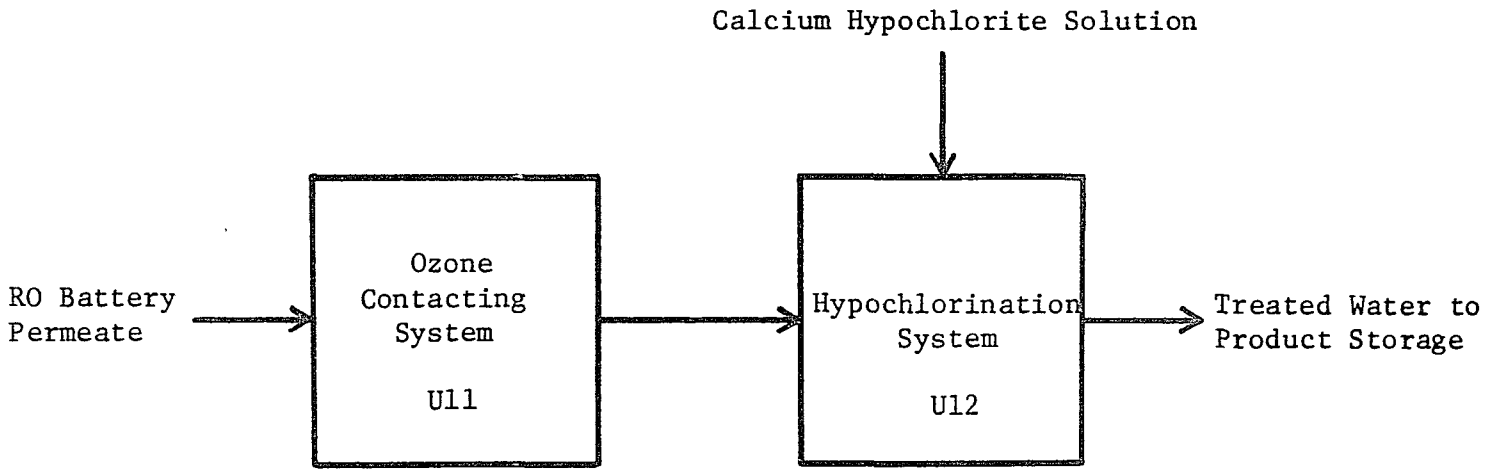

Figure 7.5. Expanded Ozonation and Hypochlorination Systems

Table 7-4. Parameter Estimation Results for Ultrafiltration (UF)
(Hospital Composite Waste Water)

Average Flux (gm/m^2-hr)		UF Permeate Solids Concentration (gm/m^3)		UF Permeate TOC Concentration (gm/m^3)		UF Module Inlet Flow Rate (m^3/hr)	UF Feed Solids Concentration (gm/m^3)	UF Feed TOC Concentration (gm/m^3)
Data	Model	Data	Model	Data	Model			
225900	216300	517	458	--	24.5	6.81	1240	229
152900	161200	869	746	--	81.4	6.81	2090	766
83230	87380	1560	1710	--	229.	6.81	7920	2170
71340	66180	2120	2296	--	457.	6.81	13400	4320
--	190900	539	572	104	52.3	4.54	1240	350
--	55560	6271	2886	683	489	4.54	12200	3350
--	25840	14285	6221	1328	1810	4.54	37200	12300

Inlet ΔP = 3.4 atm

Tube Pressure Loss = 2.0 atm

Temperature = 311°K

Table 7-5. Parameter Estimation Results for Reverse Osmosis (RO)
(Hospital Composite UF Effluent)

RO Permeate Flow Rate (m^3/hr)		RO Permeate Solids Concentration (gm/m^3)		RO Permeate TOC Concentration (gm/m^3)		RO Feed Concentration Solids (gm/m^3)	RO Feed Concentration TOC (gm/m^3)
Data	Model	Data	Model	Data	Model		
.363	.335	104.	105.	31.	29.9	12100	581
.461	.448	39.6	37.5	17.	20.0	3460	191
.477	.544	14.8	15.4	12.	8.61	845	44

Inlet Flow Rate = 1.02 m^3/hr

Inlet ΔP = 54.4 atm

Temperature = 303°K

Table 7-6. Parameter Estimation Results for Ozonation (Hospital Composite RO Effluent)

Stage	TOC, gm/m^3	
	Data	Model
Pre-Contactor	10.5	10.1
1	8.3	8.2
2	6.6	6.8
3	5.7	5.8
4	5.2	5.2
5	4.8	4.7
6	4.3	4.3

Inlet Ozone Concentration = 0.012222 moles O_3/moles carrier gas

Inlet Gas Flow Rate = 1.698 m^3/hr

Liquid Flow Rate = 0.06 m^3/hr

pH = 9 (controlled)

Temperature = 318°K

Inlet TOC Concentration = 11.6 gm/m^3

Stage Volume = $0.05/m^3$

Stage H = 1.829 m

CLEN = 1.

CWIDTH = 0.02789

} for small contactor

Figures 7.6 through 7.18 show several printer plots generated by the flow simulator package for this example study.

An interesting observation is the steady degradation in the quality of the reverse osmosis (RO) composite permeate beginning soon after starting operation. Since the reverse osmosis concentrate is recycled back into the RO feed tank, concentrations in the tank tend to increase. This in turn results in a harder separation in the RO modules and higher concentrations in the permeate.

The effects of the low purity RO permeate are transmitted downstream but are dampened somewhat by the liquid volumes of the ozonation and hypochlorination systems.

It might also be noted that the TOC levels of the ozonation system influent are much higher than those of the data points used to determine model parameters for this unit process. The accuracy of the solution under these conditions is questionable; however, the ozonation system behavior is reasonable even so.

The point is that the quality of the overall model is limited in this case by the available experimental data used in obtaining the component model parameters.

The complete discussion of this example is contained in a technical report to the Army (12).

The remainder of this chapter is devoted to comments concerning possible extensions of the work performed.

A substantial effort has been made in structuring the model so that it will remain a viable tool for continued research in the area of water re-use technology. It has already been mentioned in Chapter I that the simulator package formulation facilitates the addition or modification

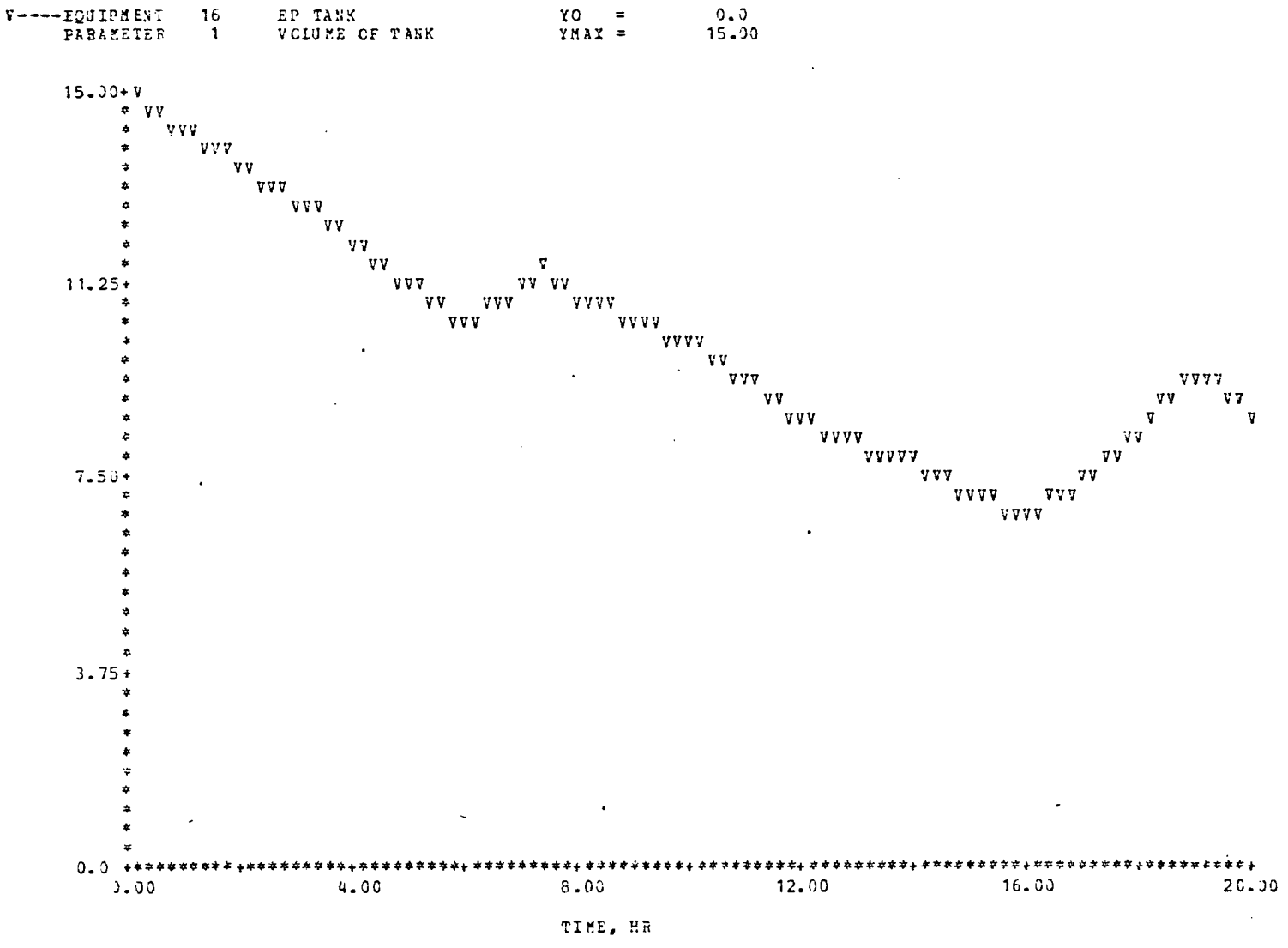

Figure 7.6. Volume of E/P Tank (m^3)

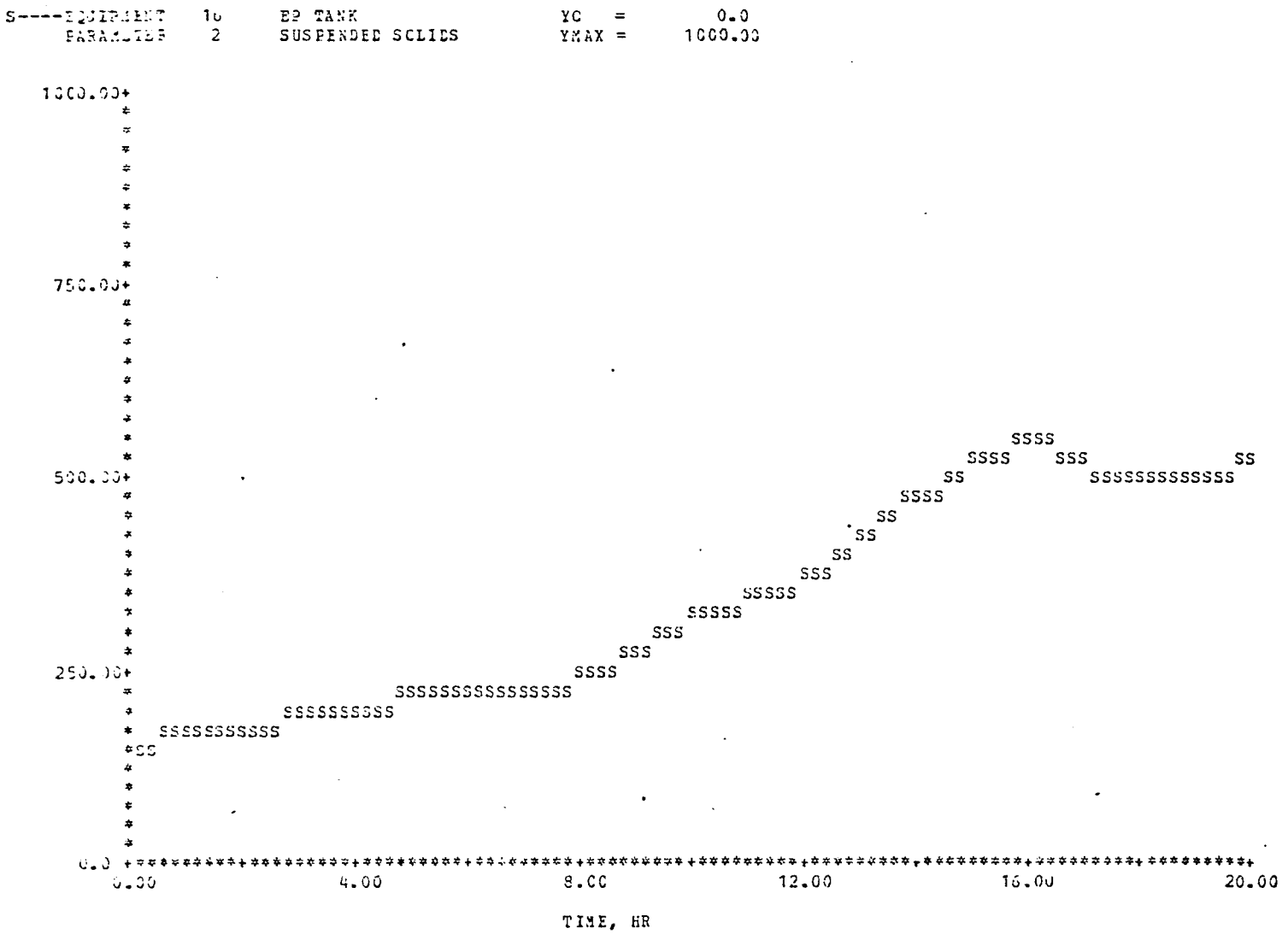

Figure 7.7. Suspended Solids Concentration of E/P Tank (gm/m^3)

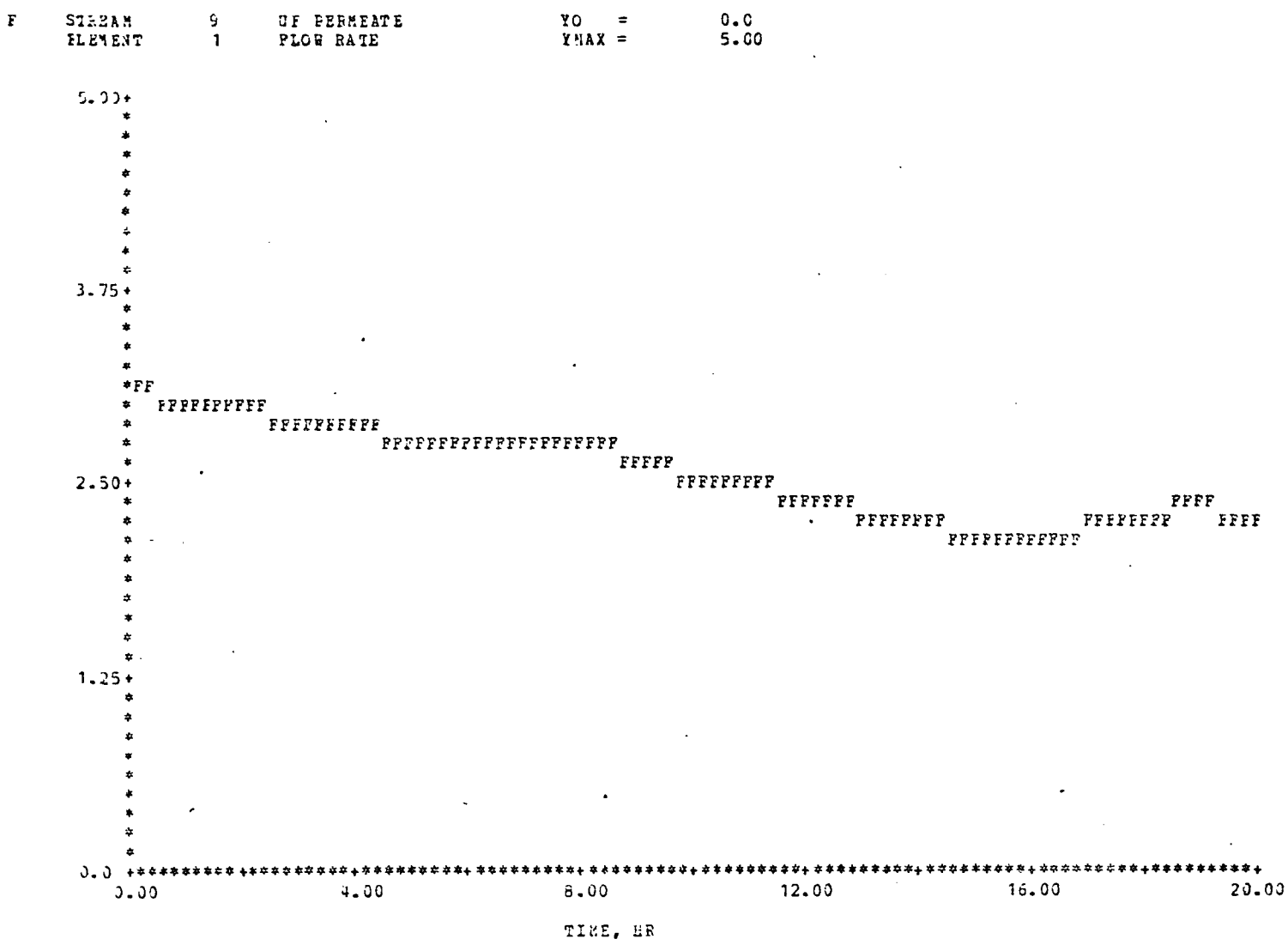

Figure 7.8. Flow Rate of UF Permeate (m^3/hr)

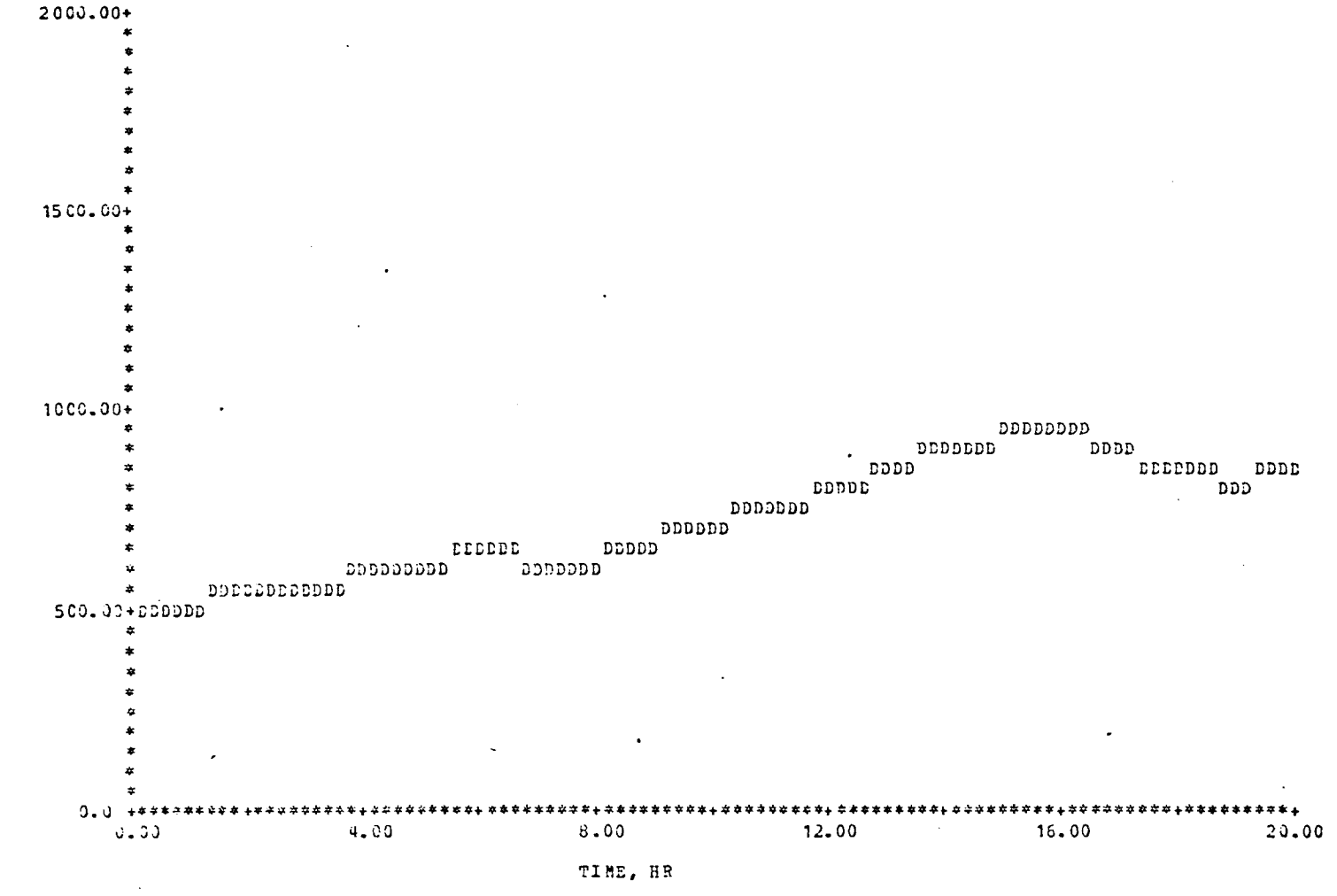

Figure 7.9. Dissolved Solids Concentration of UF Permeate (gm/m^3)

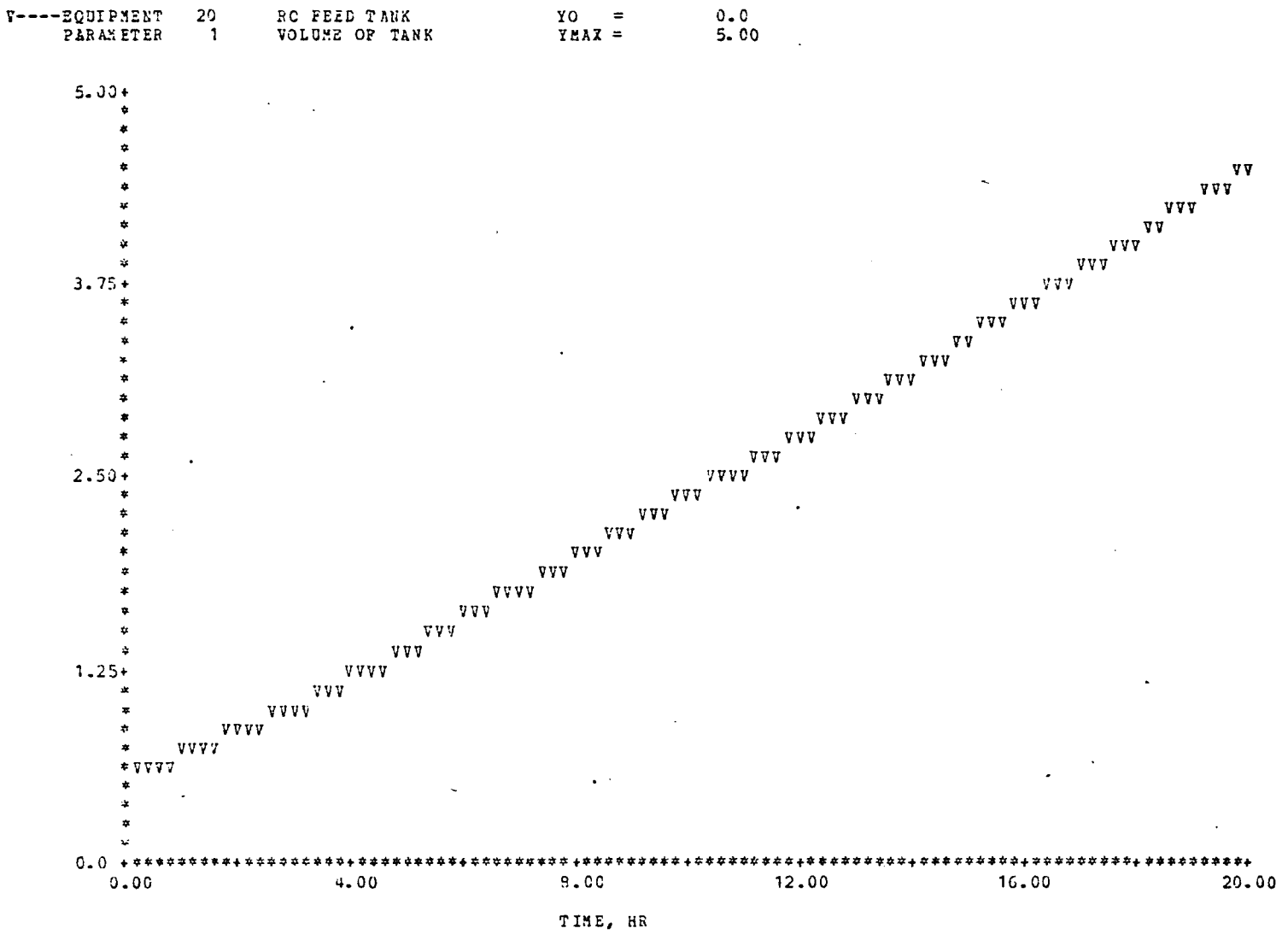

Figure 7.10. Volume of RO Feed Tank (m^3)

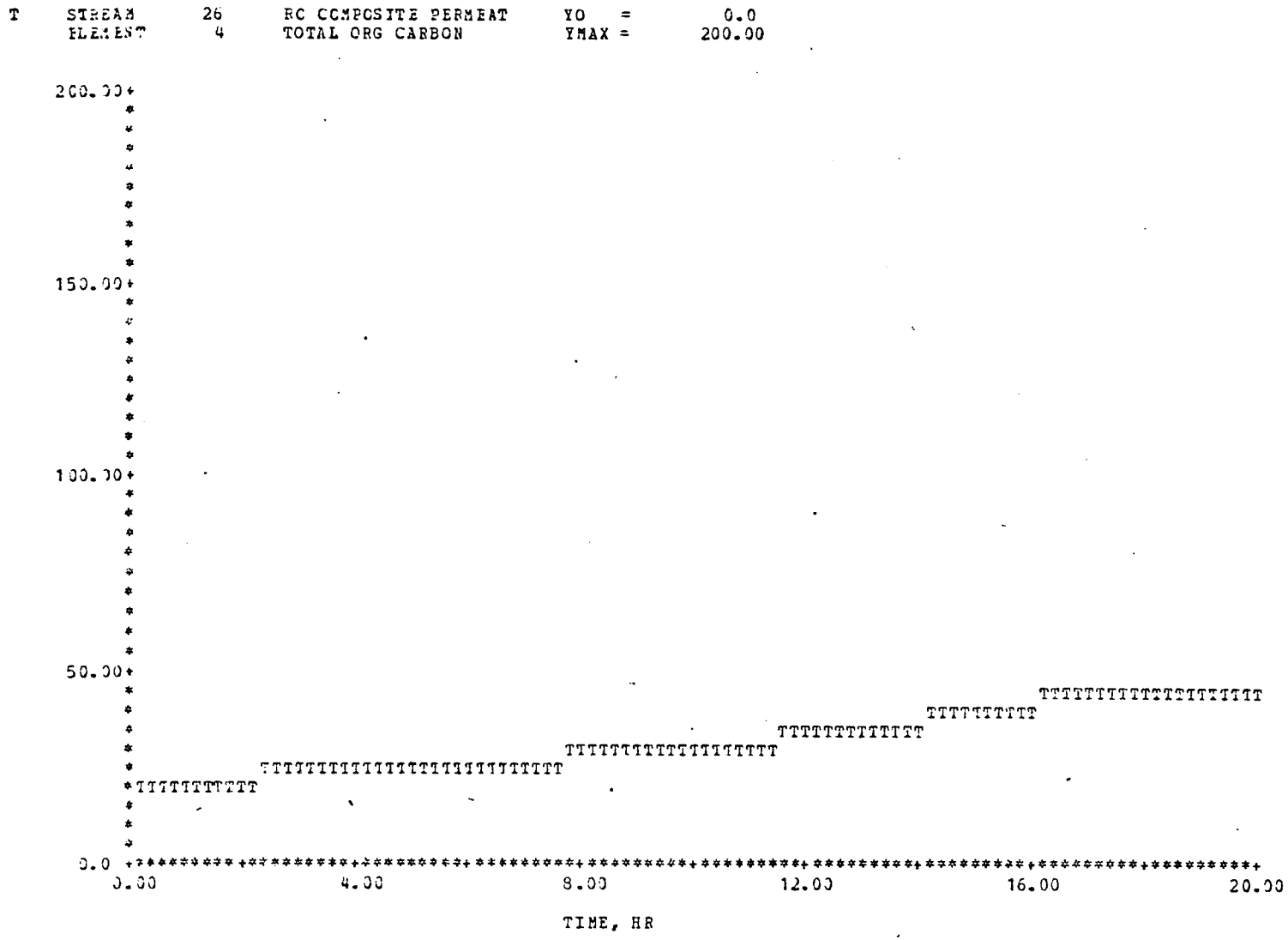

Figure 7.11. TOC Concentration of RO Composite Permeate (gm/m^3)

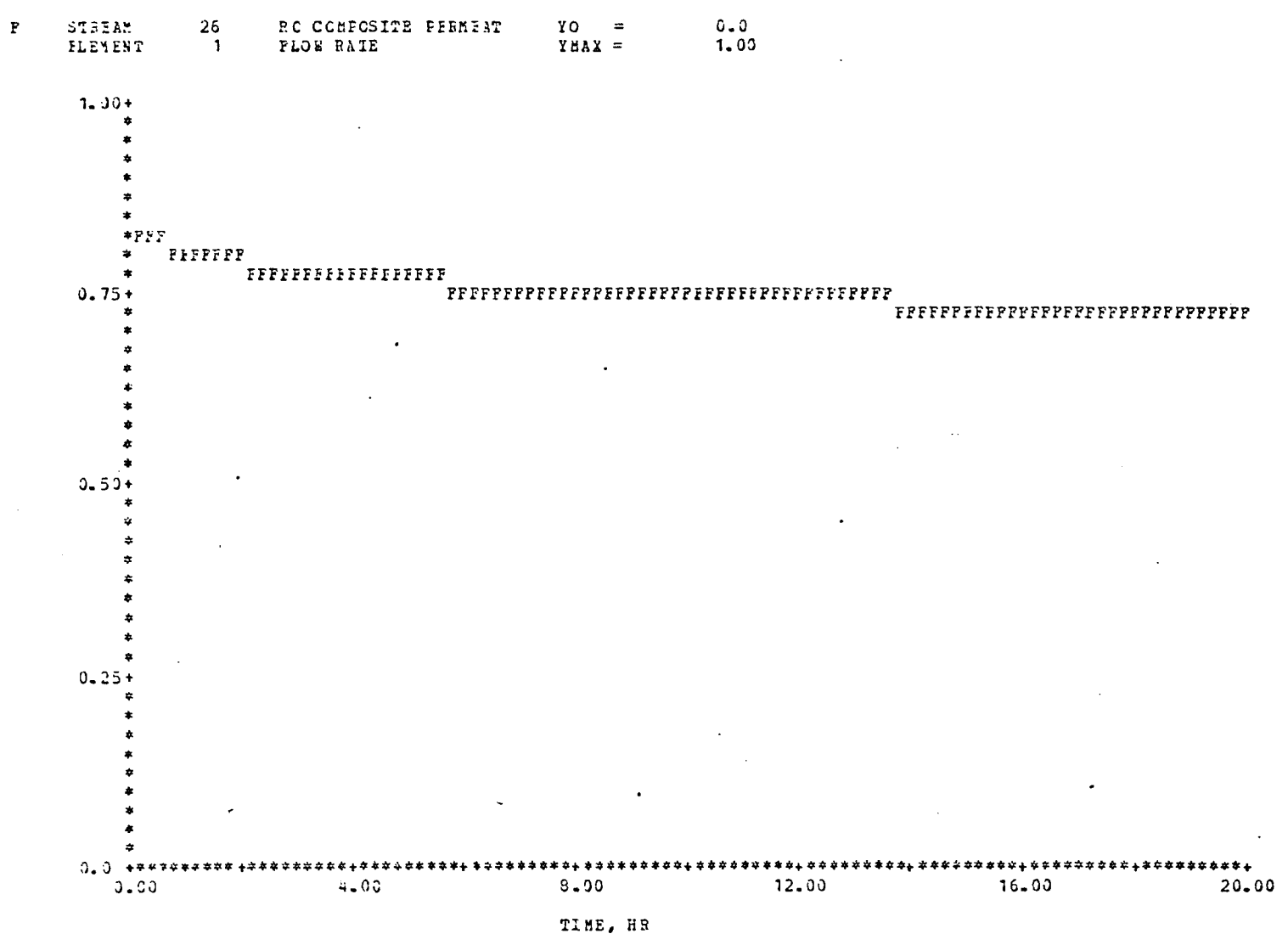

Figure 7.12. Flow Rate of RO Composite Permeate (m^3/hr)

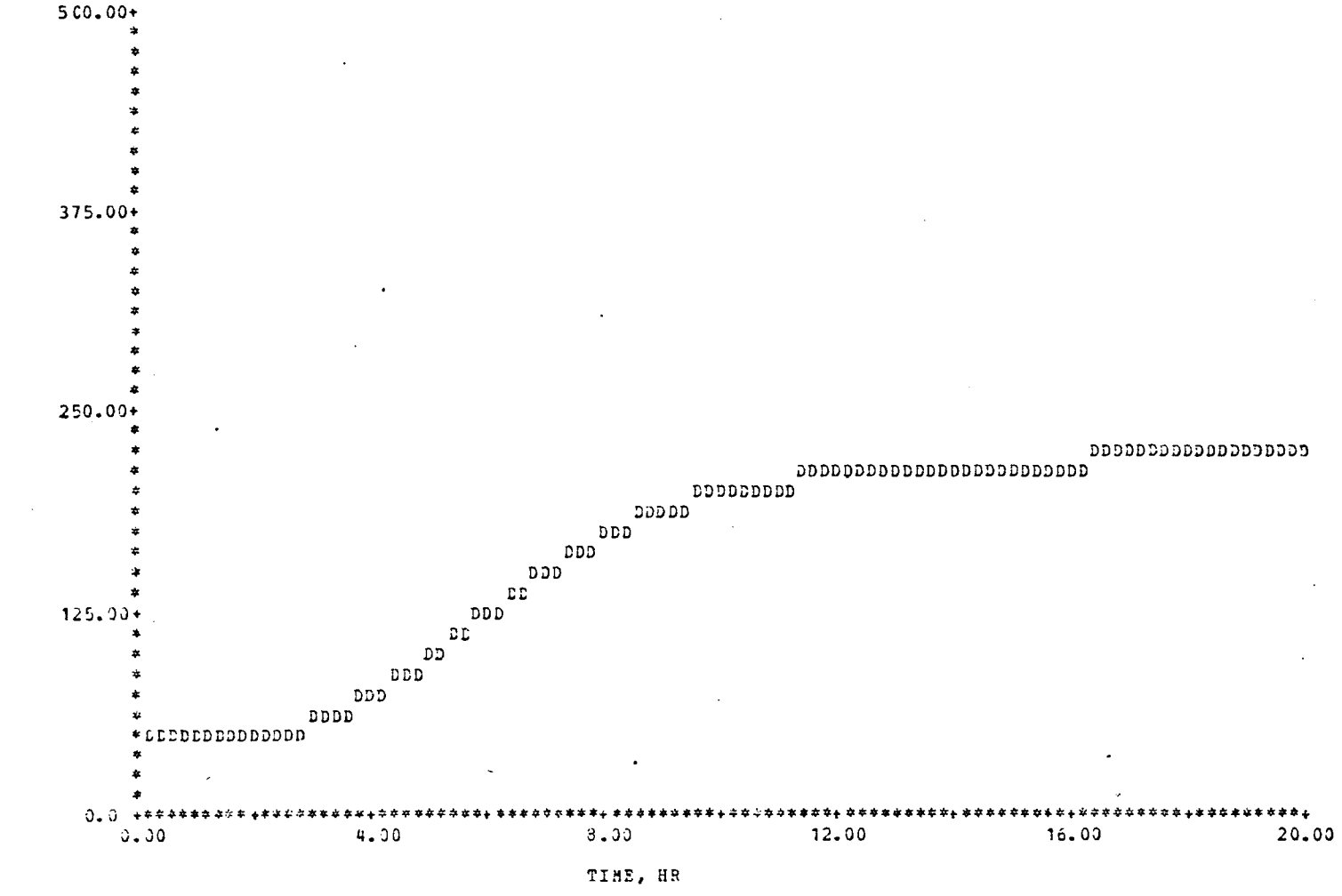

Figure 7.13. Dissolved Solids Concentration of Ozonation System Effluent (gm/m^3)

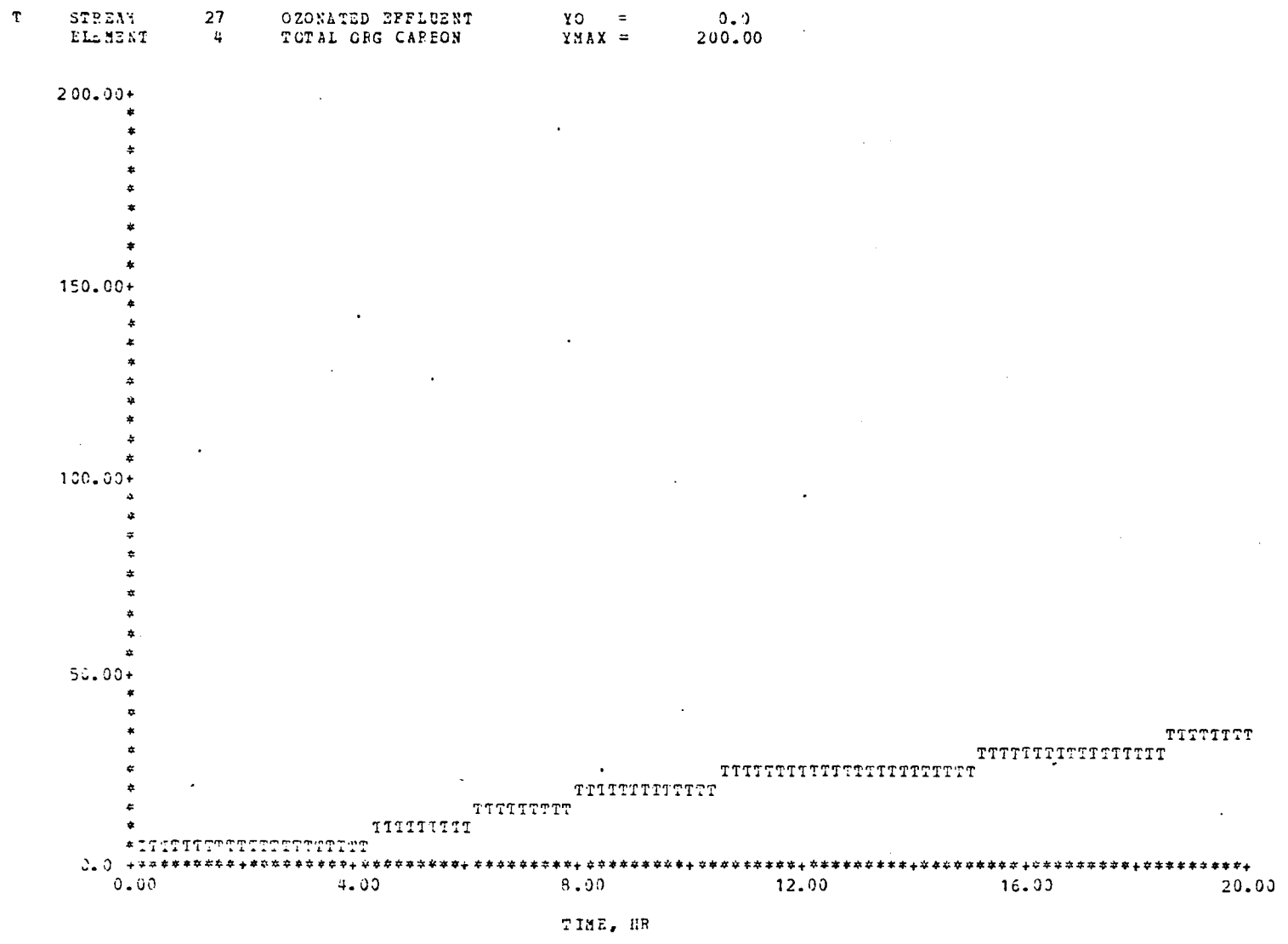

Figure 7.14. TOC Concentration of Ozonation System Effluent (gm/m^3)

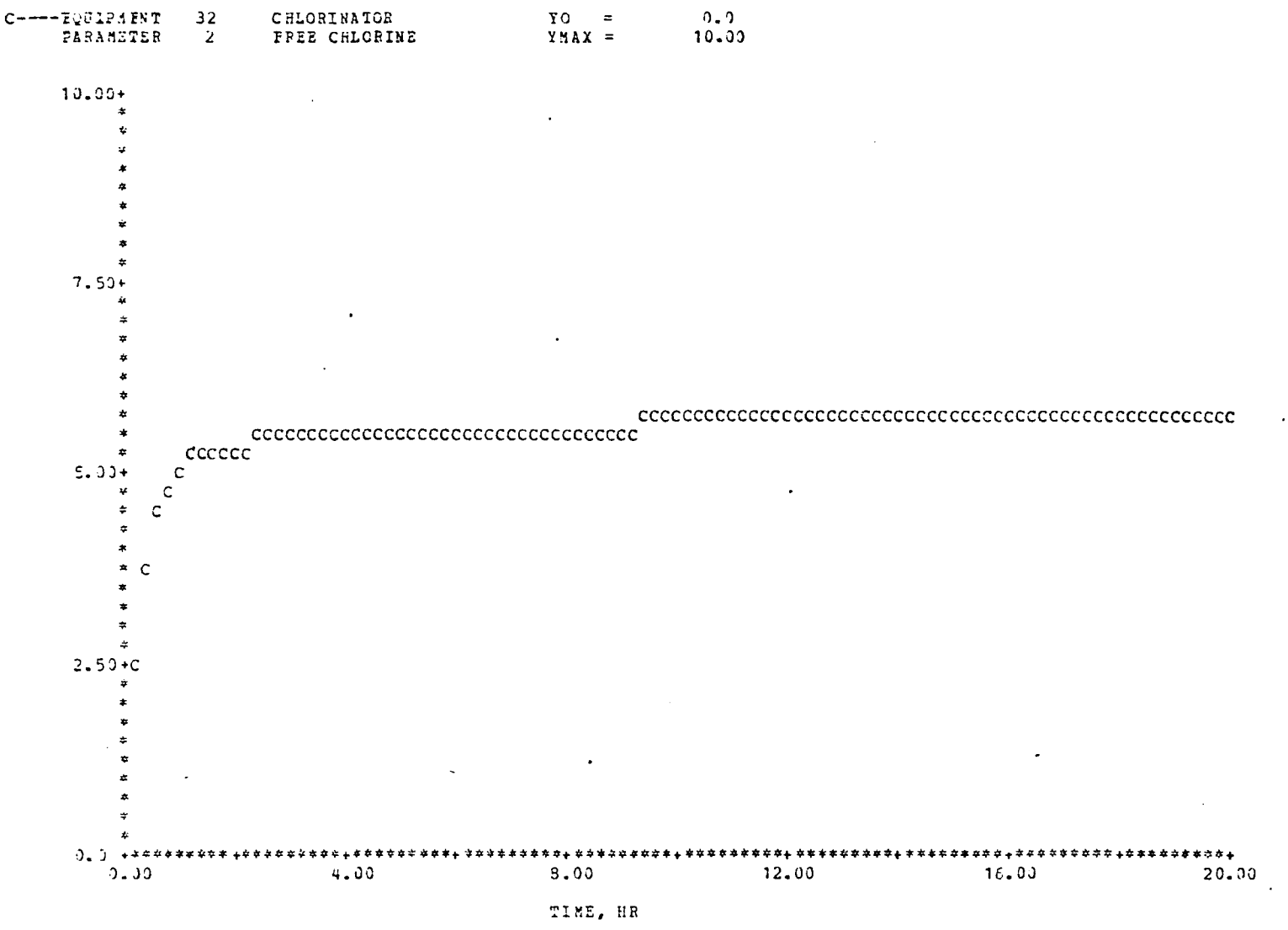

Figure 7.15. Free Available Chlorine Concentration of Chlorinator Effluent (ppm)

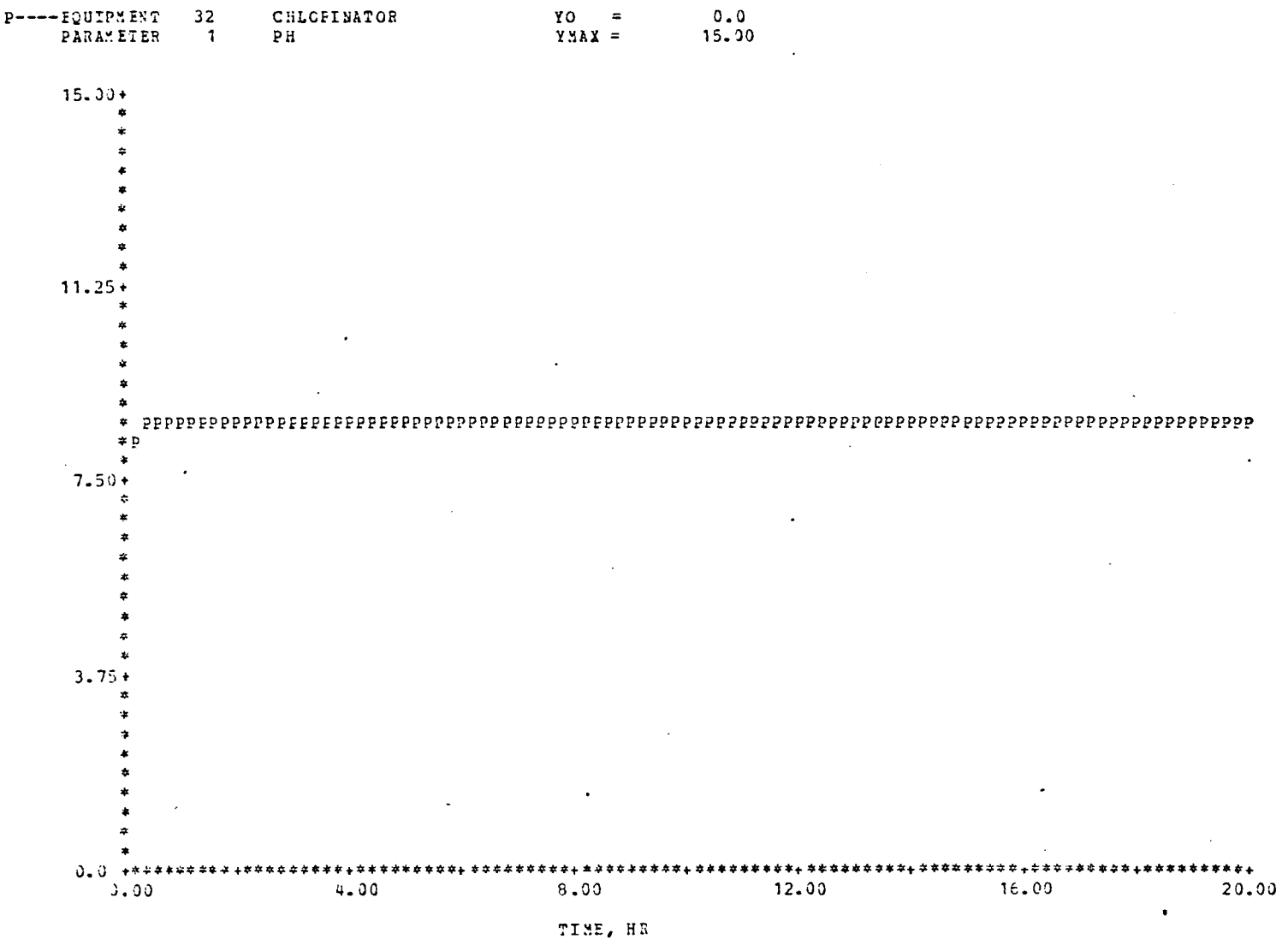

Figure 7.16. pH of Chlorinator Effluent

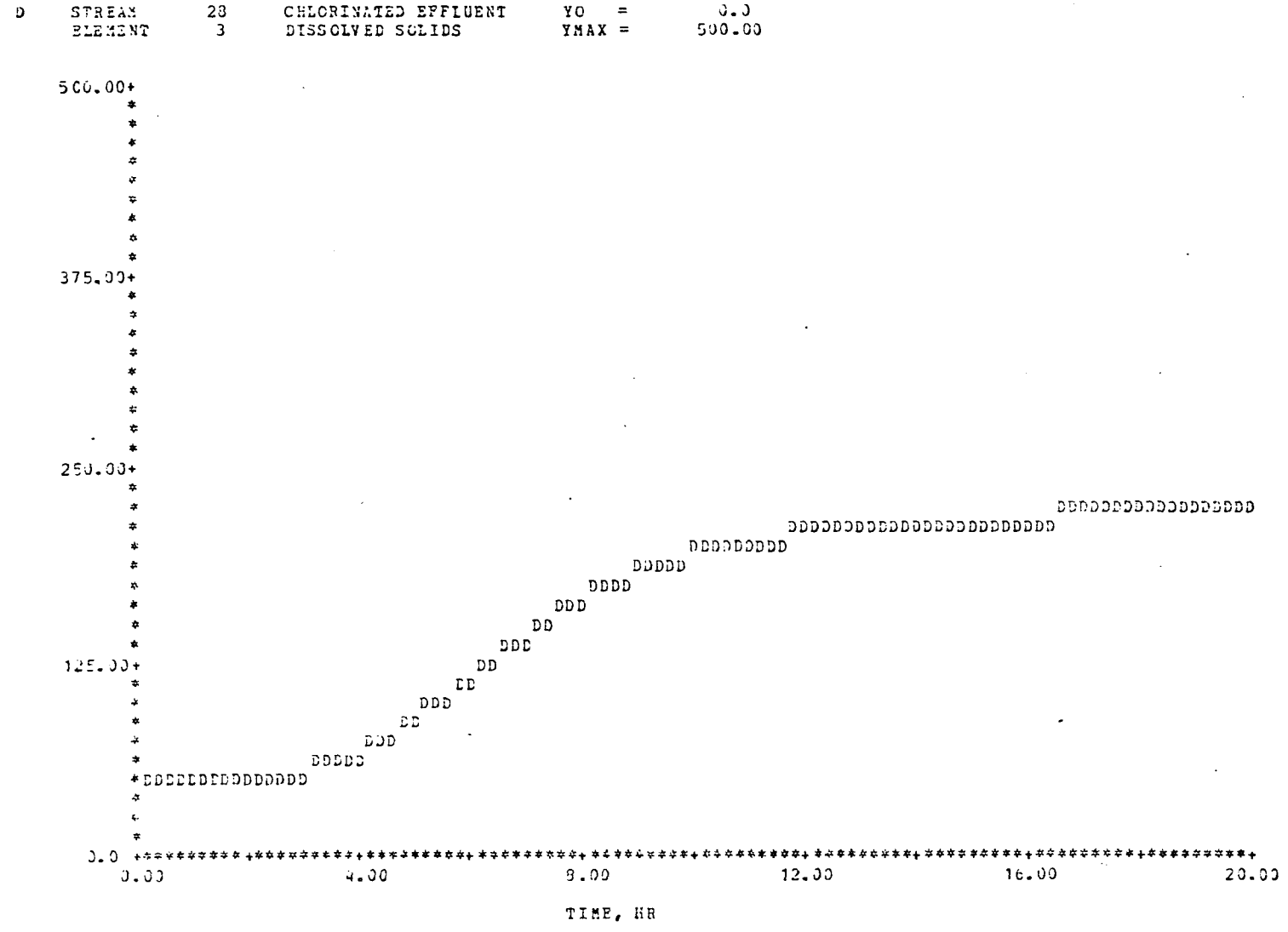

Figure 7.17. Dissolved Solids Concentration of Chlorinator Effluent (gm/m^3)

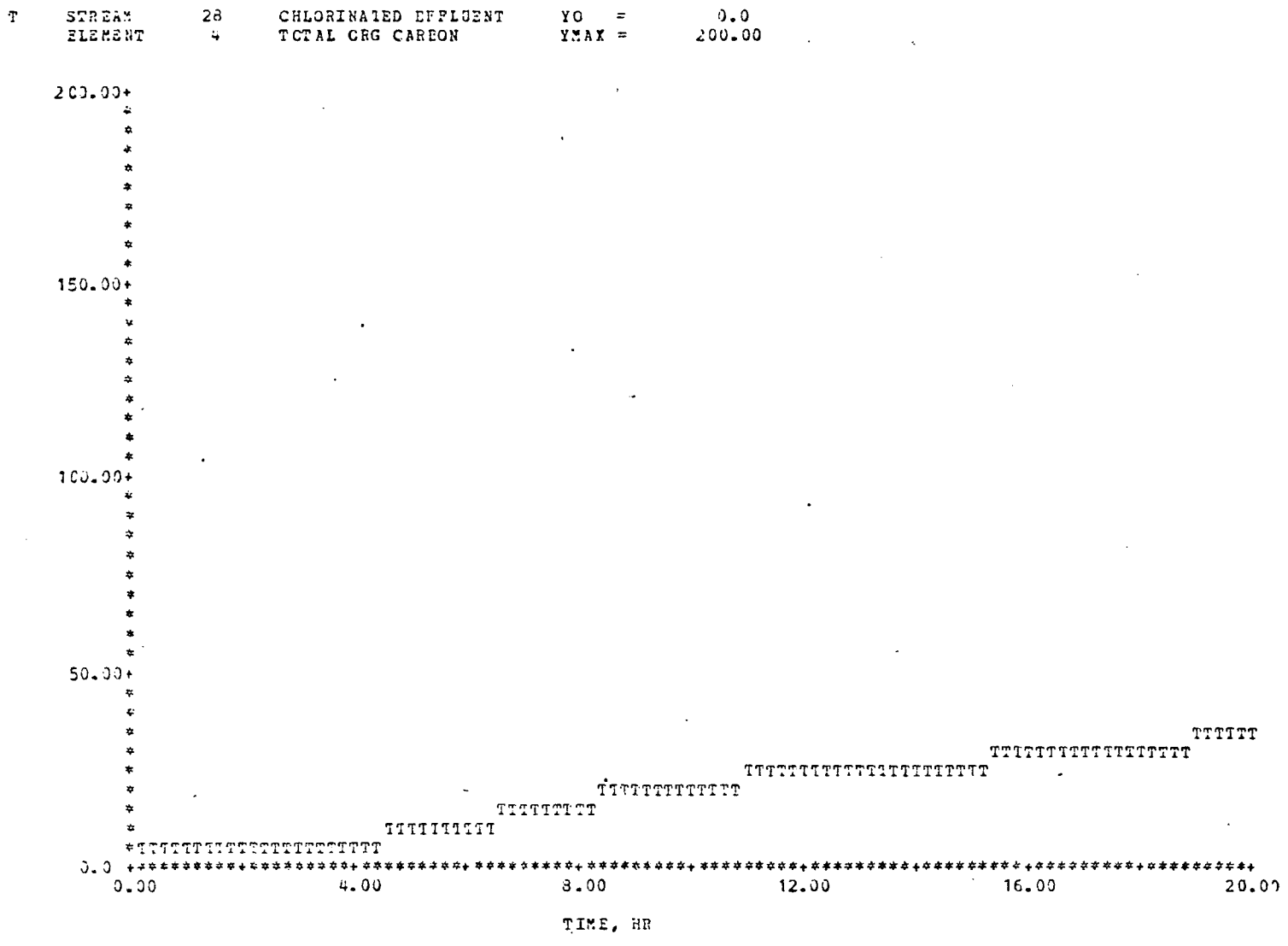

Figure 7.18. TOC Concentration of Chlorinator Effluent (gm/m^3)

of unit process models; however, this capability also extends to the implementation of other network systems. Two of interest to the author are:

1. A sensor network
2. A control element network

These additional features would be added in a way analogous to that for new unit process models. That is, these networks could be appended onto the process flow simulator by writing models for each of the control elements or sensors and then writing an interfacing routine for linkage to the simulator package.

Thus, the development of a tailored, comprehensive model of virtually any process configuration could be handled in a straightforward and standardized manner.

REFERENCES

1. Smith, C. L., and D. M. Starks, "A Mathematical Model of a Tubular Ultrafiltration Unit for Water Re-Use Systems", for USAMRDC, Contract No. DAMD 17-77-C-7040, Aug. 1978.

2. Harriott, P. and R. M. Hamilton, Chem. Eng. Sci., 20:1073 (1965).

3. Flory, P. J., Principles of Polymer Chemistry, Cornell University Press, Ithaca, New York (1957).

4. Hooke, R. and T. A. Jeeves, "'Direct Search' Solution of Numerical and Statistical Problems", J. Assoc. Comp. Mach., 8, 2 (April 1961) pp. 212-229.

5. Smith, C. L., "The Pattern Search Optimization Technique", for USAMRDC, Contract No. DAMD 17-77-C-7040, Aug. 1978.

6. Smith, C. L., and D. M. Starks, "A Mathematical Model of the Hollow Fiber Reverse Osmosis Unit for Water Re-Use Systems", for USAMRDC, Contract No. DAMD 17-77-C-7040, Aug. 1978.

7. Perry and Chilton, eds., Chemical Engineering Handbook, 5th edition, McGraw-Hill, New York, NY

8. Smith, C. L., and D. M. Starks, "A Mathematical Model of an Ozonation Contacting Unit for Water Re-Use Systems", for USAMRDC, Contract No. DAMD 17-77-C-7040, Aug. 1978.

9. Chian, E. S. K., Third Quarter Report (Jan-Mar 1977) for "Fundamental Study on the Post Treatment of RO Permeates from Army Wastewaters", Project, Contract No. DAMD 17-75-C-5006, May 1977.

10. Torricelli, A., Advances In Chemistry, Series 21, p. 453, 1958.

11. Smith, C. L., and D. M. Starks, "A Mathematical Model of a Hypochlorination Unit for a Water Re-Use System", for USAMRDC, Contract No. DAMD 17-77-C-7040, Aug. 1978.

12. Smith, C. L., and D. M. Starks, "A Dynamic Model for Application in Water Re-Use Systems", for USAMRDC, Contract No. DAMD 17-77-C-7040, Aug. 1978.

13. Gollan, A. Z. et al., "Final Report on Evaluation of Membrane Separation Processes, Carbon Adsorption, and Ozonation for Treatment of MUST Hospital Wastes", for USAMRDC, Contract No. DAMD 17-74-C-4066, Aug. 1976.

14. Chian, E. S. K., et al., "Final Report on Evaluation of New Reverse Osmosis Membranes for the Separation of Toxic Compounds from Wastewater", for USAMRDC, Contract No. DADA 17-73-C-3025, June 1976.

15. Bansal, B. and W. N. Gill, "A Theoretical and Experimental Study of Radial Flow Hollow Fiber Reverse Osmosis", presented at the 66th Annual AIChE Meeting, Session on Fundamentals in Transport Processes, Philadelphia.

16. Sourirajan, S., Reverse Osmosis, Academic Press, New York, NY, 1970.

17. See, Gary G., "WPE Pilot Plant Final Design Manual", for USAMRDC, Contract No. DAMD 17-76-C-6063, October 1976.

18. Chian, E. S. K. and P. P. K. Kuo, First Annual Report, USAMRDC, Contract No. DAMD 17-75-C-5006, July 1974-June 1975.

19. Hill, A. G., and H. T. Spencer, "Mass Transfer in a Gas Sparged Ozone Reactor", Proceeding of the First International Symposium on Ozone, Ozone Institute, Hampson Press, 1975.

20. deFilippi, R. P., and R. L. Goldsmith, "Application and Theory of Membrane Processes for Biological and Other Macromolecular Solutions", in "Membrane Science and Technology", J. E. Flinn, ed., Plenum Press, New York, 1970, pp. 33-46.

21. Goldsmith, R. L., "Macromolecular Ultrafiltration with Microporous Membranes", Ind. Engr. Chem. Fund., Vol. 10, No. 1, pp. 113-120 (1971).

22. Michaels, A. S., et al., "Solute Polarization and Cake Formation in Membrane Ultrafiltration: Causes, Consequence, and Control Techniques", in "Membrane Science and Technology", J. E. Flinn, ed. Plenum Press, New York, (1970), pp. 47-97.

23. Starks, D. M. and Cecil L. Smith, "A Dynamic Model of a Water Treatment Unit", presented at the 1977 IEEE Conference on Decisions and Control, New Orleans, Louisiana, December 7-9, 1977.

24. Starks, D. M. and Cecil L. Smith, "A Model of a Reverse Osmosis Unit for Water Re-Use Systems", presented at the Ninth Annual Modeling and Simulation Conference, sponsored by the University of Pittsburgh, Pittsburgh, Pennsylvania, April 27-28, 1978.

25. Starks, D. M. and Cecil L. Smith, "A Model of an Ultrafiltration Unit for Water Re-Use Systems", presented at the 1978 Summer Computer Simulation Conference, LaJolla, California, July 27-29, 1978.

VITA

David M. Starks is the son of Nell and Clarence C. Starks of the Central Community near Baton Rouge, Louisiana.

David graduated from Central High School in May 1971, and entered Louisiana State University in the fall of that year. He graduated from LSU with a Bachelor of Science in Computer Science and entered the LSU Graduate School, receiving a Master of Science in Chemical Engineering in 1977. He is presently a candidate for the degree of Doctor of Philosophy in Chemical Engineering.

David married the former Faye Plattsmier of Washington, Louisiana, in May 1975. Faye is a registered nurse.

Both enjoy camping in the beautiful mountains of the Eastern United States.

EXAMINATION AND THESIS REPORT

Candidate: David Milton Starks

Major Field: Chemical Engineering

Title of Thesis: A Dynamic Model for the Simulation of Water Re-Use Units

Approved:

Major Professor and Chairman

Dean of the Graduate School

EXAMINING COMMITTEE:

Date of Examination:

July 17, 1978